1. THE KINETIC ENERGY CYCLE

1.1 An overview of the kinetic energy cycle in the atmosphere

Atmospheric fluid motions may be divided into two broad classes, both of which owe their existence to the uneven distribution of diabatic heating in the atmosphere:

(a) Motions driven either directly or indirectly by horizontal heating gradients in a stably stratified atmosphere account for more than 98% of the atmospheric kinetic energy. Nearly all this kinetic energy is associated with the synoptic- and planetary-scale horizontal wind field, which has a globally averaged root mean square velocity ~12-15 m s^{-1}.

(b) Motions driven by convective instability account for the remainder of the atmospheric kinetic energy. Convection is continually breaking out within discrete regions of the atmosphere as a consequence of the vertical gradient of diabatic heating. The resulting motions have space scales ranging from about 30 km in the largest thunderstorms down to less than 1 mm in microscale motions within the surface layer. Despite their small contribution to the atmospheric kinetic energy, convectively driven motions play an important role in the upward transport of latent and sensible heat.

The term *general circulation* is used by some meteorologists to denote the totality of atmospheric fluid motions, while others in the field use the term in a more restrictive sense, to denote motions described under (a).

Defined either way, the general circulation can be viewed in the context of a *kinetic energy cycle* in which atmospheric fluid motions continually draw on the reservoir of potential energy inherent in the spatial distribution of atmospheric mass in order to maintain themselves against frictional dissipation, which is continually transforming the kinetic energy of fluid motions into the internal energy of random molecular motions. In the presence of this continual drain, the potential energy of the mass field is maintained by the spatial gradients of diabatic heating which, in a statistical sense, are always acting to lift the center of gravity of the atmosphere.

From a dynamical point of view, large-scale horizontal motions owe their existence to the pressure gradient force which drives a slow horizontal flow across the isobars from higher toward lower pressure. In the presence of the earth's rotation this flow across the isobars induces a circulation parallel to the isobars whose speed tends toward a state of geostrophic balance[1] with the horizontal pressure gradient (and thermal wind balance with the temperature gradient). From an energetic point of view, the same cross-isobar flow, together

[1]Gradient wind balance when the flow is strongly curved.

with its attendant vertical motions, is responsible for the conversion from potential to kinetic energy.

In lower latitudes, most of the atmospheric kinetic energy is contained in quasi-steady, *thermally driven circulations* which are directly related to the geographical distribution of sources and sinks of heat; as a result, the observed weather over most of the tropics varies relatively little from day to day (apart from diurnal variations) at a fixed location, although it may vary greatly from one location to another. These thermally driven circulations include the seasonally varying *monsoons*, which are the atmospheric response to land-sea heating contrasts, and a large-scale meridional overturning over the mid-Atlantic and Pacific Oceans which gives rise to the *intertropical convergence zone*, a narrow east-west band of heavy cloudiness and precipitation.

In middle and high latitudes much of the kinetic energy is associated with moving disturbances called *baroclinic waves*, which develop spontaneously within zones of strong horizontal temperature gradients. Most of the significant day-to-day weather changes at these latitudes can be attributed to the passage of these systems with their attendant mesoscale frontal zones.

Planetary- and synoptic-scale atmospheric disturbances are subject to frictional dissipation, which causes them to gradually lose their kinetic energy. The energy is not transferred directly from the large-scale motions into random molecular motions. Through processes such as shear instability, and convection, and mechanically driven turbulence in the presence of vertical wind shear, it is siphoned off by small-scale fluid motions which interact among themselves to transfer energy to smaller and smaller scales and ultimately down to the random molecular motions.

Roughly half the frictional dissipation takes place within the lowest kilometer of the atmosphere, as a result of turbulent motions generated mechanically by flow over irregularities in the underlying surface. The other half takes place higher in the atmosphere in discrete patches where small-scale disturbances are generated as a result of convection or shear instability of the vertical wind profile.

In a gross sense the atmosphere may be viewed as a vast but inefficient heat engine to which heat is added at a high temperature and removed at a somewhat lower temperature. The mechanical output of the heat engine is the supply of kinetic energy required to maintain the general circulation against frictional dissipation. Since the atmosphere receives heat at a higher effective temperature than it radiates it away to space, it may be viewed as working to increase the entropy of the universe.

The physical processes responsible for the generation and maintenance of large-scale atmospheric motions can be demonstrated by means of two simple laboratory analogs.

1.1.1 A "before and after" analog

Figure 1.1a shows a tank filled with equal volumes of two homogeneous immiscible liquids of differing densities, placed side by side and separated by a movable partition. The shaded liquid on the right is more dense than the unshaded liquid. In (b) the partition has been removed and fluid motion has developed. We will not be concerned about the details of the motion, but only the final state after friction has brought the liquids to rest. In the new equilibrium configuration shown in (c) the heavy fluid occupies the bottom half of the tank.

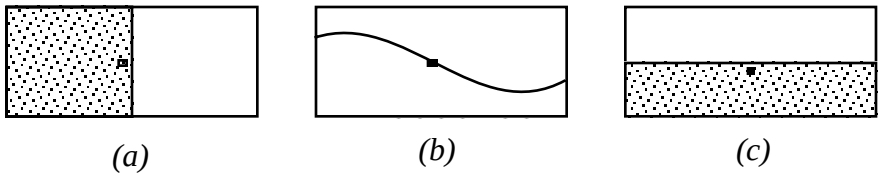

Fig. 1.1 (a) Heavier (shaded) and lighter fluids separated by a movable partition. The dot represents the center of gravity of the two-fluid system. (b) Fluids in motion following the removal of the partition. (c) Equilibrium configuration of the fluids after the motion has been dissipated by friction.

Now let us consider this sequence of events from the point of view of the energetics. In the initial configuration, the center of gravity of the fluid, denoted by the dot, is exactly halfway between the top and bottom. After the partition is removed, the center of gravity drops as the denser liquid slides under the lighter one. Through the sinking of denser liquid and the rising of lighter liquid [indicated in (b)] potential energy is converted into the kinetic energy of fluid motions. Frictional dissipation eventually converts all the fluid motions to random molecular motions so that, in the final state (c), the only evidence of the conversion that took place is the drop in the center of gravity of the system and a very slight increase in the temperatures (or internal energy) of the liquids. The energy cycle is summarized in Fig. 1.2. Note that only a small fraction of the potential energy inherent in the initial state is available for conversion to kinetic energy, since no matter what kind of motions develop the center of gravity cannot possibly drop below the level shown in (c).

Fig. 1.2 The kinetic energy cycle.

Questions:

1.1 In the experiment described above the depth of the tank is 1 m and two fluids have specific gravities of 1.1 and 0.9, and the same specific heat of 4×10^3 J kg $^{-1}$ deg^{-1}. What is the maximum possible root mean square (rms) velocity of fluid motion that can be realized in the experiment. How much does the temperature increase as a result of frictional dissipation? (Assume that the rms velocity and the temperature rise are the same for the two fluids.)

1.2 What kinds of processes contribute to the irreversible mixing of denser and lighter fluid in the atmosphere?

1.3 By how much would the center of mass of the atmosphere have to drop to release enough potential energy to account the observed kinetic energy of the general circulation? (For the kinetic energy, assume that the root-mean squared velocity associated with fluid motions is 15 m s^{-1}.)

1.1.2 A "steady-state" analog

In the real atmosphere, potential energy is constantly being replenished by diabatic heating so that there is a continuous flow of energy through the cycle indicated in Fig. 1.2. The following "steady-state" laboratory analog will help to illustrate this situation. Figure 1.3 shows a tank full of liquid, which has internal heat sources along the bottom and left wall and matching heat sinks along the top and right wall. The liquid expands with increasing temperature.

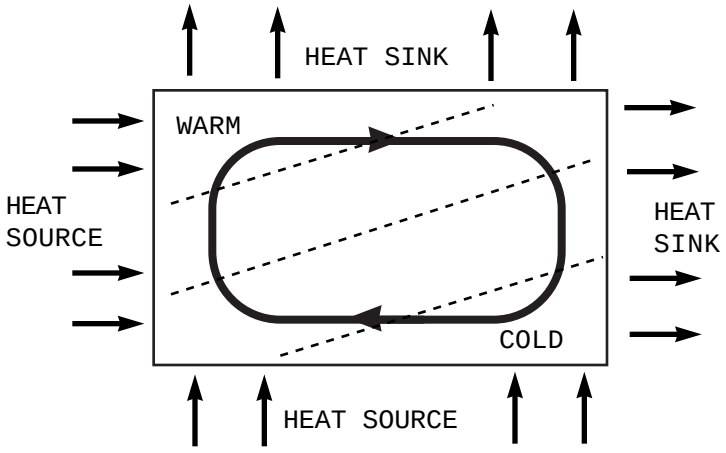

Fig. 1.3 Steady state circulation (heavy arrows) in a liquid, driven by the distribution of heat sources and sinks as indicated. Dashed lines denote isotherms.

The gradient of heating drives a slow, clockwise circulation cell, as represented in the figure. As a parcel of fluid is carried around the tank in this cell it grows warmer as it passes along the bottom of the tank and as it ascends along the left wall. Then it grows cooler as it moves across the top of the tank and down along the right wall to complete the circuit. In order to be consistent with these temperature changes, the isotherms must slope from lower left to upper right, as indicated by the dashed lines in the figure. Since temperature increases with height, the fluid in the tank is stably stratified.

In applying the above arguments to the atmosphere, the compressibility of air must be taken into account by considering changes in potential temperature (rather than temperature) as an air parcel moves around the circulation cell. The isotherms in the figure are thus indicative of isentropes in the atmosphere, where an increase of potential temperature with height is the criterion for stable stratification.

At any given level in the tank, lighter fluid is rising along the left-hand side of the tank and an equal volume of heavier fluid is sinking along the right-hand side. This vertical exchange of equal volumes of fluid with different densities produces a net downward flux of mass which should tend to lower the center of gravity of the fluid, just as in the previous analog, converting potential energy to kinetic energy. In this steady-state model, the conversion proceeds at exactly the same rate as the kinetic energy of the fluid motions is being destroyed by frictional dissipation. The lowering of the center of gravity of the fluid is opposed by diabatic heating which is always warming and expanding the fluid near the bottom of the tank, and cooling and compressing the fluid near the top. In order to accommodate this expansion and compression, a very small mean upward motion is required at intermediate levels. This mean upward mass flux exactly cancels the downward mass flux due to the circulation cell so that the center of gravity of the fluid remains at a constant level.

In the laboratory analog, the heat source and sink adjacent to the side walls of the tank represent the horizontal gradients of diabatic heating in the earth's atmosphere. The heat source near the bottom of the tank represents the combined effects of the absorption of solar radiation, the exchange of infrared radiation with the earth's surface, and, most important, the input of sensible heat associated with convectively driven motions in the mixed layer and the release of latent heat in clouds. Collectively, these processes result in a strong input of energy into the lower troposphere. The atmospheric heat sources and sinks overlap in the vertical, but the 'center of mass' of the sinks is slightly higher in the troposphere than that of the sources.

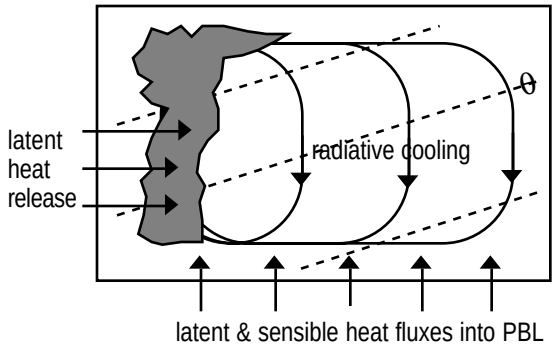

Fig. 1.4 Atmospheric analogue of the steady state, thermally driven circulation in the previous figure. It may be viewed as representing the tradewind/ITCZ circulation.

A specific example of such a circulation cell in the atmosphere is shown in Fig. 1.4. The rising branch corresponds to the regions of deep convection over the tropical monsoons and the intertropical convergence zone, where air parcels may ascend from the troposphere to the upper troposphere in a matter of an hour. Vast quantities of latent heat are released as the water vapor in these updrafts condenses into liquid water and ice. The air detrained from the anvils of these clouds subsides slowly, over a period of a week or so, cooling by the emission of infrared radiation, which nearly always exceeds the heating due to the absorption of solar and infrared radiation. Hence, these subsiding air parcels cross the isentropes toward lower values of potential temperature. When they reach the ~1.5 km level are entrained into the planetary boundary layer (PBL), where the air is being heated and moistened by the fluxes through the underlyng surface. Hence, air parcels cross the isentropes toward higher values of potential temperature as they flow toward the tropical rain belts.in the lower branch of the circulation cell. Shallow convection has the effect of vertically mixing the heat and moisture added at the lower surface through the depth of the PBL. A discrete jump in moist static energy is observed at the top of the PBL.

The importance of atmospheric water vapor in these large-scale thermally driven circulations is worth emphasizing. Latent heat added to the atmosphere in the lower branch of the cell is converted into sensible heat when the water vapor condenses in the rising branch. This additional source of heating serves to enhance the horizontal heating contrasts that would have existed in the absence of the cell. As a result, thermally driven circulations tend to be much stronger than they would be in an atmosphere without water vapor.

The maintenance of large-scale thermally driven circulations requires both horizontal and vertical gradients of diabatic heating. In the absence of horizontal heating contrasts, the heat source / sink at the bottom and top of the tank destroy the stable stratification and

initiate convectively driven motions on a scale much smaller than the dimensions of the tank. In these convection cells, bubbles of warm light fluid rise, and are replaced by cooler, denser fluid from above. In the equilibrium situation the downward mass flux in the convection cells is just enough to maintain the center of gravity of the fluid at a constant level.

Questions:

1.4 Consider how the slopes of the isotherms (or isentropes) in Fig. 1.3 depends upon the relative magnitudes of the horizontal and vertical heating gradients

1.5 How would the circulation cell in Fig. 1.3 be affected if the vertical heating gradients were turned off? How could a steady state ultimately be achieved? Hint: as an analogue, consider a room with a radiator on one side and a cold window on the other side.

1.3 Kinetic energy generation in a hydrostatic fluid

In applying the two above examples to the atmosphere, one important distinction needs to be kept in mind. In experiments of laboratory size proportions, the horizontal and vertical components of the motion are likely to be of the same order of magnitude so that an appreciable fraction of the kinetic energy associated with the fluid motions resides in the vertical component. This energy is converted from potential energy when imbalances between the forces in the vertical equation of motion propel buoyant parcels of fluid upward and denser parcels downward. In effect, gravity does work on the fluid, just as it does work on a falling object. In a hydrostatic fluid there is no vertical equation of motion and no kinetic energy associated with the vertical motion component. Kinetic energy is realized when the horizontal component of the pressure gradient force does work on parcels of fluid as they move across the isobars from higher toward lower pressure on level surfaces. The relation between this cross-isobar flow and the release of potential energy will become fully apparent when we consider the governing equations. However, one can get some intuitive feel for it from Fig. 1.4, which shows an the slope of the pressure surfaces that would develop in association with the steady state circulation considered in the previous figure. In agreement with the hypsometric equation, the vertical spacing between pressure surfaces (i.e., the thickness) is higher on the warm side of the tank than on the cold side. It follows that the horizontal flow in the clockwise circulation cell must be primarily directed down the horizontal pressure gradient, as required for the generation of kinetic energy. Hence, the rising of warmer fluid and sinking of colder fluid implies cross-isobar horizontal flow toward lower pressure and vice versa.

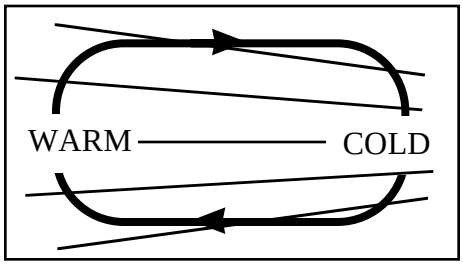

Fig. 1.4 The pressure field that would develop in association with the steady state circulation cell shown in the previous figure. The solid lines represent pressure surfaces.

Question:

1.6 For a homogeneous (constant density) fluid in a tank with a flat bottom, vertical walls, and no top:

(a) show that the average potential energy per unit area is given by $1/2\rho g\overline{z^2}$, where z is the height of the free surface of the fluid and the overbar denotes an average over the area of the tank.

(b) Show that the average potential energy per unit area that is available for conversion into kinetic energy is given by $1/2\rho g\overline{z}^2$, where $z' = z - \bar{z}$. {Hint: Begin by substituting in the expression for potential energy per unit area. Note that $\overline{\bar{z}z'} = \bar{z}\overline{z'} = 0$.}

(c) Show that the average rate of conversion from potential to kinetic energy is given by $-\rho g\overline{wz}$, where w is the vertical velocity of the free surface. Give a physical interpretation of this result in terms of flow across the isobars.

1.2 Lorenz's concept of available potential energy

The foundation for quantitative studies of the atmospheric kinetic energy cycle is the formalism introduced by Lorenz (1955), which was inspired by much earlier work by Margules (1903) on the energetics of storms. Central to this formalism is the concept of *available potential energy*. In Lorenz's words:

> The strengths of the cyclones, anticyclones, and other systems which form the weather pattern are often measured in terms of the kinetic energy that they possess. Intensifying and weakening systems are then regarded as those which are gaining or losing kinetic energy. When such gains or losses occur, the source or sink of kinetic energy is a matter of importance. Under adiabatic motion, the total energy of the whole atmosphere would

remain constant. The only sources or sinks for the kinetic energy of the whole atmosphere would then be potential energy and internal energy.

In general the motion of the atmosphere is not adiabatic. The only nonadiabatic process which directly alters kinetic energy is friction, which ordinarily generates internal energy while it destroys kinetic energy.... The remaining nonadiabatic processes, including the release of latent energy, alter only the internal energy directly. Hence the only sources for the kinetic energy of the whole atmosphere are atmospheric potential energy and internal energy, while the environment may also act as a sink.

It is easily shown (cf. Haurwitz, 1941) that the potential and internal energies within a column extending to the top of the atmosphere bear a constant ratio to each other, to the extent that hydrostatic equilibrium prevails. Hence, net gains of kinetic energy occur in general at the expense of both potential and internal energy, in this same ratio. It is therefore convenient to treat potential and internal energy as if they were a single form of energy. The sum of the potential and internal energy has been called *total potential energy* by Margules (1903).

Evidently the total potential energy is not a good measure of the amount of energy available for conversion into kinetic energy under adiabatic flow. Some simple cases will serve to illustrate this point. Consider first an atmosphere whose density stratification is everywhere horizontal. In this case, although total potential energy is plentiful, none at all is available for conversion into kinetic energy. Next suppose that a horizontally stratified atmosphere becomes heated in a restricted region. This heating adds total potential energy to the system, and also disturbs the stratification, thus creating horizontal pressure forces which may convert total potential energy into kinetic energy. But next suppose that a horizontally stratified atmosphere becomes cooled rather than heated. The cooling removes total potential energy into kinetic energy. Evidently removal of energy can be as effective as addition of energy in making more energy available.

We therefore desire a quantity which measures the energy available for conversion into kinetic energy under adiabatic flow. A quantity of this sort was discussed by Margules (1903) in his famous paper concerning the energy of storms. Margules considered a closed system possessing a certain distribution of mass. Under adiabatic flow, the mass may become redistributed, with an accompanying change in total potential energy, and an equal and opposite change in kinetic energy. If the stratification becomes horizontal and statically stable, the total potential energy reaches its minimum possible value, and the gain of kinetic energy thus reaches its maximum. This maximum gain of kinetic energy equals the maximum amount of total potential energy available for conversion into kinetic energy under any adiabatic redistribution of mass, and as such may be called the *available potential energy.*

Available potential energy in this sense can be defined only for a fixed mass of atmosphere which becomes redistributed within a fixed region. The storms with which Margules was primarily concerned do not consist of fixed masses within fixed regions, nor do any other systems having the approximate size of storms. It is perhaps for this reason

that available potential energy has not become a more familiar quantity.

It is in considering the general circulation that we deal with a fixed mass within a fixed region -- the whole atmosphere. It is thus possible to define the available potential energy of the whole atmosphere as the difference between the total potential energy of the whole atmosphere and the total potential energy which would exist if the mass were redistributed under conservation of potential temperature to yield a horizontal stable stratification.

The available potential energy so defined possesses these important properties:

(1) The sum of the available potential energy and the kinetic energy is conserved under adiabatic flow.

(2) The available potential energy is completely determined by the distribution of mass.

(3) The available potential energy is zero if the stratification is horizontal and statically stable.

It seems fairly obvious that the available potential energy so defined is the only quantity possessing these properties, although a rigorous proof would be somewhat involved. Moreover, it possesses the further property:

(4) The available potential energy is positive if the stratification is not both horizontal and statically stable.

It follows from property (1) that available potential energy is the only source for kinetic energy. On the other hand, it is not the only sink. When friction destroys kinetic energy it creates internal energy, but in doing so it increases the minimum total potential energy as well as the existing total potential energy. Thus the loss of kinetic energy exceeds the gain of available potential energy.

There is no assurance in any individual case that all the available potential energy will be converted into kinetic energy. For example, if the flow is purely zonal, and the mass and momentum distributions are in dynamically stable equilibrium, no kinetic energy at all can be realized. It might seem desirable to redefine available potential energy, so that, in particular, it will be zero in the above example. But the available potential energy so defined would depend upon both the mass and momentum distributions. If it is desired to define available potential energy as a quantity determined by the mass distribution, the definition already introduced must be retained.

1.3 A simplified derivation

Consider an atmosphere at rest with a globally averaged temperature profile *T(p)* or *T(z)*, but with undulations in the potential temperature surfaces (isentropes) so that locally

$$T(x,y,z) = \overline{T}(z) + T''(x,y,z) \tag{1.1}$$

If the isentropes are allowed to flatten out by means of an adiabatic readjustment of mass, potential energy will be released as cold, heavy air sinks and warm, light air rises in the process, so that the center of gravity of the atmosphere drops by a small amount. Alternatively, we may view this release of potential energy as work done on the atmosphere by gravity. This so-called available potential energy of the atmosphere, divided by the area of the atmosphere ($4\pi R_E^2$), will be denoted by the symbol $\overline{A}$. We will now derive an expression for $\overline{A}$.

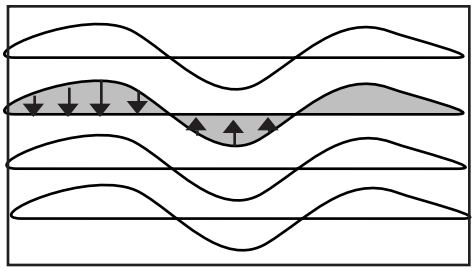

Fig. 1.5. Idealized vertical cross-section of density, denoted by the curved lines, in a stably stratified fluid. The horizontal lines represent the mean level of the density surfaces, averaged over the domain. Vertical arrows denote the restoring force due to the departure of the density from the domain averaged value

The downward directed force that exists on any air parcel, of unit mass, by virtue of the undulations in the isentropes is given by

$$F = \frac{\rho''}{\overline{\rho}} g \cong \frac{-T''}{\overline{T}} g \cong \frac{g(\Gamma_d \pm \Gamma)}{\overline{T}} z'' \tag{1.2}$$

where z'' is the vertical displacement of the air parcel from the mean level of its isentrope. (For a more thorough derivation, see Wallace and Hobbs, Problem 2.12, p. 82). The work done by gravity (or the potential energy released) in allowing this parcel to move down (or up) to the mean level of its isentrope is given by

$$W = \pm \int_{z''}^{0} F\, dz = \frac{g(\Gamma_d \pm \Gamma)}{\overline{T}} \int_{0}^{z''} z\, dz = \frac{g(\Gamma_d \pm \Gamma)}{\overline{T}} \frac{z''^2}{2} \tag{1.3}$$

where we have assumed that the undulations are small enough so that T and $(\Gamma_d - \Gamma)$ can be taken outside the integral sign. Since $z'' = T''/(\Gamma_d - \Gamma)$, we can write

$$W = \frac{g}{2\bar{T}} \frac{T''^2}{(\Gamma_d - \Gamma)} \tag{1.4}$$

To obtain an expression for available potential energy, we simply integrate *W* over the entire mass of the atmosphere and divide it by the area of the earth's surface. These operations are equivalent to integrating (1.4) over pressure divided by *g*, and averaging it over the area of the earth: hence

$$\bar{A} = \frac{1}{2} \int_0^{p_0} \frac{1}{\bar{T}} \frac{\overline{T''^2}}{(\Gamma_d - \bar{\Gamma})} \, dp \tag{1.5}$$

where p_O is the globally averaged value of pressure at the earth's surface, and $\bar{T}$ and $\bar{\Gamma}$, the environmental temperature and lapse rate now refer to globally averaged values at pressure level *p*.

In the above derivation we have made three kinds of approximations:

(1) We have done some linearizing in getting to equations. (1.2) and (1.3). This approximation is based on the assumption that the isentropes in the earth's atmosphere are relatively flat.

(2) In the final step we have treated the lapse-rate Γ as if it were a function of pressure only. Strictly speaking, we should have written:

$$\bar{A} = \frac{1}{2} \int_0^{p_0} \frac{1}{\bar{T}} \overline{\frac{T''^2}{(\Gamma_d - \Gamma)}} \, dp \tag{1.6}$$

In effect, the approximation in (1.5) amounts to a further linearization. Since T''^2 is everywhere positive and $(\Gamma_d - \Gamma)$ is always positive and does not vary widely in the horizontal (except within a thin layer near the tropopause) this approximation should be acceptable, provided that one doesn't choose to worry too much about the PBL, where the expression locally "blows up"in neutrally stratified regions.

(3) By terminating our vertical integration at the pressure surface p_O rather than at a potential temperature surface, we have, for the sake of convenience, chosen to ignore the fact that isentropes intersect the earth's surface both because of topography and, more importantly, because of the substantial horizontal temperature gradients at the earth's surface. This complication is dealt with more explicitly in Lorenz's derivation.

(4) Available potential energy, as defined in (1.5) would vanish if all the isentropes coincided

with surfaces of constant pressure. If the pressure surfaces were not flat, such an atmosphere could still contain a reservoir of energy that could be converted into kinetic energy through horizontal motions across the isobars. Available potential energy of the kind defined by Lorenz could exist by virtue of the horizontal density gradients in the fluid associated with "internal waves". Not included in Lorenz's formulation is the potential energy associated with "external waves" which involve undulations in the free surface.

Following Lorenz, if we assume that T'' is the earth's atmosphere is on the order of 15K, $\bar{T}$ is about 250 K and $\bar{\Gamma}$ ~ 2/3 Γ_d ~ 6.5K km^{-1}, then $\bar{A}$ is given by

$$\frac{1}{2}\times\frac{15^2\mathrm{K}^2}{250\mathrm{K}\times 3.5\mathrm{K\,km^{-1}}}\times 10^3\mathrm{m\,km^{-1}}\times 10^5\mathrm{N\,m^{-2}} = 10^7\mathrm{J\,m^{-2}}$$

It is of interest to compare this figure with the average kinetic energy per unit vertical column of the atmosphere based on an r.m.s. velocity of 15 m s^{-1}:

$$\frac{1}{2}\times\left[15^2\mathrm{m^2s^{-2}}\right]\times\left[\frac{10^5\mathrm{N\,m^{-2}}}{9.8\mathrm{m\,s^{-2}}}\right]\approx 10^6\mathrm{J\,m^{-2}}$$

Hence the existing reservoir of available potential energy is about an order of magnitude larger than typical values of the global kinetic energy.

It is important to note that $\bar{A}$ is by nature a globally integrated quantity that can't be separated neatly into the contributions that come from various geographical regions (e.g., tropics vs. extratropics) as kinetic energy can be. For example, suppose that the temperature on a certain pressure level is a uniform value T_1 in the tropical half of the atmosphere and another uniform value T_2 in the extratropics. Then the variance of temperature about the global mean $(T_1 + T_2) / 2$ is $(T_1 - T_2)^2 / 4$. However the variance of the temperature within these two uniform regions about their respective means T_1 and T_2 is identically equal to zero. In other words, the variance of the whole is greater than the sum of the variances of the parts. It follows that A has a unique and unambiguous definition only if it is based on a global domain (or a hemispheric domain, where one makes the assumption of equatorial symmetry).

It is possible to partition $\bar{A}$ into the contributions from various layers or from various harmonic components. For example, one may speak of the available potential energy of zonal wavenumber 1 in the 100-10 mb layer. We will also have occasion to speak of the zonal symmetry and "eddy" components of the available potential energy. In certain situations, one

may also speak of the available potential energy associated with some particular dynamical entity which is confined to a limited region of the atmosphere (e.g., African waves, the quasi-biennial oscillation, a hurricane).

Because of the constraint of thermal wind equilibrium, the only way that all the available potential energy inherent in the mass distribution can be realized is to generate disturbances that are purely barotropic. Since atmospheric disturbances always have some degree of baroclinity, it follows that $\bar{A}$ never really approaches the theoretical limit of zero; that is to say, not all the available potential energy is really available.

Questions:

1.7 Show that the sum of the potential plus internal energy of a unit column of the atmosphere is given by $P + I = \frac{c_p}{g}\int_0^{p_0} T\,dp$.

1.8 Are the assumptions which underlie the definition of available potential energy more valid in the troposphere or in the stratosphere?

1.9 How does the ratio of $\bar{K}/\bar{A}$ differ between troposphere and stratosphere? How does it vary with the horizontal and vertical scales of atmospheric disturbances?

1.10 Can you think of any large-scale atmospheric phenomenon for which *K>>A?*

1.11 Suppose that the observed rate of kinetic energy dissipation in the earth's atmosphere is 10^5 J m^2 d^{-1}. On the basis of the estimates of $\bar{K}$ and $\bar{A}$ given in this section, estimate the characteristic decay time of atmospheric motions if sources of *K* were turned off. (Assume an exponential decay with a constant ratio of $\bar{K}/\bar{A}$.)

1.12 Define the available potential energy of a stratified Boussinesq fluid enclosed within a container with a flat bottom, vertical walls, and no top. Be sure to take the free surface into account. Assume that fluid parcels conserve density.

1.13 Derive an expression for the true available potential energy of a purely barotropic atmosphere.

1.4 The Budget of Available Potential Energy

It is evident from (1.5) that available potential energy can be changed by any process that is capable of changing:

(a) the variance of temperature on pressure surfaces;

(b) the mean static stability of the atmosphere;

(c) the mean temperature of the atmosphere.

We regard (c) as unimportant for the purposes of this discussion. The observed distribution of diabatic heating in the earth's atmosphere tends to increase the variance of temperature on pressure surfaces, since in the long term mean diabatic heating is acting to increase the equator to pole temperature gradient, particularly in the winter hemisphere. Diabatic heating also tends to destabilize the atmosphere by heating it from below (by sensible heat flux from the earth's surface and latent heat release) and cooling at upper tropospheric levels (by infrared emission to space). Hence the observed distribution of diabatic heating functions as a source of available potential energy.

In a similar manner, atmospheric motions draw on the reservoir of available potential energy in two different ways when warm (light) air rises and cold (dense) air sinks:

(a) horizontal temperature contrasts, which determine the variance of temperature on pressure surfaces, tend to be reduced as the rising warm air undergoes adiabatic cooling as it expands while the sinking cold air undergoes adiabatic warming as it is compressed.

(b) the upward transport of heat by these same vertical motions increases the static stability.

Hence, if we are interested in doing a really comprehensive diagnosis of the budget of available potential energy, we have to consider changes in variance $\overline{T''^2}$ and in static stability ($\overline{\Gamma}-\Gamma_d$). There have been a number of such studies by Dutton and Johnson (1967) and collaborators over the years, based on isentropic analysis techniques.

In most general circulation studies a further simplification is employed: the static stability is treated as if it doesn't vary with time; processes which contribute to time variations of static stability are assumed to be in a state of balance, so that there is no need to be concerned about them. With this simplification, the task of keeping track of the budget of available potential energy is essentially reduced to the task of accounting for changes in the variance of temperature on pressure surfaces. When we consider the general circulation from a global perspective this simplification is justifiable because globally averaged static stability does change very little with time.

The nature of this simplification can perhaps be made a little clearer by the use of an analogue from the realm of economics. Let us think of available potential energy as the analogue of the wealth in the federal treasury and kinetic energy as the analogue of the material goods that could be purchased with that wealth. The wealth in the treasury is equal to the

amount of currency in the treasury (the analogue of $\overline{T''^2}$) divided by the amount of currency required to buy material goods, or the "cost of living index" (the analogue of static stability). If the federal treasury were to rapidly accumulate or dispose of large amounts of currency the value of that currency might be affected and with it, the national wealth. For example, a wild spending spree would not only decrease the amount of currency remaining in the federal coffers, but it would also deflate the value of that currency by inflating the "cost of living index". [Likewise, a large uncompensated conversion from $A \rightarrow K$ would reduce $\overline{T''^2}$ and it would also deflate $(\Gamma_d - \bar{\Gamma})$.] So long as the value of the currency is stable, it is sufficient for budgeting purposes to keep track only of the amount of currency held in reserve. Fortunately, the static stability of the earth's atmosphere does not appear to be subject to "inflation", or large short-term fluctuations, and thus, we are justified in regarding $\overline{T''^2}$ as if it alone is a true measure of $\bar{A}$.

In recognition of this simplification let us rewrite the expression for available potential energy in the form

(1.7)

where

(1.8)

Note that *s* is a function of pressure only.

Questions:

1.14 Contrast large scale motions in a stably stratified atmosphere versus convection with respect to the way in which they draw upon the reservoir of available potential energy, as defined in (1.7).

1.15 Is the assumption made in this section more easily justified for the troposphere or for the stratosphere? Is it more easily justified for a global study or for the study of an individual storm?

1.5 Generation and Release of Available Potential Energy

Consider the First Law of Thermodynamics written in the form

$$\frac{\partial T}{\partial t} = -\vec{V} \cdot \nabla T + s\omega + Q \tag{1.9}$$

where we make the approximation that $s = s(p)$ only. If we average (1.9) over the entire earth's surface on a given pressure level, we obtain

$$\frac{\partial \overline{T}}{\partial t} = \overline{Q} \tag{1.10}$$

Horizontal advection can move the isotherms around on a pressure surface, but it can't act to systematically raise or lower the mean temperature of the layer. Furthermore, it is clear that $\overline{\omega} = 0$ on any pressure level, since there are no appreciable sources or sinks of atmospheric mass. (Here we ignore the small, systematic upward mass flux of water vapor.) Subtracting (1.10) from (1.9) we obtain

$$T'' \frac{\partial T''}{\partial t} = -T'' \vec{V} \cdot \nabla T + s\omega T'' + Q'' T''$$

Finally, we average over the surface of the earth to obtain

$$\frac{1}{2} \frac{\overline{\partial T''^2}}{\partial t} = s\overline{\omega T} + \overline{Q'' T''} \tag{1.11}$$

where we have thrown out the horizontal advection term because horizontal advection can only distort the shapes of the isotherms; it can't change the area enclosed by any isotherm, and therefore it can in no way change the variance or any of the higher moments of temperature. We have also made use of the fact that $\overline{\omega T''} = \overline{\omega T}$, since the continuity of mass requires that $\overline{\omega} = 0$ on pressure surfaces. The first term on the right hand side is associated with the conversion from available potential energy to kinetic energy. On average in the earth's atmosphere warm air rises and cold air sinks, so there is a negative correlation between ω and T on pressure surfaces, and since $\overline{\omega} = 0$, this effect contributes to a decrease in the variance of temperature; that is, a release of available potential energy. The reservoir of available potential energy is maintained by the diabatic heating term $\overline{Q'' T''}$, which involves the spatial correlation between diabatic heating and temperature. At tropospheric levels Q and T tend to be positively correlated since on average, the tropical atmosphere receives more heat than it radiates to space and the polar atmosphere radiates more away than it receives. [For a further discussion, see Wallace and Hobbs (1977), §9.9.] There is an additional positive correlation between Q and T, even at a given latitude, because of the tendency for precipitation and latent heat release to occur preferentially in rising warm air masses; the most spectacular example is the case of hurricanes,

but from a global perspective the positive correlation between Q and T due to latent heat release in monsoons is far more significant.

There are limited regions in the atmosphere in which Q and T are negatively correlated so that diabatic heating is acting to destroy the existing temperature gradients. For example desert regions undergo strong radiative cooling in comparison to their surroundings, as reflected in the net radiation at the top of the atmosphere. The equatorial tropopause is far below its radiative equilibrium temperature, while in middle latitudes temperatures at these levels are above radiative equilibrium. Hence in the lower stratosphere, diabatic heating functions as a sink of available potential energy. The same is true of the mesopause level, where the summer pole is cold and the winter pole is warm. From a thermodynamic point of view, these localized regions of the atmosphere function as refrigerators rather than heat engines, with temperature gradients being maintained by an influx of mechanical energy (work) supplied by other regions of the atmosphere.

Combining (1.7) and (1.11) we can express the conversion from available potential energy to kinetic energy in the form

$$\frac{\partial \overline{A}}{\partial t} = -C + G \tag{1.12}$$

where

$$C = -\frac{R}{g}\int_0^{p_0} \overline{\omega T} d\ln p \tag{1.13}$$

We have introduced a minus sign so that the conversion $A \rightarrow K$, which corresponds to the usual situation in the earth's atmosphere, will correspond to a positive value of C. Substituting for T from the equation of state $p\alpha = RT$, we can write

$$C = -\frac{1}{g}\int_0^{p_0} \overline{\omega\alpha}\, dp \tag{1.14}$$

which can be interpreted as the rising of lighter air and the sinking of denser air which results in a net downward flux of mass and a lowering of the center of gravity of the atmosphere. If we substitute from the hydrostatic equation for dp, the conversion can be written

$$C = -\int_0^{\infty} \overline{\omega}\, dz \tag{1.15}$$

which tells us that if $A \rightarrow K$ then in an average over the *volume* of the atmosphere air parcels are undergoing a decrease in pressure.[2] The same is true of the working fluid in any heat engine,.as implied by the clockwise sense of the loop in a plot of pressure versus volume.

Returning to (1.14) we can substitute for α from the hydrostatic equation and integrate by parts so that the conversion takes the form

---

[2] Note that this expression involves the global average of ω on constant height, rather than constant pressure surfaces. On constant height surfaces, $\partial p/\partial t$ must vanish in the global average, but not dp/dt.

$$C = \frac{1}{g}\int_0^{p_0} \overline{\omega \frac{\partial \Phi}{\partial p}} = \frac{1}{g}\int_0^{p_0} \frac{\partial}{\partial p}\overline{\omega\Phi}\, dp - \frac{1}{g}\int_0^{p_0} \overline{\Phi \frac{\partial \omega}{\partial p}} dp \qquad (1.16)$$

The term $\omega\Phi/g$ represents the rate at which work is being done by (on) the part of the atmosphere below the pressure level in question on (by) the part of the atmosphere above that level by vertical motions. It can be viewed as the mechanical stirring of one part of the atmosphere by another part. Note that $\omega\Phi/g$ has units of Force $\times$ Velocity / Area or, alternatively Work / (Area $\times$ Time). If the air parcels on a pressure surface are being pushed up in high pressure regions and down in lows, then $\omega\Phi < 0$ and the layer of air below the pressure surface is doing work on the layer of air above it. The term $g^{-1}\partial/\partial p(\omega\Phi)$ represents the energy exported upward and downward from level p through work done by vertical motions. We will discuss this term further in the next section.

Now it is clear that $\overline{\omega\Phi} = 0$ at the top of the atmosphere, since $\omega \rightarrow 0$ as $p \rightarrow 0$, and the atmosphere cannot be doing mechanical work on empty space. The spatial correlation between ω and Φ does not vanish at the earth's surface or on the 1000 mb level. However, it is true that at the earth's surface tends to be about an order of magnitude smaller than at mid-tropospheric levels. Were it not for the existence of large mountain ranges like the Himalayas and Rockies the work done on the atmosphere by the earth's surface or vice versa would play only a minor role in the atmospheric kinetic energy budget. For the present, let us treat the surface of the earth as if it were flat, so that the lower boundary corresponds to a surface of constant geopotential Φ, and let us also assume that the 1000 mb pressure surface is also rather flat and/or ω is small there so that $\omega\Phi$ is vanishingly small at the bottom boundary. With this assumption

(1.17)

so that

(1.18)

At this point we begin to see the conversion C in the context of atmospheric dynamics (as opposed to thermodynamics). The term $\partial\omega/\partial p$ may be viewed as the vertical stretching of "vortex lines" associated with the absolute vorticity of the horizontal flow. Following air parcels in large-scale motions, the primary source/sink of vorticity is the stretching term

where η is absolute vorticity. Since ∂ /$\partial p = 0$, we can go through an analogous set of

operations so that which we performed in (1.9)-(1.12) to show that

$$\frac{1}{2}\frac{\partial}{\partial t}\overline{\eta''^2} = f\,\overline{\eta\frac{\partial \omega}{\partial p}}$$

that is to say, the variance of absolute vorticity on a pressure surface will be increased if vertical stretching is occurring in regions of high vorticity (i.e., "lows") and vertical squashing is occurring in regions of low vorticity (in highs). In other words, vertical stretching accelerates the circulation around lows and vertical squashing accelerates the circulation around highs, so that if $\Phi\,\partial\omega/\partial p < 0$, the geostrophic flow in the atmosphere will be speeded up.

Next we substitute from the continuity equation to obtain

$$C = \frac{1}{g}\int_0^{p_0} \overline{\Phi \nabla \cdot \vec{V}}\, dp \tag{1.19}$$

Energy is being converted from *A* to *K* if Φ and $\nabla \cdot \vec{V}$ are positively correlated on pressure surfaces so that air diverges out of highs and converges into lows (as is observed, for example, in the planetary boundary layer). It is impossible to draw a realistic picture of air diverging out of highs and converging into lows in the horizontal without having air flowing across the isobars from higher toward lower pressure. We can express *C* explicitly in terms of the cross isobar flow by integrating (1.19) by parts to obtain

(1.20)

The term is the horizontal counterpart of the $\omega\Phi$ term discussed above. It too is a work term involving the horizontal flux of geopotential or, in (x,y,z) coordinates, it involves Pressure Velocity or (Force/Area) Velocity. It represents the horizontal flux of energy across a vertical "wall", such as a latitude circle, by mechanical stirring. Now since the atmosphere has no horizontal boundaries there is no external region for it do work on. Formally, from the divergence theorem

where *dS* is an element of surface area and the horizontal integration is carried out over the entire surface of the earth, *s* is an element of arc length around the perimeter of *S*, and V_n represents the component of the horizontal velocity directed outward through this perimeter. For an integration over the entire earth's surface there is no perimeter and so the integral vanishes. Hence, (1.20) reduces to

(1.21)

and the conversion can be expressed in terms of the cross-isobar flow from higher toward lower pressure.

It is possible to derive (1.21) directly from the horizontal equation of motion, expressed in

pressure coordinates:

$$\frac{d\vec{V}}{dt} = -\nabla\Phi - f\vec{k} \times \vec{V} + \vec{F} \tag{1.22}$$

where $\vec{F}$ is the frictional force per unit mass. Taking the dot product with $\vec{V}$, averaging over the area of the earth's surface and integrating over the vertical coordinate *p/g*, we obtain

$$\frac{\partial}{\partial t}\frac{1}{2g}\int_0^{p_0}\overline{\vec{V}\cdot\vec{V}}\,dp = -\frac{1}{g}\int_0^{p_0}\overline{\vec{V}\cdot\nabla\Phi}\,dp + \frac{1}{g}\int_0^{p_0}\overline{\vec{F}\cdot\vec{V}}\,dp \tag{1.23}$$

which can be expressed symbolically as

$$\frac{\partial\bar{K}}{\partial t} = C - D \tag{1.24}$$

where *D*, the frictional dissipation term is always positive as defined here, since and $\vec{V}$ tend to be in the opposite direction. Equation (1.12) can also be expressed in symbolic form

$$\frac{\partial\bar{A}}{\partial t} = -C + G$$

If the existing reservoirs of $\bar{A}$ and $\bar{K}$ are maintained over long periods of time, then *C*, *G* and *D* must all be equal to one another. We can express this equality in terms of the following "flow chart" of the kinetic energy cycle, which is really just an elaboration of Fig. 1.2.

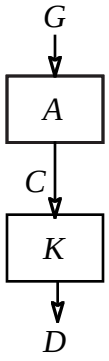

Fig. 1.6 Schematic illustration of the kinetic energy cycle.

Thermally direct circulations are those in which $A \rightarrow K$, so that warm, light air is rising, cold, dense air is sinking, and air is flowing across the isobars toward lower pressure; and thermally indirect circulations are those in which the opposite conditions prevail. In the average,

motions in the atmosphere tend to be thermally direct, but there are local exceptions which correspond to those phenomena or regions of the atmosphere which behave as refrigerators. The work required to run these refrigerators is supplied by the $\omega\alpha\Phi$ and or $\vec{V}\Phi$ terms, which will be discussed in more detail in the next section.

Since *G*, *C* and *D* are equal in the long-term mean, it is possible to get a sense of how fast kinetic energy is generated and dissipated in the atmosphere by evaluating *C* in any one of its various forms. A particularly convenient form is (1.21), for which the absolute value of the integrand can be expressed in the form , making use of the geostrophic equation. Since and are of comparable magnitude, the absolute upper limit of this expression is $f V^2 \quad (p_o/g) \sim 10^{-4}\ s^{-1} \quad (15\ m\ s^{-1})^2 \quad (10^5\ Pa\ /9.8\ m\ s^{-2}) \sim 200\ W\ m^{-2)}$, and this limit would be approached only if and were systematically oriented at right angles to one another. Since the cross-isobar flow tends to be smaller than the geostrophic wind by a factor of the Rossby Number (almost an order of magnitude), it follows that *C* cannot be more than 20-30 W m^{-2} and that value would be approached only if the cross-isobar flow were systematically toward lower (or higher) pressure. Within the planetary boundary layer, the cross-isobar flow tends to be systematically directed toward lower pressure, but in the free atmosphere there is a good deal of compensation between up- and down-gradient flow. Hence, *C* is not likely to be more than a few watts per square meter. Estimates by Oort (1964) and many others since then place it in the range of 2-3 W m^{-2}, which amounts to ~1% of the.solar radiation incident on the top of the atmosphere reduced by the fraction reflected directly back to space. Hence, the thermal efficiency of the atmospheric heat engine is on the order of 1%. This low figure indicates that the effective temperatures of the the atmospheric heat source and heat sink cannot differ by more than a few degrees (e.g., see Wallace and Hobbs, §2.8.1).

Questions:

1.16 If *C* as defined in (1.14) tends to be positive in the earth's atmosphere, why doesn't the center of gravity drop?

1.17 Why is it that $\overline{\omega} = 0$ on pressure surfaces and not $\overline{\omega\alpha} = 0$? Hint: Remember the definition of ω and think of a pressure surface as a material surface.

1.18 If *C* as defined in (1.15) tends to be positive in the earth's atmosphere, what keeps the pressure of air parcels from continually dropping?

1.19 How would the treatment in this section have to be modified in order to make it applicable to convective scale motions?

1.20 Write an expression for *C* in terms of velocity $\vec{V}$ and the ageostrophic velocity $\vec{V}_a$ in component form.

1.6 The Local Kinetic Energy Cycle

It should be emphasized that the equality between the release of available potential energy, as manifested in the $-\overline{\omega T}$ and $-\overline{\omega\alpha}$ terms, and the generation of kinetic energy, as manifested in the $\overline{\vec{V}\cdot\nabla\Phi}$ term holds only for integrals over the entire mass of the atmosphere. Locally there may be large imbalances between these terms which are compensated by imports or exports of energy through the $\overline{\omega\Phi}$ or terms. For example, most of the release of potential energy in the earth's atmosphere takes place in the middle troposphere where the vertical motions are largest, whereas most of the kinetic energy generation occurs in the planetary boundary layer and in the vicinity of the jetstream level, where the strongest frictional dissipation is taking place. The middle troposphere is continually doing work on the upper and lower troposphere, through the $\overline{\omega\Phi}$ term to complete the balance. Let us consider this situation in more detail.

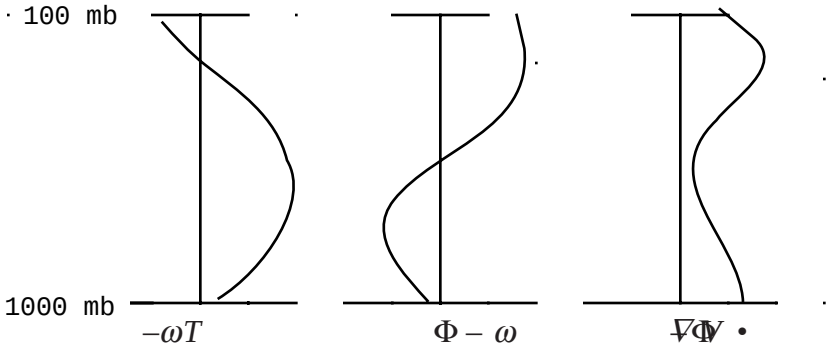

Fig. 1.7 Schematic representation of the vertical profiles of $-\overline{\omega T}$ or – , $-\overline{\omega\Phi}$ and $-\overline{\vec{V}\cdot\nabla\Phi}$.

Combining (1.13), (1.14), (1.16), (1.18), (1.19), and (1.20) it is (more easily than it sounds) shown that

$$-\overline{\omega\alpha} = \frac{\partial}{\partial p}\overline{\omega\Phi} - \overline{\vec{V}\cdot\nabla\Phi} \qquad (1.26)$$

Hence, all the available potential energy released at a particular level can be accounted for either in terms of export, through the work term, or generation of kinetic energy at that same level. Fig. 1.7 shows idealized vertical profiles of the three terms in (1.26) in the earth's atmosphere. We know that – < 0 at the top of the planetary boundary layer for the following reasons:

(1) high pressure regions at the earth's surface tend to be clear and dry and low cloudy with precipitation

(2) cross-isobar flow toward lower pressure associated with frictional veering within the

boundary layer implies a downward mass flux in the highs and an upward mass flux in the lows at the top of that layer.

In contrast to conditions at the earth's surface, at upper troposphere levels, regions of ascent and enhanced precipitation tend to correspond to upper air ridges (e.g., see Wallace and Hobbs, Fig. 5.38, p. 262) which is consistent with a reversal in the sign of $\overline{\omega\Phi}$ between upper and lower troposphere. The shape of the $-\overline{\vec{V}\cdot\nabla\Phi}$ profile is indicated both by direct measurements of Kung (1966) and many others, and by our knowledge of the vertical distribution of kinetic energy dissipation in turbulence in the boundary layer and in the free atmosphere. The $-\overline{\omega\alpha}$ and profiles are also well established on the basis of observations. There are some minor differences between tropics and mid-latitudes, but the shapes of all the profiles are qualitatively similar to those shown in Fig. 1.2.

It is also evident from Fig. 1.7 that the troposphere does work on the stratosphere through the $\overline{\omega\Phi}$ term. As noted above, the lower stratosphere is one of those passive regions of the earth's atmosphere, whose motions are driven by an influx of energy from elsewhere. This influx of energy is mainly accomplished through the "mechanical stirring" brought about by the term. There also exist situations in which the mechanical stirring is provided by the term. For example, some of the transient disturbances in the tropics are driven by an influx of energy from higher latitudes as manifested in the observed negative correlation between v and Φ in the subtropical upper troposphere (Mak, 1969). Evidently, some of the available potential energy released in middle latitudes is being used to generate kinetic energy in the tropics.

A full treatment of the kinetic energy cycle for localized regions of the atmosphere requires consideration of additional terms involving boundary fluxes of kinetic energy and available potential energy. In this discussion we have considered only the leading terms. A comprehensive formulation has been developed by Muench (1964) for studying the kinetic energy cycle in the stratosphere.

Questions:

1.21 Consider the hypothetical situation in which the flow in the free atmosphere above the PBL is purely barotropic so that all the work done on the PBL by the – term is at the expense of the kinetic energy of the free atmosphere. Complete the sketch of the pressure perturbations and the cross-isobar flow in an idealized vertical cross-section (i.e., fill in the cross-isobar flow (the horizontal arrows) in the free atmosphere, assuming that the vertical motion and the cross-isobar flow satisfy continuity in the plane of the section and the vertical integrated cross-isobat flow is equal to zero.

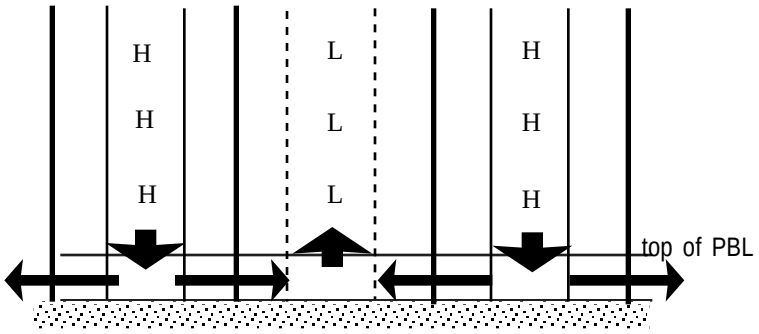

Make an analogous sketch for the contrasting situation in which the kinetic energy generated in the PBL is all at the expense of the available potential energy of the free atmosphere? [Hint: imagine a two-layer free atmosphere consisting of a baroclinic lower layer and an upper layer with no horizontal pressure gradients. Assume that all the cross-isobar flow required to satisfy continuity is concentrated in the upper layer.]

1.22 Describe the latitudinal profile of [$\Phi^* v^*$] in relation to the "storm track" or monsoon disturbances centered at latitude ϕ_0.

1.23 What other boundary term besides the work term $\overline{\omega\Phi}$ enters into the kinetic energy budget for the stratosphere? (Hint: start with (1.22) with the time rate of change term expressed as a local derivative and repeat the operations that led to (1.23), except perform the vertical integration only down to a pressure level which corresponds to the base of the stratosphere.

1.7 Subdivision of the Kinetic Energy Cycle

The Lorenz (1955) paper is notable not only for its useful definition of available potential energy, but also for its subdivision of the kinetic energy cycle in terms of zonally averaged and eddy components as illustrated in Fig. 1.8.

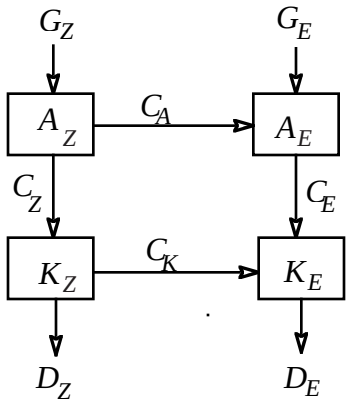

Fig. 1.8 The kinetic energy cycle, as formulated by Lorenz (1955).

Here the zonal kinetic energy, K_z is the kinetic energy of the zonal wind component, $[u]^2 / 2$; and eddy kinetic energy, K_E is $(u^{*2} + v^{*2})/2$. The kinetic energy associated with mean meridional motions $[v]^2/2$ is neglected for reasons that will become more clear in subsequent chapters.

In order to partition A into zonal and eddy parts, A_z and A_E, we expand the temperature into global mean, the zonally averaged departure from the global mean and the eddy part $T = \bar{T} + [T]'' + T^*$, from which it is easily shown that

$$\overline{T''^2} = \overline{[T]''^2} + \overline{T^{*2}} \tag{1.27}$$

The various quadratic terms associated with C (i.e., $\overline{\omega T}$, $\overline{\omega\alpha}$, $\overline{\vec{V} \cdot \nabla\Phi}$, etc.) can be partitioned into C_Z and C_E in a similar manner, where the zonal component

$$C_Z = -\frac{1}{g}\int_0^{p_0} \overline{[\omega][\alpha]}\, dp = -\frac{1}{g}\int_0^{p_0} \overline{[v]\frac{\partial[\Phi]}{\partial y}}\, dp \tag{1.28}$$

is associated entirely with mean meridional motions because the zonally averaged zonal flow $[u]$ is, by definition, nondivergent and parallel to the zonally averaged geopotential height contours. Hence the mean meridional motions play a crucial role in the kinetic cycle even though they account for only a minute fraction of the kinetic energy reservoir. These simple two-dimensional circulations provide a convenient illustration of the energy conversion process:

The Hadley circulation is obviously thermally direct, with C >0. It is characterized by the rising of warm, light air in equatorial latitudes and the sinking of colder, denser air in subtropical latitudes ($-\overline{\omega\alpha}$ >0); low level equatorward flow out of the subtropical high pressure belt into a belt of low pressure along the equator (> 0); and upper tropospheric flow out of the equatorial belt and into subtropical latitudes in the presence of a westerly flow in which $[\Phi]$ decreases with latitude (again > 0). Note the resemblance of the Hadley cell to the circulation cell in Fig. 9.4a of Wallace and Hobbs, p. 418.

The middle latitude "Ferrel cell" which extends between approximately 30° and 60° latitude is, in many respects, a mirror image of the Hadley cell. Relatively warm, light air sinks in the subtropics while colder, denser air rises at higher latitudes. The cross-isobar flow is poleward, toward lower pressure at low levels, and equatorward, toward higher pressure at high levels. However, since $[u]$ increases with height at these latitudes, (i.e., $-\partial[\Phi]/\partial y$ is larger aloft) it is clear that the up-gradient flow in the upper troposphere must dominate in the average over the cell. Hence the Ferrel cell is thermally indirect with $C < 0$. Observations indicate that the conversions in the Ferrel and Hadley cells nearly cancel one another, so that in the global average the numerical value of C_Z is, in effect, a small difference between two large numbers, each of which has some uncertainty associated with it. Hence, even the sign of C_Z is uncertain in a global average.

Returning to Fig. 1.8 we note that C_E represents the eddy part of the conversion $-\overline{\omega^* \alpha^*}$ or $-\overline{\vec{V}^* \cdot \nabla \Phi^*}$, where it is readily verified that

$$\overline{\omega\alpha} = [\overline{\omega}][\overline{\alpha}] + \overline{\omega^* \alpha^*} \tag{1.29}$$

and

$$\overline{\vec{V} \cdot \nabla \Phi} = [v]\frac{\overline{\partial[\Phi]}}{\partial y} + \overline{u^* \frac{\partial \Phi^*}{\partial x}} + \overline{v^* \frac{\partial \Phi^*}{\partial y}} \tag{1.30}$$

The eddy conversion is associated with phenomena such as monsoons and baroclinic waves which are characterized by strong deviations from zonal symmetry with large and systematically interrelated fluctuations in $T^*, \alpha^*, \omega^*, u^*, v^*$, and Φ^*. We will discuss these phenomena further in Chapter 5.

The conversions C_A and C_K involve the advection of temperature and momentum, respectively. For example, if horizontal temperature advection is tending to distort the isotherms from a zonally symmetric configuration into a more perturbed one, with larger values of T^*, then $A_Z \rightarrow A_E$. In a similar manner, if the horizontal advection of zonal momentum is tending to smooth out a zonally averaged jet, then $K_Z \rightarrow K_E$. We will consider these processes in further detail in Chapter 5.

The generation term $\overline{Q''T''}$ in (1.12) can be partitioned in a manner entirely analogous to (1.29) and dissipation can be classified as D_Z or D_E. It is evident that G constitutes a major input of energy into the kinetic energy cycle because of the large equator to pole heating gradient in the troposphere. Latent heat release in the troposphere makes strong positive contributions to both G_Z and G_E while Newtonian cooling at stratospheric levels represents a sink of eddy available potential energy ($G < 0$). It is possible to imagine an idealized steady state atmosphere, not drastically unlike our own, in which all the input of energy into the kinetic energy cycle is through G_Z and energy flows from the A_Z reservoir to the other reservoirs and is destroyed mainly by frictional dissipation D_Z and D_E.

In Lorenz's formulation, the zonal mean and eddy fields are spatially orthogonal so that spatial variance and covariance quantities such as $u, v, T, \omega T, \overline{Q''T''}, -\overline{\vec{V} \cdot \nabla \Phi}$, etc. can be partitioned as in (1.27), (1.29) and (1.30). A similar partitioning can be carried out among any set of spatially orthogonal fields. For example, the eddy energies and conversion processes in Fig. 1.8 can be expanded in terms of zonal wavenumber components so that A is partitioned into $A_1, A_2, A_3 \ldots A_k$, where k refers to zonal wavenumber, and similarly for G, C, and D, as illustrated in Fig. 1.9.

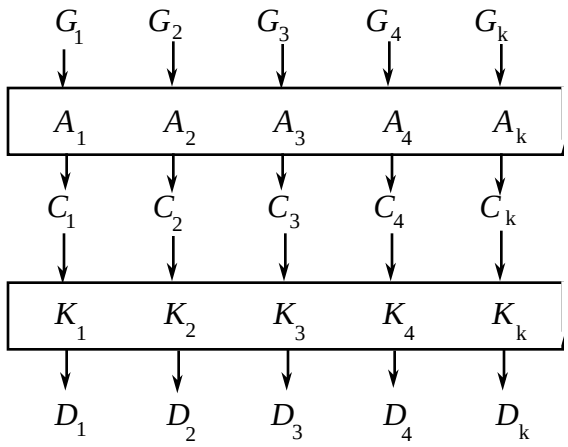

Fig. 1.9 The kinetic energy cycle, subdivided in terms of zonal wavenumbers.

A and *K* are exchanged among the various harmonic components by means of advective processes similar to those described above. The nonlinear wave-wave interactions as well as the interactions between each wave component can be expressed in terms of formulae involving the coefficients of the various harmonics (Saltzman, 1970) and different components in the wavenumber-frequency domain (Kao, 1968; Kao and Chi, 1978). With these formulations it is possible to gain some insight into the contributions of various dynamical entities to *G* and *C*. For example, the processes associated with the monsoon circulations are represented, for the most part, by k = 1-3, whereas baroclinic waves fall largely within the range k = 6-10. Because of the large number of possible interactions between the various wave components, the job of keeping track of the kinetic energy cycle depicted in Fig. 1.9 is rather complex and tedious. A considerable reduction in complexity can be realized if the waves are grouped into a few categories such as planetary waves (k = 1-3), long waves (k = 4-5), synoptic scale waves (k = 6-15) etc.

Relationships analogous to (1.27), (1.29) and (1.30) can also be derived by components of the general circulation which are orthogonal in the time domain. The simplest subdivision of this type would be a partitioning between time mean components, A_M , K_M , C_M , etc. and time varying or transient components A_T , K_T, C_T , etc. Such a breakdown would allow one to distinguish between geographically fixed phenomena such as the monsoons and the wintertime standing waves in the Northern Hemisphere, versus propagating disturbances such as baroclinic waves and transient planetary waves. Temporal subdivision can be extended in a manner analogous to Fig. 1.9 by means of power spectrum analysis in the time domain. Mixed space/time subdivisions are possible and spherical harmonics or other spatially orthogonal

functions can be used in place of zonal harmonics. It is also possible to subdivide motion systems in terms of vertical structure (e.g., barotropic vs. baroclinic systems). Hence there are numerous possible variants of Lorenz's formulation. In practice, it seems to have worked out that the number of valuable new insights derived from such studies is inversely proportional to the number of subdivisions. The most successful studies have tended to be those in which dynamical considerations have motivated the choice of subdivisions.

Questions:

1.24 Prove that $A_M + A_T = A$, $C_M + C_T = C$, etc., where M refers to time mean and T to transient.

1.8 Steady state vs. time dependent formulations

Lorenz's formulation of the kinetic energy cycle has been used to study the maintenance of the general circulation over long periods of time like a season, in which case it is assumed that the amounts of energy in the various reservoirs are not changing with time so that, for example, in the case of Fig. 1.8 we can write the balance equations

$$\begin{aligned} G_Z - C_Z - C_A &= 0 \\ G_E - C_E + C_A &= 0 \end{aligned} \qquad (1.31)$$

for the zonal and eddy available potential energy reservoirs and

$$\begin{aligned} C_Z - C_K - D_Z &= 0 \\ C_E + C_K - D_E &= 0 \end{aligned} \qquad (1.32)$$

for the zonal and eddy kinetic energy reservoirs. Note that (1.31) and (1.32) correspond, respectively, to forms of (1.24) and (1.25). By adding the two equations in (1.31) together one obtains (1.24) and by adding the two equations in (1.32) together one obtains (1.25). With such a steady state formulation one can discern the nature of the kinetic energy cycle from a simple visual inspection of flow charts such as Figs. 1.8 and 1.9 with numerical values printed on them.

For time scales shorter than a month or so, the time rate of change terms in (1.12) and (1.23) are not necessarily small in comparison to the generation, conversion and dissipation terms and hence the zeroes on the right-hand sides of (1.31) and (1.32) have to be replaced by time rates of change of A_Z , A_E , K_Z and K_E , respectively. Similar time dependent balance equations can be written for the subdivision in terms of zonal harmonics.

The time dependent formulation has proven useful for studies of sudden stratospheric

warmings and form vacillation cycles in the troposphere, both of which are hemispheric in extent and have characteristic time scales on the order of a week or two. It has also been used to diagnose the energetics of the growth of baroclinic waves in numerical experiments with spectral models. Because of the constraints of thermal wind balance, energy tends to "slosh back and forth" laterally in flow charts such as those in Figs. 1.8 and 1.9 so that, to a first approximation, A and K for each component undergo simultaneous increases and decreases. This constraint is particularly evident at the shorter time scales.

References

Haurwitz, B. 1941: *Dynamic Meteorology*, McGraw-Hill, New York, 365pp.

Dutton, J.A. and D.R. Johnson, 1967: The theory of available potential energy and a variational approach to atmospheric energetics. *Advances in Geophysics,* 12.

Kao, S.K., 1968: Governing equations and spectra for atmospheric motion and transports in wavenumber frequency space. *J. Atmos. Sci.*, **25**, 32-38.

Kao, S.K.and C.N. Chi, 1978: Mechanism for the growth and decay of long- and synoptic-scale waves in the mid-troposphere. *J. Atmos. Sci.*, **35**, 1375-1387.

Kung, E.C.,1966: Large-scale balance of kinetic energy in the atmosphere. *Mon. Wea. Rev.*, **94**, 627-640.

Lorenz, E.N., 1955: Available potential energy and the maintenance of the general circulation. *Tellus,* **7**, 157-167.

Mak, M., 1968: Laterally driven stochastic motions in the tropics. *J. Atmos. Sci.*, **26**, 41-64..

Margules, M., 1903: Über die Energie der Stürme. *Jahrb. Zentralanst. Meteor.*, Vienna, 1-26, English translation: Abbe, C., 1910: *The Mechanics of the Earth's Atmosphere.* 3rd. Coll.. Washington, Smithsontan Inst., 533-595.

Muench, H.S.,1964: *Stratospheric Energy Processes and Associated Long-wave Structure in Winter*. PhD thesis, University of Washington, 129pp.

Oort, A.H., 1964: On estimates of the atmospheric energy cycle. *Mon. Wea. Rev.*, **92**, 483-493.

Saltzman, B., 1970: Large-scale atmospheric energetics in the wavenumber domain. *Rev. Geophys. Space Phys.*, **8**, 289-302.

Wiin Nielsen, A., 1962: On the transformation of kinetic energy between the vertical shear flow and the vertical mean flow in the atmosphere. *Mon. Wea. Rev.*, **90**, 311-323.

2. THE ANGULAR MOMENTUM BALANCE

2.1 Angular momentum conservation for the 'earth system'

The angular momentum per unit mass of an air parcel is given by

$$m \equiv R_E \cos\phi \left[\Omega R_E \cos\phi + u\right] \tag{2.1}$$

where R_E is the radius of the earth (6.37 x 10^6 m), ϕ is the latitude, Ω is the angular rotation rate of the earth (7.29 x 10^{-5} s^{-1}), and u is the zonal wind. By definition, m is positive where the relative angular momentum is in the same sense as the earth's rotation: in regions of westerlies the atmosphere is rotating slightly faster than the solid earth and in regions of easterlies it isn't rotating quite as fast. The first term in (2.1) may be recognized as the angular momentum associated with the earth's rotation and the second as the angular momentum of the air parcel relative to the rotating earth. Since ΩR_E = 465 m s^{-1}, it is evident that the first term is dominant, except at very high latitudes.

For the atmosphere, oceans and solid earth as a single system, total angular momentum is conserved, but for tidal interactions with the moon, which are conspicuous because they are quasi-periodic, and predictable on the basis of theory. The angular momentum of the solid earth can be monitored by taking precise measurements of the length of the day (*l.o.d.*). Rosen and Salstein (1983) have shown that if the angular momentum of the molten core of the earth is assumed to be constant on time-scales of a year or so, changes in length of day and angular momentum of the solid earth obey the linear relation

$$\Delta lod \;=\; -1.68 \text{ x } 10^{-29}\, \Delta M_E$$

where Δlod is expressed in units of seconds and M_E in units of kg m^2 s^{-1}. The mean length of the day has varied by several milliseconds on the decadal time scale over the course of the past century which, according to the above relation, imply gains and losses in angular momentum an order of magnitude larger than the atmosphere could have possibly experienced on these time-scales. These gradual changes are believed to be due to core-mantle coupling (Lambeck, 1980).

Fig. 2.1 shows higher frequency fluctuations in atmospheric angular momentum M and *l.o.d.*, plotted on the same axis. The fluctuating part of M is obtained by integrating the relative component of m in (2.1) over the mass of the atmosphere

$$M = \frac{2\pi R_E^3}{g} \int_0^{p_o} \int_{-\pi/2}^{\pi/2} [u] \cos^2\phi \, d\phi \, dp \tag{2.2}$$

The integral is based on analyses from the the U.S National Meteorological Center (NMC) operational analyses for levels up to 100 mb, and zonal wind data compiled by I.Hirota (Univ. of Kyoto) from analyses prepared by the U.K. Meteorological Office. The time mean has been removed from both time series and the tidal component has been smoothed out of the *l.o.d.*

record. The level of agreement of the two curves is quite remarkable, considering the inaccuracies in the zonal wind data and the neglect of the oceanic angular momentum. The curves exhibit a pronounced seasonal march, with a brief period of low values around August of each year. The unusually high values in 1982-83 were ascribed to the strong warm episode in the ENSO cycle observed that year; similar peaks have been observed during other warm episodes. The higher frequency variability in the record exhibits a spectral peak around a period around 40- 50 days.

Questions

(1) Why are we justified in ignoring time variations in the earth's rotation rate Ω in evaluating M in (2.2)?

(2) Show that for a zonally symmetric ring of air, angular momentum per unit mass and circulation are linearly related.

INSERT Fig. 2.1

Fig. 2.1 Time series of 3-day mean length of day (corrected to remove the tidal component) and atmospheric angular momentum After Salstein and Rosen (1986).

2.2 The climatological mean distribution of zonal wind

Figure 2.2 shows pole-to-pole cross-sections of the climatological mean [$\bar{u}$] based upon the compilation of general circulation statistics compiled by Hoskins et al. (1989), from 11 years of daily operational analyses of the European Centre for Medium-Range Weather Forecasting (ECMWF). Since the vertical coordinate is linearly proportional to pressure equal vertical increments contain equal amounts of mass. In this coordinate system the stratosphere doesn't show up very well. [Note that if we wished to display the data in the format most directly related to the global integral in Equation (2.2) we would have also had to distort the meridional scale so as to stretch the tropics and compress the higher latitudes.] Cross-sections are shown for the two extreme seasons, DJF and JJA.

Note that the prevailing zonal motion is from west to east, which is indicative of a net superrotation relative to the solid earth. The dominant features in the cross-sections are the westerly jetstreams at the tropopause level. The tropospheric jet is stronger and located at lower latitudes in the winter hemisphere. The Northern Hemisphere jet exhibits a much stronger annual cycle, which dominates the annual march of total atmospheric angular momentum in Fig. 2.1. Easterlies are largely restricted to the tropics: only in the subtropical lower troposphere of the summer hemisphere do they exceed 5 m s^{-1}.

Let us consider the distribution of zonal wind at the jetstream level in the Northern winter in more detail. Fig. 2.3 shows isotachs of climatological mean wind speed. In the regions of strong winds it is virtually identical to the distribution of $\bar{u}$, since jetstreams tend to be zonally oriented. Note the strong jet extending from the subtropical Atlantic across the Sahara, the middle East, and the Himalayas to a maximum over Japan, where wind speeds reach 70 m s^{-1}. A second, much weaker jet extends east-northeastward from Baja California to a maximum over Washington DC. These jets occur at the longitudes of the longwave troughs in the climatological mean 250 mb height field, which shown in the right-hand panel. The lower panel shows the eddy component of the climatological mean streamfunction field, $\overline{\psi}^*$. It is similar to the corresponding distribution for the geopotential height field, but it shows more clearly how the patterns extend into the tropics. Note the tendency for north-south oriented dipole patterns straddling 35°N.

Questions

2.1 Why doesn't the stratosphere show up well in Fig.2.2. What function of pressure would be convenient as a vertical coordinate if we wished vertical increments in the figure to correspond to the geometric thickness of the layer, rather than to the mass of air within it?

2.2 If one wished to design a cross section in which equal increments along the horizontal axis correspond to equal areas on the earth's surface, how would you scale the horizontal coordinate? What latitude would lie halfway between equator and pole in the diagram?

2.3 If one wished to design a cross section in which the contribution of an element of area δA in the section to the relative angular momentum of the atmosphere is equal to $[\bar{u}]\delta A$, regardless of its position on the section, how would you scale the axes?. What latitude would lie halfway between equator and pole in the diagram?

Fig. 2.2 Vertical cross section of climatological mean zonally averaged zonal wind and potential temperature: top DJF; bottom JJA. After Hoskins et al. 1989.

Fig. 2.3 Climatological mean wind speed, geopotential height, and eddy component of the streamfunction at the 250 mb level for DJF. After Hoskins et al., 1989.

2.3 Transfer of angular momentum through the atmosphere's lower boundary

The atmosphere exerts a *torque* (i.e., a force acting at a distance $R_E \cos \phi$ from the earth's axis) on the solid earth or ocean beneath it (or vice versa) through two processes: zonal pressure differences across mountain ranges and zonal wind stresses at the earth's surface. These processes are commonly referred to as *mountain torques* and *frictional torques*, respectively.

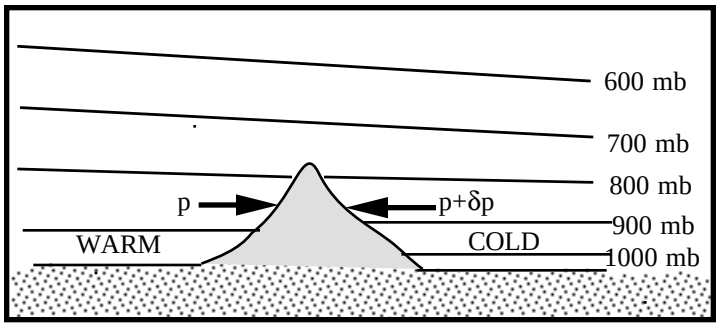

Fig. 2.4 The force exerted by the atmosphere upon a mountain range.

Pressure differences sometimes develop across mountain ranges as a hydrostatic response to temperature contrasts between the air masses on the two sides, as illustrated in Fig. 2.4, or as a dynamical response to strong flow over the mountains. In these situations, the atmosphere exerts a net horizontal force upon the mountain range and vice versa, even in the absence of any atmospheric motions whatsoever. As an example of how such a force can act to transfer angular momentum between the atmosphere and the solid earth, Fig. 2.5 shows composite sea-level pressure distributions for "high and low index" circulation types as defined the strength of $[u_g]$ averaged between 35° and 55°N, after Willett (1944). The high index pattern is characterized by higher pressure to the west of the Rockies and lower pressure to the east. Warm "chinook" winds are often observed along the lee slopes of the Rockies in these situations. The isobars were drawn very smooth on this map, but on more detailed analyses it is evident that much of the east-west pressure gradient is concentrated in along ridges such as the Continental Divide in Montana and Colorado and the Cascades in Washington. It is evident that the atmosphere is exerting an eastward torque on the Rockies, so the solid earth is gaining angular momentum from the atmosphere. In the contrasting low index pattern, pressures are higher over the Great Plains, to the east of the Rockies in association with a pattern typical of major cold outbreaks. In this case the atmosphere is exerting a westward torque on the Rockies, slowing down the rate of rotation of the earth. Hence, the torque on the Rockies cause the atmosphere to lose angular momentum to the solid earth in the high index composite and gain angular momentum from it in the low index composite—which may be viewed as a negative

feedback. In the climatological mean sea-level pressure pattern, shown in Fig. 2.6, the zonal gradient across the Rockies is so weak that its sign is in questionable. The same is true of most of the other mountain ranges in the hemisphere. Hence, it does not appear that the mountain torque term plays a major role in the climatological mean angular momentum balance, though it may be of first order importance (perhaps as a negative feedback) on short time scales.

Fig. 2.5 Composite sea-level pressure patterns for "high and low index" circulation regimes, based upon the zonally averaged sea-level pressure gradient between 35 and 55°N. After Willett (1944).

Fig. 2.6 Climatological mean 1000 mb height or sea-level pressure pattern for DJF and JJA, after Hoskins et al., 1989. Contour interval, 30 m or 4 mb.

The frictional torque at the earth's surface can be inferred from the distrubution of surface wind, shown in Fig. 2.7. It is evident that easterlies prevail over the tropical half of the globe (30°N-30°S) during both seasons. The strongest easterlies are observed in association with the traewinds over the Atlantic and Pacific and over the southern Indian Ocean. Westerlies prevail at higher latitudes (beyond the limits of these maps), as is evident from an examination of the sea-level pressure patterns in the previous figure. They are particularly strong between 40°S and 60°S, the belt that was referred to as "the roaring 40's" in the days of sailing ships.

Fig. 2.7 Climatological mean surface winds for DJF and JJA. After Hoskins et al., (1989)

The atmosphere exerts a frictional torque on the ocean or land below it in the same sense as the surface wind; i.e., it is acting to slow down the rotation of the earth equatorward of 30°, where easterlies prevail, and to increase it at higher latitudes, in the regions of surface westerlies. From the point of view of the atmosphere, the frictional torque is acting as a source of angular momentum at low latitudes and a sink at higher latitudes.

The actual stress is determined from the surface wind using the bulk aerodynamic formula

$$\tau_x = \rho C_D (Vu) \qquad (2.3)$$

where V is the scalar wind speed at the anemometer level and C_D is an empirically determined, dimensionless drag coefficient which is on the order of 1.2 x 10^{-3} over the sea[3] (Smith, 1980; Large and Pond, 1981). Note that for a time average such as a climatological mean involves both mean and transient terms. For example, if we ignore the contribution of the meridional wind component to the wind speed, the scalar value of the stress is given by $\tau_x = \rho C_D\left(\bar{u}^2 + \overline{u^{*2}}\right)$. Note that because of the nonlinearity inherent in these relationships, the stress tends to be concentrated in regions of high surface wind speeds and, (other things being equal) it tends to be larger in regions of large temporal variability such as the northern oceans than over regions such as the trades, where the winds are much more steady from day to day.

Questions

2.4 If were of the same sign at all latitudes, the zonal winds in the atmosphere could not possibly be in a steady state. Explain.

2.5 Prove that on any pressure surface that doesn't intersect the ground the zonally averaged zonal pressure gradient force [ ] is identically equal to zero.

2.6 How does the ocean transmit the large amounts of westward angular momentum that it acquires from the atmosphere in the tropics to the solid earth? [Hint: consider the fact that sea-level tends to be higher on the western side of tropical ocean basins than on the eastern side.]

2.4 Poleward transport of angular momentum within the atmosphere

From the foregoing discussion it is evident that the portion of the atmosphere that lies within 30° of the equator is gaining angular momentum through the frictional drag on the tradewinds, while the part that lies poleward of 30° is losing angular momentum through the frictional drag on the surface westerlies. Since the atmosphere is close to a steady state, it follows that there exists a *balance requirement* for the poleward transport of angular momentum across 30°, as discussed in famous essays on the atmospheric general circulation by Jeffreys (1926) and Starr (1948) and in a related paper on the vorticity balance by Rossby

[3] The drag coefficient increases slightly with wind speed.

(1947). The nature of the balance is illustrated schematically in Fig. 2.8. It can be expressed symbolically in the form

$$-2\pi R_E^3 \int_{eq}^{30^\circ} \left[\overline{\tau_x}\right] \cos^2\phi \, d\phi = \frac{2\pi R_E \cos\phi}{g} \int_{30^\circ} \left[\overline{mv}\right] dp \qquad (2.4)$$

where τ_x is the stress exerted by the atmosphere upon the underlying surface.

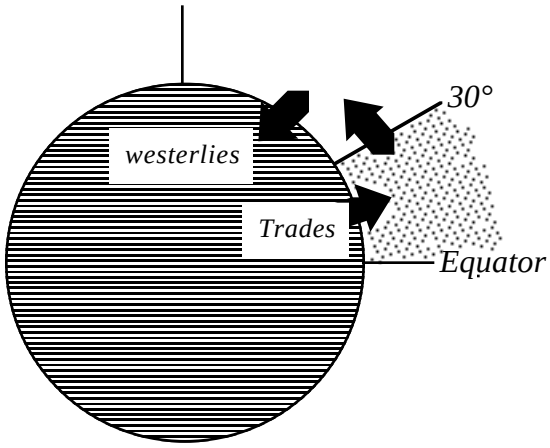

Fig. 2.8 Balance requirement for the poleward transport of angular momentum in the earth's atmosphere.

The poleward transport is given by the integral

$$\frac{2\pi R_E \cos\phi}{g} \iint_\phi \overline{[mv]}\, dp = \frac{2\pi\Omega R_E^3 \cos^3\phi}{g} \iint_\phi \overline{[v]}\, dp + \frac{2\pi R_E^2 \cos^2\phi}{g} \iint_\phi \overline{[uv]}\, dp \qquad (2.5)$$

We envision the integration as being performed over an imaginary wall extending all the way around a latitude circle at latitude ϕ, and from the ground to the "top" of the atmosphere. The overbar refers to time averages over some rather long interval like a season. The first calculations of these integrals were performed by Widger (1949)

The first term on the right-hand side represents the transport of the component of the angular momentum that can be attributed to the earth's rotation. It is proportional to the net poleward flux of mass across the latitude circle: if the atmosphere as a whole, were to draw closer to its axis of rotation, it would rotate faster in the same sense as the earth's rotation (from west to east) just as an ice skater spins more rapidly by drawing in his/her arms. The center of mass of the earth's atmosphere undergoes a small latitudinal shift with the seasons, but it isn't anywhere near large enough to account for the observed seasonal changes in zonal wind speed. When we examine the hydrologic cycle we will see that in the statistical average, water vapor is always being transported poleward through middle latitudes. However it constitutes such a small fraction ($\cong$ 1%) of the atmospheric mass that its contribution to the angular momentum

flux is minimal.[4] Hence we conclude that this term cannot account for the poleward flux of angular momentum in the earth's atmosphere.

The second term involves the component of the angular momentum associated with the zonal motion of air parcels relative to the rotating earth. It can be identified with exchange processes (i.e., the exchange of equal amounts of mass containing differing amounts of relative angular momentum). This term can be rewritten in the form

$$\frac{2\pi R_E^2 \cos^2\phi}{g}\int_0^{p_0}\left[\overline{uv}\right]dp$$

where the term in brackets refers to a zonal average. The integrand $\left[\overline{uv}\right]$ can be evaluated by calculating the product *uv* at each gridpoint and time and averaging around the latitude circle and over time in either order. However, the nature of the dynamical processes responsible for the transport becomes more clearly evident if we expand it in terms of various types of exchange processes as explained in Appendix I.

Particularly illuminating is the expansion

$$\underset{(a)}{\left[\overline{uv}\right]} = \underset{(b)}{[\bar{u}][\bar{v}]} + \underset{(c)}{\left[\bar{u}^*\,\bar{v}^*\right]} + \left[\overline{u'v'}\right] \qquad (2.6)$$

Term (a) is clearly identified with mean meridional motions, since it is proportional to $[\bar{v}]$. Since the net vertically integrated meridional mass flux is very small, we can assume that this term is associated with mean meridional cells, characterized by poleward motion at some levels and equatorial motions at others. The observed distribution of mean meridional cells in the earth's atmosphere is shown in Fig.2.9, superimposed upon the zonal wind field In the winter hemisphere the mean meridional motions are rather strong, but note that there is no exchange of mass across 32°N, which marks the transition zone between the thermally direct "Hadley cell" in the tropics and the thermally indirect "Ferrel cell" which prevails in middle latitudes. Hence it is clear that the mean meridional cell term does not contribute to the required transport of angular momentum from the tropics into middle latitudes during the winter season. In the summer hemosphere, the mean meridional motions are so weak that even the sign of the transport of angular momentum is uncertain.

The mean meridional circulations do produce fluxes of angular momentum across other latitude circles. Throughout most of the troposphere, zonally averaged temperature [*T*] decreases with latitude, and mean zonal wind [*u*] increases with height, as required by the thermal wind equation. Hence the direction transport of westerly (positive) angular momentum is in the same sense as the mean meridional motion in the upper branch of the cell; that is to say,

[4] This term is of first order importance in the Martian atmosphere during the equinoctial seasons, when massive amounts of carbon dioxide are subliming from the polar cap of the spring hemisphere, crossing the equator and precipitating out to form a polar cap in the autumn hemisphere. This large meridional mass flux tends to induce easterlies in the spring hemisphere and westerlies in the autumn hemisphere.

the Hadley cell transports westerly angular momentum poleward and the Ferrel cell transports it equatorward. For example, in the upper branch of the Hadley cell (say, at 15° latitude of the winter hemisphere), $[\bar{u}]$ and $[\bar{v}]$ are both positive and hence $[\bar{u}][\bar{v}]$ is positive there. In the lower branch, $[\bar{v}]$ is negative in the equatorward flow and $[\bar{u}]$ is negative in association with the tradewinds. Hence $[\bar{u}][\bar{v}]$ at low levels does not cancel the large contribution to the vertical integral that comes from upper troposphere levels: on the contrary, it contributes in the same sense, since $[\bar{u}][\bar{v}]>0$.

Fig.2.9 Zonally averaged mean meridional circulations, superimposed upon the corresponding zonal wind fields. See arrow for scale. Easterlies are shaded. Upper panel DJF, lower panel JJA. After Hoskins et al., 1989.

Having eliminated the possibility of the required transport of angular momentum across 30° latitude being accomplished by mean meridional circulations (term (a)) we must conclude that it is accomplished by eddy transports (terms (b) and (c)). Both terms are associated with the meridional tilt of the "eddies" or "waves" in the horizontal plane, as shown in Fig. 2.11. In disturbances that tilt eastward with increasing latitude, poleward moving air is characterized by larger (westerly) angular momentum than equatorward moving air. The exchange of equal masses of air containing differing amounts of angular momentum per unit mass results in a net poleward transport of angular momentum at a given level. Term (b) represents the effect of *standing eddies* or *stationary waves*: longitudinally dependent features of the flow which appear on the time mean maps, while term (c) represents the effect of the *transients*.

Fig. 2.10 Northward transport of westerly momentum by the transients (left panels) and the standing eddies or stationary waves (right panels) for DJF (upper panels) and JJA (lower panels). Contour interval 5 m^2s^{-2}, Regions of southward transport are indicated by stippling.

It is evident from the sections presented in Fig. 2.10 that both terms contribute to the required poleward transport of angular momentum across 30°N. The fluxes are largest precisely where they are needed. Note also the weaker equatorward transports across 65°S, which marks the boundary between the belt of surface westerlies in middle latitudes and a ring of easterlies centered along the Antarctic coast. There is a suggestion of a similar feature in the

Northern Hemisphere during wintertime. In all the sections the fluxes tend to be concentrated near the jet stream level: the lower troposphere contributes very little to the mass weighted transport. In both hemispheres and in both seasons the transients make the dominant contribution to the transport: only in the northern hemisphere during winter do the climatological mean stationary waves make an appreciable contribution. The Northern Hemisphere exhibits a much larger annual cycle in the magnitude of the fluxes.

The magnitude of the eddy transports has been compared against the amount of angular momentum required to balance the frictional torque associated with the middle latitude surface westerlies and, within the range of uncertainty of the estimates (~20-30%) the agreement appears to be satisfactory. For example, the Southern Hemisphere exhibits much stronger summertime westerlies and it also exhibits a much stronger summertime poleward transport of westerly momentum.

Wherever the eddy flux of angular momentum is poleward, the zonal momentum of the poleward flowing air in the eddies must be larger than that of the equatorward flowing air. Regardless of the the direction or meridional shear of the zonal flow upon which the eddies are superimposed, this difference in zonal momentum implies that the axes of the waves or eddies shift eastward as one moves poleward, as pictured in Fig. 2.11. In this example, the individual contours are virtually sinusoidal and they are all identical. Therefore, it is not the shape of the contours but, rather, their eastward shift with latitude that makes the zonal momentum larger in the poleward flow than in the equatorward flow. From a careful inspection of Fig. 2.3 it is evident that at at latitudes around 30°N, the major features in the distribution of the $\overline{\psi}^*$ field in the Northern Hemisphere winter circulation exhibit the required northeast-southwest tilt, consistent with the large poleward standing eddy flux of angular momentum across this latitude in Fig. 2.10.

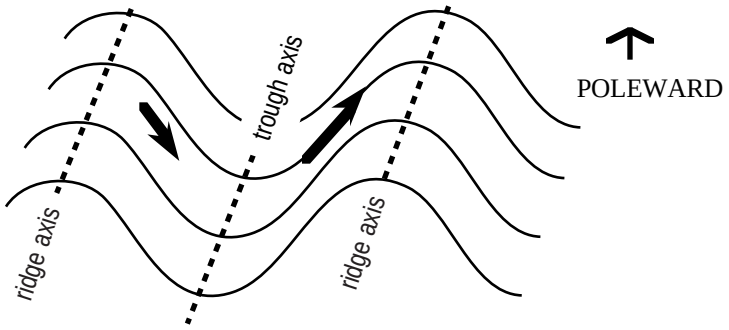

Fig. 2.11 Idealized pattern of streamfunction or geopotential height contours consistent with the poleward momentum fluxes, emphasizing the importance of the latitudinal tilt of the axes of the waves

Questions

2.7 The poleward flux of angular momentum across 30° latitude, as estimated by in a number of different studies, is on the order of 30 x 10^{18} kg m^2s^{-2} (e.g., see Obasi, 1963 and the references therein) Make your own estimate based on the wind stress equatorward of 30° latitude. [Hint: start by assuming representative zonal wind and scalar wind speeds in the tradewind belt.]

2.8 On the basis of the data presented in this section, estimate the poleward transport of angular momentum across 30° latitude. Compare your results with those from Problem 2.7.

2.9 On 30°N at the jetstream level during DJF, $\left[\overline{u^*v^*}\right]$=30 m^2s^{-2}, and $\left[\overline{u^2}\right] = \left[\overline{v^2}\right]$ = 200 m^2s^{-2}. Calculate the correlation coefficient between *u* and *v* in the transients.

2.10 Suppose that the eddies consisted of waves in which the perturbations in *u* and *v* both had amplitudes of 10 m^2s^{-2} and were 60° out of phase. Calculate [u*v*] and the correlation coefficient between *u** and *v** in the eddies.

2.5 Contribution of the high frequency transients to the transport

Fig. 2.12 shows the contribution of the "high frequency" component of the transients to the momentum fluxes in Fig. 2.10. It is generated by digitally filtering the time series of *u* and *v* at each gridpoint so as to eliminate fluctuations with periods longer than a week. The pattern closely resembles the one for the unfiltered transients in Fig. 2.10, with strong poleward fluxes across 30° and much weaker equatorward fluxes across 65°. Comparing amplitudes it is evident that the high frequencies account for ~40% of the total poleward flux of angular momentum across 30° latitude.

Fig. 2.12 As in the left panels of Fig. 2.10, but for the high frequency transients with periods shorter than a week. DJF left; JJA right. Contour interval 5 m^2s^{-2}.

Fig. 2.13 Distribution of kinetic energy at the 250 mb level associated with transient variability with periods shorter than a week. DJF only. After Hoskins et al. (1989).

In order to shed some light on the nature of these "high frequency transients", we show in Fig. 2.13 the corresponding hemispheric distributions of kinetic energy at the jetstream (250 mb) level. In both hemispheres, the variance tends to be concentrated within zonally elongated bands centered along 45° latitude. In the Southern Hemisphere the band can be traced all the way around the laritude circle, but the variability is largest in the Indian Ocean sector. In the Northern Hemisphere the zonal asymmetries in the distribution are more prominent. The bands of largest variability of the high frequency transients are concentrated over the Atlantic and Pacific sectors, whereas the Eurasian sector is relatively quiescent. The bands of high variability are suggestive of the notion of "storm tracks". Similar features are observed in all seasons and at all levels. The same banded structure is apparent in the temporal variances (or standard deviations) of the highpass filtered geopotential height, vorticity, and vertical velocity fields. Note that the axes of the "storm tracks" do not lie along 30°, the latitude of the strongest poleward fluxes of angular momentum: they lie ~15° poleward of that latitude.

Fig. 2.14 One point correlation maps based on a highpass filtered 500 mb height time series at the gridpoint indicated by the heavy dot over the central North Pacific: DJF data for 11 winters. Upper panel 250 mb height; lower panel 850 mb height. Contour interval 0.05. Dashed contours denote negative correlations with the reference time series. After Lim (1989).

It is possible to get further insight into the structure of the high frequency transients by taking a "reference (highpass filtered) time series" of some variable at a specified gridpoint located along the axis of one of the stormtracks and correlating it with (or regressing it upon) time series of any desired field over an entire array of gridpoints and plotting the corresponding correlation (or regression) coefficients in the form of a map. Fig. 2.14 shows such a pair of maps, constructed by taking highpass filtered 500 mb height at the gridpoint (41°N, 178°E, along the Pacific stormtrack) as the reference time series and correlating it with unfiltered 250 and 850 mb height over the entire Pacific sector, using DJF data only.

The correlations in the figure are modest but the pattern that emerges is remarkably clean nonetheless. It is suggestive of a zonally oriented wavetrain in which the disturbances exhibit a zonal wavelength of ~50° of longitude (~4000 km). The patterns at the two levels are simillar, but upon close inspection it is evident that the various features at the 250 mb level are displaced slightly to the west of their counterparts at the 850 mb level, indicating that the waves tilt westward with height. The phase speed of the waves, as deduced from the displacements of the primary "centers of action" on lag correlation maps is 10-15 m $s^{-1,}$ which is comparable to the wind speed at the 700 mb level (Wallace et al., 1988). Hence, the structure and evolution of the high frequency transients is consistent with an interpretation in terms of baroclinic waves.

The wavetrains at the two levels are oriented slightly differently: at the upper level it extends in an west-northwest—east-northeast direction, whereas at the lower level it follows the 40°N latitude circle almost exactly. Because of this minor difference in orientation, the individual positive and negative centers at the 250 mb level tilt poleward with increasing latitude much more than those at the 850 mb level. This difference is consistent with the much larger poleward fluxes of angular momentum at the higher level in the previous figure. The tilt is largest ~30°N (halfway between the two southernmost latitude circles), precisely where the contribution of the high frequency transients to the poleward flux of angular momentum is largest. The characteristic "kidney bean" shape of the individual centers is a reflection of the fact the poleward transport of westerly momentum is much stronger on the southern flank of the stormtrack than on the northern flank, which is also consistent with the previous figure.

Hence, the distribution of the flux of angular momentum in zonally averaged cross-sections is a reflection of the horizontal shape of the disturbances that produce it. From an inspection of correlation patterns such as the one shown in Fig.2.14 it is possible to deduce the sense of the fluxes. These results suggest that waves that disperse equatorwards tend to be associated with poleward momentum fluxes and vice versa.

Questions

2.11 Consider the balance requirements for the conservation of angular momentum within a

hurricane, which can be assumed to be in a steady state. Assume that the storm exhibits circular symmetry about the "eye" and imagine a porous circular "wall" at a radius large enough to enclose most of the strong winds. The large loss of angular momentum associated with frictional drag at the ocean surface must be balanced by the radial transport through the wall. Assume that the inflow is mostly occurring within the planetary boundary layer and that the outflow is just below the tropopause, and neglect the fluxes associated with the large-scale flow pattern in which the hurricane is embedded. Does the angular momentum associated with the earth's rotation play an important role in the transport?

2.12 Consider the balance requirements for the conservation of angular momentum within an intense and rapidly deepening extratropical cyclone. In particular, consider the transport across a circular "wall" concentric with the center of the cyclone at the earth's surface and enclosing the strong and intensifying low-level circulation. Assume that the associated trough at the jetstream level lies about one quarter of a wavelength to the west of the deepening cyclone. Take into account the transports associated with the nondivergent component of the wind at upper levels.

2.13 By means of sketches analogous to 2.11, show that the result deduced from that figure is valid regardless of whether the background flow is from the west or from the east, or whether is is present or not.

2.14 Write an analytic expression for a flow similar to the one pictured in Fig. 2.11. Evaluate the eddy flux [u^*v^*] and show that it depends upon the tilt of the wave axes with latitude.

2.15 The sketches below are based on a single contour, replicated many times. In the left panel the contours are shifted meridionally, whereas in the right panel they are shifted both meridionally and zonally. In which panel is the poleward flux of zonal momentum identically equal to zero? Why?

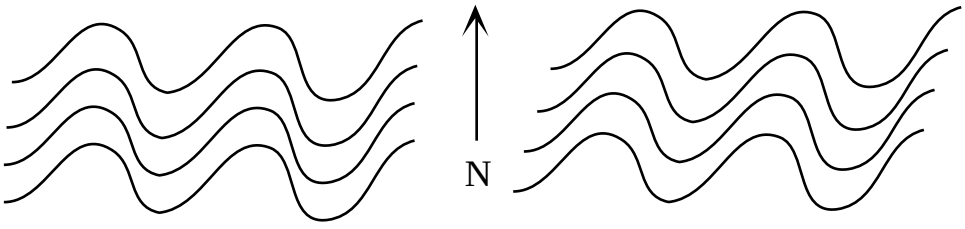

2.6 The vertical transports

We have seen that the atmosphere's major source of angular momentum is in the planetary

boundary layer in the tradewind belt and its major sink is in the planetary boundary layer in the westerlies at much higher latitudes. Yet most of the poleward transport of angular momentum within the earth's atmosphere takes place near the jet stream level. It remains to be shown how the angular momentum gets transferred upward from the boundary layer to the jet stream level equatorward od 30° and back down poleward of 30°. Is this vertical transport accomplished by some sort of turbulent mixing, as in the planetary boundary layer, or is some other mechanism involved?

A simple laboratory experiment can provide a surprising amount of insight into both questions. Consider a cylindrical tank, filled with a homogeneous liquid, in solid body rotation about its axis of symmetry. At some instant in time the motor for the turntable is turned off so that the walls of the tank abruptly become stationary. The fluid continues to rotate for a period of time under laminar flow conditions, until its angular momentum is removed by frictional drag at the walls. How long does this "spindown" process take? If the boundary effects were transmitted to the interior of the fluid by molecular diffusion, one should expect that the spindown time would be on the order of hours for a laboratory-size tank and minutes for a "teacup size" demonstration model. By comparison, the observed spindown time is remarkably short; minutes for a laboratory-size apparatus and much less than a minute for a teacup. Evidently some other much more efficient process is at work. The tendency for tea leaves to pile up in the middle of the cup during such an experiment provides a clue as to the nature of this process.

Let us consider the motions in the tank during the spindown process. Throughout most of the tank the tangential flow is close to a state balance between the inward directed horizontal pressure gradient force associated with the parabolic shape of the free surface (not shown) and the outward directed centrifugal force associated with the curvature of the trajectories. However, within the very thin molecular boundary layer adjacent to the bottom wall of the tank this balance is continually being upset by the frictional drag which is slowing down the tangential flow so that the centrifugal force is unable to balance the pressure gradient force. The situation is analogous to sub-geostrophic flow in the planetary boundary layer of the earth's atmosphere. As a result of the imbalance, fluid drifts inward toward the axis of rotation along the bottom of the tank; hence the pile of tea leaves in the middle of the teacup. This frictionally driven radial inflow requires a very slow return flow above the boundary layer, as shown in Fig. 2.15. The character of the return flow is highly dependent upon whether the fluid in the tank is homogeneous (constant density) or stably stratified. If it is homogeneous, then the flow must be barotropic: there is no way to generate horizontal density gradients so there can be no vertical shear of the tangential flow. In this case the radial outflow must be uniformly

distributed throughout the interior of the tank. As an element of fluid drifts inward along the bottom of the tank it loses most of its angular momentum. Thus, by the time it completes a full circuit of the radial circulation cell, the spin-down of the tank should be almost complete. The stably stratified (baroclinic) case has been investigated by Holton (J.A.S., 1965).

Fig. 2.15 Streamlines for the frictionally induced flow in a rotating cylinder during "spindown". The outer part of the cylinder and the parabolic free surface are not shown. After Holton (1979).

The radial circulation cell in the tank is the analogue of mean meridional cells in the zonally symmetric atmospheric circulations. Let us examine how such cells transport angular momentum vertically in the atmosphere. The vertical flux of angular momentum through any horizontal plane in the atmosphere is given by

$$\frac{\Omega R_E^2}{g}\iint -\overline{\omega}\cos^2\phi\, dxdy + \frac{R_E}{g}\iint \overline{u\omega}\cos\phi\, dxdy$$

where x and y have their usual meanings as defined in the context of a spherical coordinate system. Performing the indicated zonal integration, we obtain

$$\frac{2\pi\Omega R_E^3}{g}\int[-\overline{\omega}]\cos^3\phi\, dy + \frac{2\pi R_E^2}{g}\int\left[\overline{u\omega}\right]\cos^2\phi\, dy$$

Expanding the $\left[\overline{u\omega}\right]$ term and combing the $[\overline{u}][\overline{\omega}]$ part of it with the first term, we obtain the total contribution of mean meridional circulations to the vertical transport of angular momentum

$$\frac{2\pi R_E^2}{g}\int[-\overline{\omega}]\left(\Omega R_E\cos\phi+[\overline{u}]\right)\cos^2\phi\,dy \qquad (2.7)$$

In the above expression the first term exhibits a much wider range of variation with latitude than the second. For example, for the latitude range of the Hadley cell (0–30° latitude), $\Omega R_E \cos\phi$ varies from ~465 m s^{-1} to 402 m s^{-1} and for the latitude range of the Ferrel cell (30–60° latitude) it varies from 402 to 232 ms^{-1}. Thus the air in the rising branch of the Hadley cell contains much more angular momentum per unit mass than the air in the sinking branch and hence the Hadley cell transports angular momentum upward from the planetary boundary layer into the upper troposphere, south of the jet stream. The eddies at the jet stream level transport this angular momentum poleward into middle latitudes.

The Ferrel cell then transports the angular momentum downward into the planetary boundary layer where it serves to maintain the surface westerlies in the presence of frictional dissipation, as shown in Fig. 2.16. During wintertime, there is an analogous, but much weaker transport of angular momentum from the polar cap regions into middle latitudes, as indicated in Fig. 2.16.

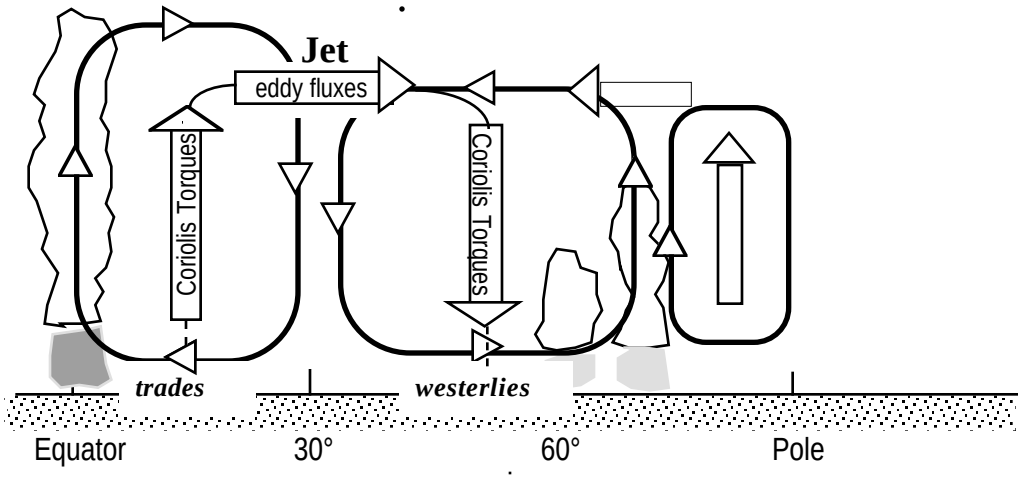

Fig. 2.16 Schematic of the transport of atmospheric angular momentum in the earth's atmosphere.

The mean meridional circulations extract angular momentum from the flow at one level and impart it to the flow at another level by means of the cross isobar flow which induces a zonal Coriolis force. For example, in the lower branch of the Hadley cell the equatorward flow induces a westward Coriolis force which maintains the easterly tradewinds against frictional dissipation. Meanwhile in the upper branch of the same cell, the poleward return flow induces

an eastward Coriolis force which maintains the upper level westerlies. In accordance with the discussion in Section 9.3.3 of Wallace and Hobbs (1977), the Hadley cell, which is a thermally direct circulation, serves to increase the vertical shear of the geostrophic (zonal) flow and the Ferrel cell, which is a thermally indirect circulation, serves to decrease it.

In order to obtain some estimate of the effectiveness of mean meridional circulations in the angular momentum balance of the earth's atmosphere, it is interesting to compute the "spin down time" of the westerlies in the upper branch of the Ferrel cell, say at 43°N, 250 mb during the winter season, where $[\bar{u}]$ 25 m s^{-1} and $[\bar{v}]$ 0.4 m s^{-1} (we will justify this estimate later). In the absence of any other influences

$$\frac{\partial [u]}{\partial t} = f[\bar{v}] \approx 0.4 \times 10^{-4}\,\mathrm{m\,s^{-1}} \approx 4\,\mathrm{m\,s^{-1}d^{-1}}$$

Thus the "spindown time" is on the order of only a week. The "spin up time" for the Hadley cell is of the same order of magnitude.

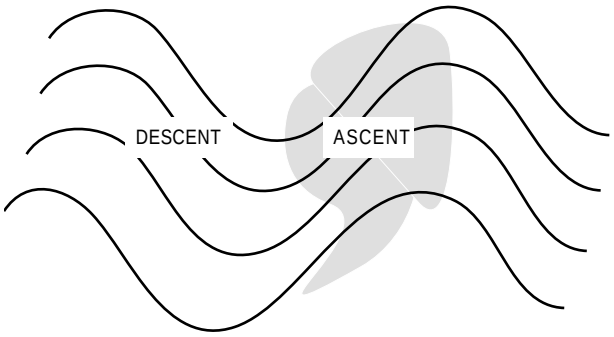

Fig. 2.17 Distribution of vertical motion in a typical extratropical motion system.

Now let us examine the vertical transport of angular momentum due to the eddies. First let us consider the sign of the transport. Fig. 2.17 shows the vertical motion field in a typical middle latitude wave disturbance as deduced from synoptic considerations; e.g., by application of the diagnostic omega equation. This distribution is consistent with typical patterns of cloudiness as manifested in satellite imagery (e.g., see Wallace and Hobbs, Fig. 5.38). It is

evident that in the middle and upper troposphere, rising air in the eddies is characterized by higher values of relative angular momentum than sinking air. Hence the vertical eddy flux of zonal momentum is upward and countergradient; that is, directed from lower values of $[\bar{u}]$ toward higher values.

Now let us consider the magnitude of the vertical eddy flux of zonal momentum. In order to be of comparable importance to the meridional flux, it needn't be nearly as large as the latter, since much shorter distances are involved in the vertical direction. On the basis of scaling considerations we can argue that the meridional and vertical fluxes should be of comparable importance in the tropospheric general circulation if $[u^*w^*]/[u^*v^*] \sim D/L$, where D is the depth of the troposphere (10 km) and L is the distance over which the eddies transport zonal momentum in the meridional direction, say from 15° to 45° latitude, or 3000 km. Hence $D/L \sim 1/300$. Now if we assume that the correlation between u and w is comparable to that between u and v, it follows from the product moment formula that

$$\frac{[u^* w^*]}{[u^* v^*]} \approx \frac{[w^{*2}]}{[v^{*2}]}$$

where the latter ratio is a measure of trajectory slopes in the eddies, projected onto the meridional plane. Hence for meridional and vertical eddy fluxes to assume comparable importance, the trajectory slopes must be of the order D/L.

The typical trajectory slopes in the mid-troposphere are much less than 1 part in 300. (We recall from the theory of baroclinic waves that they are inclined only half as steeply as the isentropes which have a slope on the order of 1 part in 1000.) Furthermore, it can be demonstrated from quasi-geostrophic scaling arguments that w/v is of the order $Ro \times D/L$ where Ro, the Rossby Number is of order 0.15. Hence we conclude that as far as the angular momentum budget is concerned, the vertical eddy flux of zonal momentum is of second order importance in comparison to the meridional transport.

Vertical eddy fluxes of zonal momentum are not always of second order importance. In the equatorial stratosphere the fluxes produced by planetary-scale, vertically propagating Kelvin-waves and mixed Rossby-gravity waves play a major role in producing the remarkable quasi-biennial oscillation (QBO) in zonal wind. Large upward fluxes of westerly momentum have been observed in association with the descent of the leading edges of successive westerly wind regimes. These fluxes play a critical role in Lindzen and Holton's (1968) theory of the QBO[5], which has been verified by Plumb's (1977) laboratory analogue

[5] see also Holton and Lindzen (1972) and Holton et al. (1987)

2.7 The local, zonally averaged zonal momentum balance

In Appendix II it is shown that the time rate of change of zonally averaged zonal wind is given by

$$\frac{\partial[u]}{\partial t} = [v]\left(f - \frac{1}{\cos\phi}\frac{\partial}{\partial y}[u]\cos\phi \right) - [\omega]\frac{\partial[u]}{\partial p} - \frac{1}{\cos^2\phi}\frac{\partial}{\partial y}[u^*v^*]\cos^2\phi - \frac{\partial}{\partial p}[u^*\omega^*] + [F_x] \tag{2.8}$$

The terms that arise as a consequence of the spherical geometry are of second order importance. Therefore, for purposes of discussion it will be useful to refer to the Cartesian approximation

$$\frac{\partial[u]}{\partial t} = [v]\left(f - \frac{\partial[u]}{\partial y} \right) - [\omega]\frac{\partial[u]}{\partial p} - \frac{\partial}{\partial y}[u^*v^*] - \frac{\partial}{\partial p}[u^*\omega^*] + [F_x] \tag{2.9}$$

The term in parentheses that multiplies [*v*] in (2.8) and (2.9), which is proportional to the meridional gradient of angular momentum *m*, plays a role analogous to the static stability in the thermodynamic energy equation. For a zonally symmetric ring of air displaced meridionally under the conservation of angular momentum, it is readily verified that $D[u]/Dt = f[v]$ [in analogy with the temperature of a sinking air parcel rising at a rate $DT/Dt = (\kappa T/p)[\omega]$. But the zonal momentum of the environmental air varies with latitude, and therefore, $\partial[u]/\partial t$ is given by the term in parentheses [just as $\partial T/\partial t$ is given by $\sigma \equiv (\kappa T/p - \partial T/\partial p)$]. Just as the static stability is a measure of the restoring (gravitational) force per unit vertical displacement, the term in parentheses is a measure of the meridional (inertial: i.e., Coriolis) restoring force per unit meridional displacement of a zonally symmetric ring of air. Just as the static stability is ordinarily positive (potential temperature increasing with height) the "inertial stability" is ordinarily positive (zonally averaged angular momentum decreasing with latitude). Note that the inertial stability for the zonally averaged flow is simply the zonally averaged absolute vorticity. If the anticyclonic shear of [*u*] were strong enough to cancel *f*, the inertial stability would vanish. On the equatorward flank of the Pacific jetstream (Fig. 2.3) $\partial\overline{u} / \partial y$ is so large that it does, in fact, approach *f* locally , but the absolute vorticity does not approach zero in the zonal average. Figure 2.18 shows the meridional profile of angular momentum (divided by the radius of the earth), together with the corresponding profiles of zonal velocity for the solid earth and for the atmosphere (in absolute coordinates), at the 200 mb level which corresponds to the core of the tropospheric jetstream, in DJF. Equatorward of the jetstream, zonal velocity is almost uniform, but even there the angular momentum still exhibits a substantial meridional gradient.

Hence, the inertial stability for the zonally symmetric flow is positive throughout the troposphere with the possible exception of a narrow region within a few degrees of the equator. Note that the jetstream at 30° marks a break in the profiles.

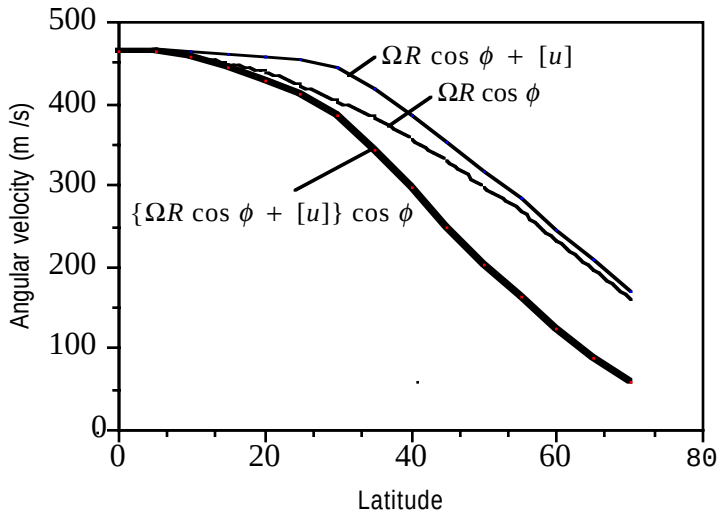

Fig. 2.18 Meridional profiles of zonal velocity of the rotating earth and the atmosphere in absolute coordinates, and angular momentum divided by the radius of the earth, based upon Northern Hemisphere data for the 200 mb level for DJF.

For the reasons discussed in the previous section, the terms involving the vertical motions are smaller than their counterparts that involve meridional motions by a factor of the Rossby Number. Neglecting these terms, (2.9) becomes

$$\frac{\partial [u]}{\partial t} = [v]\left(f - \frac{\partial [u]}{\partial y} \right) + G + [F_x] \qquad (2.10)$$

where G represents the meridional convergence ($-\partial/\partial y$) of the northward flux of westerly momentum by the eddies.

Now let us apply this equation at points *A*–*D* in Fig. 2.19. We will assume that poleward eddy fluxes are important only in the upper troposphere (points *B* and *C*), and that frictional effects are important only within the planetary boundary layer (points *A* and *D*).

At point *A* in the figure there must be a balance between the $f[v]$ term, which is producing an easterly (negative) acceleration and the frictional drag, which is trying to decelerate the surface easterlies. Thus, the easterly tradewinds are maintained against frictional dissipation by the equatorward flow in the lower branch of the Hadley cell. In a similar manner, the surface westerlies in the middle latitudes are maintained against frictional dissipation by the poleward flow in the lower branch of the Ferrel cell. Thus there is a good reason why the transition between easterly and westerly surface winds, near 30° latitude, coincides exactly with the

transition between Hadley and Ferrel cells.

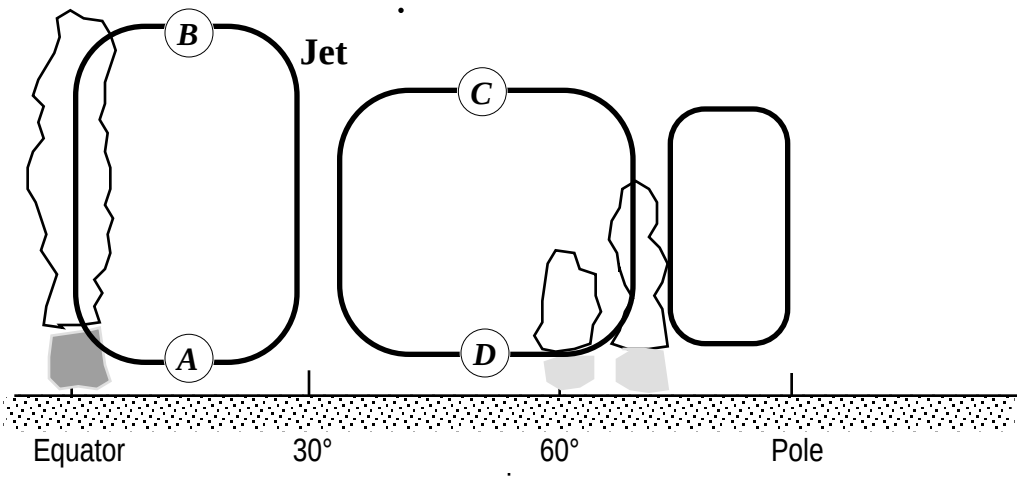

Fig. 2.19 See text for explanation.

At point *B*, the poleward eddy flux of zonal momentum is increasing rapidly with latitude. Hence, $\partial[u^*v^*] / \partial y >> 0$; that is to say, there is a strong divergence of eddy flux out of this region. Thus at *B*, the $f[v]$ term associated with the poleward flux in the upper branch of the Hadley cell supplies westerly momentum at exactly the rate that the eddies are removing it.

At point *C* the picture is just the reverse. The zonal momentum fluxed poleward by the eddies is converging into this region so that $\partial[u^*v^*] / \partial y << 0$. The Coriolis term associated with the equatorward flow in the upper branch of the Ferrel cell removes the westerly momentum as fast as the eddies bring it in, thus maintaining a steady state.

We have purposely applied the above equation to latitudes near 15 and 45 degrees, where the signs of the terms are unambiguous. Note that this equation doesn't tell us anything about the balance in the vicinity of 30°, where all the terms are near zero.

Questions

2.16 Zonally symmetric inertial instability is possible in a flow with a(n) (westerly, easterly) jet centered on the equator.

2.17 Show how the zonal momentum balance is satisfied at point *D* in Figure 2.19.

2.18 Taking into account the meridional variation of f and $[u]$ in (2.9), show that the Hadley cell must be stronger than the Ferrel cell by at least a factor of 3.

2.19 Making use of Figures 2.9 and 2.10, discuss the seasonal differences in the distribution of mean meridional circulations and relate them to relative the strength of the "eddy forcing" term G in (2.10).

2.208 Prove that if $\vec{V}^*$ is nondivergent, $G \equiv -\partial[u^*v^*]/\partial y = [v^*\zeta^*]$, where ζ^* is the relative vorticity of the eddies.

2.21 During the peak of the QBO, $[u]$ on the equator reaches values of 20 m s^{-1}. Prove that only eddy processes could be responsible for the presence of such strong westerlies in the equator.

2.8 Further remarks concerning the mean meridional circulations

It is worth noting that even in the Hadley cell, $[\bar{v}]$ is roughly an order of magnitude smaller than $\bar{v}$ at individual longitudes. Given the sparsity of observations over parts of the globe, direct estimates of $[\bar{v}]$ are subject to a considerable amount of uncertainty. Even the estimates presented in this section, which are based on sophisticated multivariate analysis schemes, should be viewed with caution, particularly in the Southern Hemisphere where much of the analysis is based upon satellite observations. Note, for example, the strong low-level outflow from the Antarctic continent, which is not compensated by any return flow aloft.

It is easily shown that on pressure surfaces that do not intersect the ground, $[v_g]$ is identically equal to zero, both instantaneously and in the long-term average. It follows that $[v]$ represents a purely ageostrophic flow. In the planetary boundary layer, both the Hadley cell and the Ferrel cell are characterized by cross isobar flow, down the pressure gradient, which maintains the zonal component of the surface wind in the presence of frictional drag. At the tropopause level, where westerlies prevail at virtually all latitudes, the poleward ageostrophic flow in the Hadley cell is also down the gradient. Hence, the Hadley cell, which has $-[\bar{v}]\dfrac{\partial[\overline{\Phi}]}{\partial y} > 0$ in both upper and lower branches is obviously thermally direct: it converts available potential energy associated with the meridional temperature gradient into kinetic energy of the zonally symmetric component of the flow. However, the equatorward flow in the upper branch of the Ferrel cell is up the pressure gradient. Furthermore, since the westerlies increase with height in the troposphere, the conversion term must be larger, in absolute value, in the upper branch of the cell than in the lower branch. It follows that the Ferrel cell is thermally indirect: it converts kinetic energy to available potential energy.

Despite the uncertainties in the analyses, we can be quite confident that they are capturing the structure and approximate magnitude of the mean meridional circulations because they are consistent with the balance requirements for angular momentum. Unlike the estimates of $[\bar{v}]$, which represents a very small difference between northward and southward winds across different sectors of a latitude circle, estimates of $\left[\overline{u^*v^*}\right]$ at the jetstream level are quite robust: $\overline{u^*v^*}$ varies with longitude, but at 30° it is poleward at almost all longitudes; consistent with the fact that one-point correlation maps for base gridpoints at that latitude exhibit wavetrains that appear to propagate out of the extratropics and into the tropics. Distributions of $\left[\overline{u^*v^*}\right]$ very similar to those shown in Fig 2.10 have been found in analyses based on operational analyses from NMC (Lau, 1979; Lau et al., 1981) and zonal averages of vertical profiles of $\overline{u^*v^*}$ based on wind statistics derived from rawinsonde stations [e.g., see Oort and Rasmusson, 1971, Oort, 1983]. In addition, we have corroborative evidence based upon estimates of surface wind stress over the oceans. Hence, there can be no question as to the reality and relative strengths of the Hadley and Ferrel cells.

Questions

2.22 Show $[u]$ contains a small ageostrophic component. If $[u]$ = 40 meters per second at 30° latitude, estimate the zonal component of the ageostrophic flow.

References

Holton, J.R. and R.S. Lindzen 1972: An updated theory for the quasi-biennial cycle of the tropical stratosphere. *J. Atmos. Sci.*, **29**, 1076-1080.

Hoskins, B.J., H.-H. Hsu, I.N. James, M. Masutani, P.D. Sardeshmukh and G.H. White, 1989: Diagnostics of the global atmospheric circulation based on ECMWF analyses 1979-1989. *World Climate Research Programme Report–27* (World Meteorological Meteorological Organization Technical Document No. 326), 217pp.

Jeffreys, H., 1926: On the dynamics of geostrophic winds. *Quart. J. R. Met. Soc.*, **52**, 85-104.

Lambeck, K., 1980: *The Earth's Variable Rotation*. Cambridge University Press, 449pp.

Lambeck, K and A. Cazenave, 1976: Long term variations in the length of day and climatic

change. *Geophys. J. Roy. Astr. Soc.*, **46**, 555-573.

Langley, R.B., R.W. King, I.I. Shapiro, R.D. Rosen, and D.A Salstein, 1981: Atmospheric angular momentum and length od day: A common fluctuation with a period near 50 days. *Nature*, **294**, 730-732.

Large, W.G. and Pond, S., 1981: Open ocean momentum flux measurements in moderate to strong winds. *J. Phys. Oceanogr.*, **11**, 324-336.

Lau, N.-C., 1979: The structure and energetics of transient disturbances in the Northern Hemisphere wintertime circulation. *J. Atmos. Sci.,* **36**, 982-995.

Lau, N.-C., G.H. White and R.L. Jenne, 1981: Circulation statistics for the extratropical Northern Hemisphere based on NMC analyses. *NCAR Tech. Note* **NCAR/TN-171,** xx pp..

Lindzen, R.S. and J.R. Holton, 1968: A theory of the quasi-biennial Oscillation. *J. Atmos. Sci.,* **25**, 1095-1107.

Obasi, G.O.P., 1963: Poleward flux of atmospheric angular momentum in the Southern Hemisphere. *J. Atmos. Sci.,* **20**, 516-528.

Oort, A.H., 1983: *Atmospheric Circulation Statistics 1958-73.* NOAA Prof. Paper No. 14, U.S. Gov't Printing Office, Washington, DC.

Oort A.H. and E.M. Rasmusson, 1971: *Atmospheric Circulation Statistics.* NOAA Prof. Paper No. 5, U.S. Gov't Printing Office, Washington, DC.

Palmén, E., 1949: Meridional circulations and the transfer of angular momentum in the atmosphere. *J. Meteorol.,* **6**, 429-430.

Palmén, E. and C.W. Newton, 198xx: *Atmospheric Circulation Systems,* Academic Press

Plumb, R.A., 1977: The interaction of two waves with the mean flow: implicatiuons for the theory of the quasi-biennial oscillation. J. Atmos. Sci., **34**, 1847-1858.

Rosen, R.D. and D.A. Salstein, 1983: Variations in atmospheric angular momentum on global and regional scales and the length of day. *J. Geophys. Res.*, **88**, 5451-5470.

Rosen, R.D. and D.A. Salstein, 1985: Contribution of stratospheric winds to the annual and semiannual fluctuations in atmospheric angular momentum and the length of day. *J. Geophys. Res.*, **90**, No. D5, 8033-8041.

Rosen, R.D., T.M. Eubanks, J.O. Dickey and J.A. Steppe, 1984: An El Niño signal in atmospheric angular momentum and earth rotation. *Science,* **225**, 411-414.

Rossby, C.G., 1947: On the distribution of angular velocity in gaseous envelopes under the influence of large-scale mixing processes. *Bull. Amer. Meteorol. Soc.*, **28**, 53-68.

Salstein, D.A. and R.D. Rosen, 1986: Earth rotation as a proxy for interannual variability in the atmospheric circulation, 1860-present. *J.C.A.M.,* **25**, 1870-1877.

Smith, S.D., 1980: Wind stress and heat flux over the ocean in gale-force winds. *J. Phys. Oceanogr.*, **10**, 709-726.

Starr, V.P., 1948: An essay on the general circulation of the earth's atmosphere. *J. Meteor.*, **5**, 39-43.

Starr, V.P.,1949: Reply. *J. Meteorol.,* **6**, 430.

Wahr, J.M. and A.H. Oort, 1984: Friction and mountain torque estimates from global atmospheric data. *J. Atmos. Sci.*, **41**, 190-204.

Widger, W.K, 1949: A study of the flow of angular momentum in the atmosphere. *J. Meteorol.,* **6**, 291-299.

3. THE ENERGY BALANCE

3.1 The global energy balance

In contrast to the angular momentum budget, in which the atmosphere, and the solid earth constitute a closed system, the global energy balance involves large fluxes through the top of the atmosphere, and the oceans and the continental ice sheets play much more important roles than the solid earth[6]. Significant variability in the energy stored in the various global reservoirs is observed on time scales ranging from a season to the age of the earth.

The annual mean global energy balance is summarized in Fig. 3.1. The small flux of geothermal energy through the earth's surface (0.1 W m^{-2}) and the equally small fluxes associated with interannual variability and climatic change are neglected, so that the net fluxes through the top and bottom of the atmosphere sum to zero.[7] The 100 units of incoming solar radiation refer to the average solar irradiance per unit area of the earth's surface (~345 W m^{-2}). Note that 70 units (~238 W m^{-2}) are actually absorbed by the earth system after the reflection associated with earth's albedo is accounted for.

It is evident from the figure that the atmosphere is heated by both solar radiation and by the exchange of infrared radiation at its lower boundary, but it emits so much infrared radiation to space that it suffers a net loss of energy at a rate of 30 units by radiative transfer which is balanced by an influx of latent and sensible heat from the earth's surface. The latent heat is converted into sensible heat when water vapor condenses in clouds, most of which occurs in the lower and middle troposphere. The net emission of infrared radiation from the earth's surface represents the difference between a large upward irradiance (113 units) from the surface and a smaller downward irradiance (92 units) from the atmosphere.

Clouds play a pervasive, and rather subtle role in the balance. On the one hand, they cool the earth's surface by reducing the amount of solar radiation that reaches the ground but, on the other hand, they warm the surface by contributing to the greenhouse effect. For low clouds, whose tops are comparatively warm, the cooling effect predominates, whereas high clouds with cold tops produce a net warming.

The energy balance at the top of the atmosphere involves only two types of measurements: the reflected solar radiation or albedo, and the outgoing longwave radiation *(OLR)* emitted by the earth-atmosphere system, both of which can be monitored to an accuracy of ~1 W m^{-2} with

---

[6] The flux of geothermal energy through the earth's surface is estimated to be on the order of 0.1 W m^{-2}, averaged over time and over the surface of the earth, which is two orders of magnitude smaller than the fluxes that we will be concerned with.

[7] For an individual hemisphere the net fluxes through the air-sea interface during the transition seasons associated with changes in heat storage on the oceanic mixed layer are quite substantial.

sensors carried aboard satellites. The balance at the earth's surface is more complicated, with upward and downward irradiances of both solar and terrestrial radiation, plus latent and sensible heat fluxes which are not easily monitored from space because of the intervening cloud cover.

The hydrologic cycle plays an important role in the global energy balance. Evaporation is a heat sink for the oceans and vegetated land surfaces, and latent heat release within the atmosphere balances most of the energy loss due to radiative transfer. Note that the latent heat is not realized until the water vapor condenses, by which time it may be far from where it entered the atmosphere.

Fig. 3.1 The annual mean global energy balance for the earth-atmosphere system. (Numbers are given as percentages of the globally averaged solar irradiance incident upon the top of the atmosphere.) See text for further explanation. [Adapted from "Understanding Climatic Change", U.S. National Academy of Sciences, Washington, D.C. (1975)].

The problem of keeping track of the latent heat can be circumvented by treating latent heat of air parcels as part of their energy. On short time scales, air parcels tend to conserve *moist static energy*; defined as the sum of the enthalpy or sensible heat, plus the latent heat, plus the gravitational potential energy

$$e \equiv c_p T + Lq + \Phi \qquad (3.1)$$

where L is the latent heat of condensation per unit mass (2.50×10^6 J kg^{-1}) and q is the specific humidity of water vapor(the mass of water vapor per unit mass of air); even when when

condensation is taking place. Enthalpy appears in this expression instead of internal energy because air parcels do work (or have work done on them) by the surrounding air as they expand (or contract) during heating (or cooling). This work is incorporated into the definition of the moist static energy[8]. The only process operating within the free atmosphere that is capable of changing it is radiative heating, which is dominated by infrared cooling. Energy is converted between latent and sensible heat when water vapor undergoes phase changes[9] and between sensible heat and potential energy when it rises and sinks. From a Lagrangian point of view, a "typical" air parcel gains substantial amounts of sensible and latent heat during the relatively brief periods that it spends in the planetary boundary layer (PBL) which increases their moist static energy. (The actual mechanism by which the latent and sensible heat is imparted to the parcel is the turbulent motions on scales smaller that the size of the parcel, which pick up heat and moisture at the earth's surface and distribute them throughout the PBL.) Air parcels suffer a more gradual but systematic loss of moist static energy through radiative transfer during the more extended periods of time in which they move about in the "free atmosphere".

Questions

3.1 Using the Stefan Boltzmann Law, calculate the effective temperatures of (a) the earth-system, as viewed from space, (b) the earth's surface, as felt by the atmosphere, and (c) the atmosphere, as sensed from the earth's surface, looking upward. [*Ans.* (a) 255 K] Explain how the atmosphere can emit more infrared radiation in the downward direction than the earth system emits in the upward direction.

3.2 How much energy would it take to raise the mean temperature of a unit (1 m^{-2}) column of the atmosphere by 1 K? (*Ans.* 1.03 x 10^7 J.)

3.3 If all the energy sources were instantly "turned off" and the atmosphere were allowed to radiate to space as a blackbody, with an effective temperature of 255 K, compute the rate at which its mean temperature would begin to drop. Neglect the interactions with the underlying surface (*Ans.* 2.07 K day^{-1})

3.4 The thermal capacity of the atmosphere is equivalent of that of an ocean how many meters deep? The specific heat of liquid water is 4218 J kg^{-1} K^{-1}. (*Ans.* 2.46 m)

3.2 The Atmosphere as a heat engine

In Problem 1.14 the reader was asked to estimate the efficiency of the atmospheric heat

---

8 For a formal derivation see Appendix III.

9 In this discussion we have ignored the latent heat absorbed and given up when cloud droplets freeze and melt.

engine by comparing the rate of conversion of available potential energy to kinetic energy, as represented by the vertical integral of $\overline{-\vec{V}\cdot\nabla\Phi}$, with the input of solar energy (238 W m^{-2}). In actual calculations, the conversion is on the order of 2-3 W m^{-2},[10] which indicates that the efficiency is ~1%. If we model the atmosphere in terms of an idealized Carnot cycle operating between temperatures T_w and T_c, we can write $(T_w - T_c) / T_w = 1\%$. It we take T_w ~ 240 K, the temperature difference comes out to ~2-3 K. Assuming a standard lapse rate of 6 K km^{-1}, the effective heat source for the heat engine that drives the large-scale motions in the earth's atmosphere is only ~400 m below the heat sink. If the kinetic energy generated within moist and dry convection is not taken into account in this calculation, the difference would be somewhat larger.

3.3 Maintenance of the observed stratification

On average, the observed lapse-rate in the troposphere is only ~2/3 of the dry adiabatic value (Γ_d = 9.8 K km^{-1}), despite the fact that radiative heating is continually acting to destroy the stable stratification: i.e., the radiative heat sink tends to be located at a slightly higher level in the atmosphere than the heat sources.

One of the processes that contributes to the observed stable stratification and to the upward transport of moist static energy is condensation heating in deep convective clouds. Deep 'penetrative convection' extending all the way up to the tropopause can erupt in regions in which the lapse-rate $-\partial T/\partial z$ is substantially less than the dry adiabatic value , provided that the buoyant 'plumes' originating in the planetary boundary layer contain sufficient moisture so that condensation heating can keep them warmer than their environment as they ascend. A necessary (but not sufficient) condition for deep convection is that the moist static energy of the air in the PBL be larger than that of a deep layer of air immediately above it. This condition is satisfied throughout most of the tropics because of the large differences between the relative humidity of the air in the PBL (~80%) and the air immediately above it (20-60%). However, convection occurs only in those regions in which plumes originating in the PBL break through the 'lifting condensation level' and ascend moist adiabatically to the 'level of free convection':i.e., the level above which the potential buoyancy inherent in the water vapor stratification is realized. These regions tend to lie over hot spots in the underlying surface and convergence of the flow in the PBL.

Fig. 3.2 illustrates how deep cumulus convection, in the presence of radiative cooling, acts to

[10] The calculated value is about a factor of 4 smaller than one would estimate by assuming that the ageostrophic component of the wind is systematically across the isobars toward lower pressure, as it is in the PBL.

maintain the observed stratification. Large volumes of boundary layer air are transported into the upper troposphere in the updrafts in cumulonimbus clouds. Updraft velocities are so large that this air conserves moist static energy as it rises. After being detrained from the tops of cumulonimbus clouds, this (former) boundary layer air subsides very slowly in the cloud-free regions and even in rain areas in the spaces in between the updrafts. As it subsides it is subject to radiative cooling rates in excess of 1 K day^{-1}. Hence, as it sinks it warms up at a rate somewhat less than the dry adiabatic lapse rate (9.8 deg km^{-1}). Since it conserves moisture as it descends, its moist static energy must decrease, as indicated in the figure. Since this sinking air occupies so much more horizontal area at any given level than the rising air in the updrafts, its vertical profile of moist static energy essentially determines the environmental static stability. In regions of strong surface heating, the lowest values of moist static energy are usually found just above the inversion that caps the mixed layer (or the cumulus cloud tops if shallow cumulus convection is present), whereas in regions of little or no surface heating the stable stratification extends all the way downward to the surface.[11]

Fig. 3.2 Schematic description of the vertical mass fluxes and environmental distribution of moist static energy observed in association with deep convection in the atmosphere.

When the vertical velocity distribution is spatially averaged on the synoptic scale, we obtain a somewhat different physical interpretation of the moist static energy balance. The distribution of moist static energy is virtually unaffected by the averaging, but the vertical velocity distribution is changed in a substantive way: the cumulus "plumes" are smeared out to form a broad area of upward motion, so that the motion field now takes the form of a large circulation

[11] In a similar manner (but upside down) the thermohaline circulation in the oceans maintains the strong stratification in the thermocline. Water sinks in convective regions in high latitudes where salt plays an important role in producing the negative buoyancy. In the much slower return flow of water parcels rising through the thermocline, the water is warmed by microscale fluxes, which mix heat downward from the surface layer.

cell. The distribution of sources and sinks of moist static energy is also affected by the smoothing: the vertical transport by cumulus convection must now be taken into account as a virtual source term. In order to show how this term arises, let us write

$$\omega = \{\omega\} + \omega_c \text{ and } e = \{e\} + e_c,$$

where the quantities in braces refer to the spatially smoothed values of ω or e, and the subscript c refers to differences between the actual values and the smoothed values due to the presence of cumulus convection. The vertical transport of moist static energy over the domain A is given by

$$\frac{1}{g}\iint \omega e \, dA = \frac{1}{g}\iint \{\omega\}\{e\} \, dA + \frac{1}{g}\iint \omega_c e_c \, dA \qquad (3.1)$$

The virtual source of moist static energy due to the convective transport term (per unit mass) is given by $-\partial\{\omega_c e_c\}/\partial p$. Now at the level of the cloud tops ω_c and e_c are everywhere very small and thus $\{\omega_c e_c\} = 0$. However, in the lower and middle troposphere, ω_c is large in absolute value and $e_c > 0$ in the updrafts; thus there is an upward flux of moist static energy by the convective scale motions; with $\{\omega_c e_c\} < 0$. It follows that in the intervening layer $-\partial\{\omega_c e_c\}/\partial p > 0$ and thus there is a virtual source of moist static energy due to the convective scale motions. In regions of heavy convective precipitation, this source term more than makes up for the losses associated with radiative cooling. In numerical models of the general circulation and numerical weather prediction models, the convective transports are parameterized in terms of the large scale field variables. All the major parameterization schemes have the effect of increasing the moist static energy in the middle troposphere in convective rain areas.

Even in the absence of deep convection, a stable stratification would be maintained throughout most or all of the atmosphere by the upward flux of moist static energy in large-scale, thermally direct circulations, in which warm, moist air rises and cool, dry air sinks. The Hadley cell, the monsoons and baroclinic waves all contribute to this flux. In general, the stronger the horizontal heating gradients in the earth's atmosphere, the stronger the thermally direct circulations, the larger the upward transport of moist static energy and the stronger the resulting stable stratification. It is not surprising, then, that the most stable lapse rates tend to be found in middle and high latitudes of the winter hemisphere, where the meridional heating gradient is very strong; and that (with a few notable exceptions) deep cumulus convection tends to be confined to the tropics and the summer hemisphere, where horizontal heating gradients are relatively weak .

Problems

3.5 At the level of free convection, suppose that the updraft air is saturated, the environmental relative humidity is 50%, and the specific humidity for saturated air is 15 g/kg. Estimate the difference between the moist static energy if the updraft air and the environmental air at the same level.

3.6 In the region of ascent in a synoptic scale disturbance, the temperature at the 900 mb level is 13°C, the specific humidity is 8 g/kg and the sea-level pressure is 995 mb, while in the region of descent, temperature at the 900 mb level is 0°C, the specific humidity is 2 g/kg and the sea-level pressure is 1020 mb. Estimate the difference in moist static energy of the air in the two regions on the 900 mb surface. Give an interpretation of the geopotential term in terms of the discussion in Section 1.5.

3.7 Do the phase changes associated with the freezing and melting of cloud droplets result in an upward or downward flux of moist static energy? Explain.

3.4 Balance requirements for the earth system

If we assume that the earth system is in a steady state with respect to total energy, the horizontal distribution of net radiation through the top of the atmosphere essentially determines the balance requirements for the horizontal transport of total energy within the system. Virtually all the required large-scale transports are accomplished by the fluid components of the system: the atmosphere and oceans. The partitioning of the transports between the atmosphere and oceans is inextricably linked to the horizontal distribution of energy fluxes (including latent heat) through the air-sea interface, as illustrated in the schematic Fig. 3.3. If the horizontal transports in either medium can be estimated on the basis of observations, the horizontal transports in the other medium as well as the vertical fluxes through the air-sea interface can be obtained as residuals. Alternatively, the horizontal transports in the two media can be estimated independently and checked for consistency. (As noted above, the total energy fluxes through the air-sea interface are difficult to estimate directly on the basis of observations.)

The motions that accomplish the horizontal transports in both media are of comparable complexity. However, the atmospheric transports can be determined with a much higher degree of confidence than the ocean transports, simply because the observing system is so much more comprehensive. Therefore, the strategy indicated in Fig. 3.3, in which the atmospheric transports are measured directly and the oceanic transports and the air-sea fluxes are inferred indirectly as residuals, is the one that has usually been pursued, starting with the work of Vonder Haar and Oort (1973). Ocean transports have been estimated on the basis of direct measurements by Bryden and Hall (1980). We will briefly review these results in

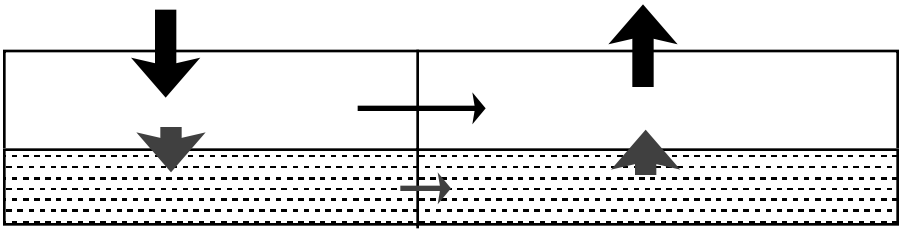

Fig. 3.3 A strategy for partitioning energy transports between atmosphere (upper layer) and ocean (lower layer). Transports and air-sea fluxes determined as residuals in the energy budget are denoted by stippled arrows. Solid vertical arrows at top denote net radiation at the top of the atmosphere.

Section 3.5, after we have discussed the distribution of net radiation at the top of the atmosphere and the horizontal transports within the atmosphere.

Before we examine the distribution of net radiation through the top of the atmosphere, let us consider some of the factors that influence it. Figure 3.4 shows a time-latitude section of the solar radiation (insolation) incident upon a horizontal surface at the top of the atmosphere, as determined by the sun-earth geometry, taking into account the obliquity of the earth's orbit. In midsummer the polar regions receive as much radiation as the tropics but the poles receive no insolation whatsoever during the 6 months between the autumnal equinox and the spring equinox. In the annual average, the North Pole receives 41.5% as much insolation as the equator and the Arctic Circle at 66.5°N receives about half as much as the equator.

Fig. 3.4 Solar radiation incident on a horizontal surface at the top of the atmosphere as a function of latitude and date, expressed in units of MJ m^{-2} day^{-1}. [Adapted from Meteorological Tables, R.J. List ed., Smithsonian Inst., Washington DC (1951)]

The albedo should be higher at high latitudes than in the tropics because of the presence of the icecaps and because of the persistent summertime cloud cover. Hence, in the annual mean the polar regions receive substantially less than half as much insolation as the tropics.

Now let us consider the meridional distribution of outgoing longwave radiation (OLR). In the absence of interference from the atmosphere, the meridional profile of OLR would be determined entirely by the effective temperature of the surface of the earth, which should be almost identical to its actual temperature. Annual average temperatures on Earth vary from roughly –15°C in the polar regions to almost 30°C in the tropics: a difference of.~15% in terms of absolute temperature. The ratio of polar to tropical OLR would be roughly $(0.85)^4 \sim 0.5$. Several aspects of the transfer of infrared radiation within the atmosphere tend to make this ratio closer to unity. Tropospheric lapse-rates tend to be steeper in the tropics than in high latitudes. Hence at the levels at which the atmosphere emits infrared radiation to space, the equator-to-pole temperature gradient is not as large as it is at the earth's surface. As documented in Fig. 3.5, water vapor, which is the among the most infrared absorbers is more abundant in the tropical atmosphere and spread through a deeper layer because its saturation mixing ratio approximately doubles for each 10°C temperature increase. Hence, the tropical atmosphere emits radiation to space from a higher level than the polar atmosphere and, since temperature decreases with height, it follows that the meridional gradient of water vapor tends to decrease the meridional gradient of OLR relative to what it would be in a dry atmosphere. Clouds act in a similar manner. It is not unusual for cloud tops in cumulonimbus to extend as high as 150 mb (14 km) in the tropics (which is still below the tropopause) and to spread out to form large areas of high overcast. At high latitudes, cloud tops rarely extend above the 250 mb (10 km) level.

Fig. 3.5 Meridional cross-section of zonally averaged specific humidity, based on 8 years of data from the ECMWF model. (From Schubert et al., 1990)

Hence, when atmospheric transmission is taken into account, we expect that the meridional

gradient of OLR should be considerably less steep than that of net downward solar radiation through the top of the atmosphere. Since the globally averaged net radiation through the top of the atmosphere, averaged over the year, should be close to zero, it follows that the net radiation must be downward at low latitudes and upward at high latitudes.

Figures showing the annual average distribution of net downward solar radiation, OLR, and net radiation through the top of the atmosphere are presented in Appendix 3.2. Also shown are the "Clear Sky" contributions to the fluxes (i.e., the values for pixels that are judged to be free of clouds) and the "Cloud Forcing" (i.e., the difference between the total fluxes and the contribution from the cloud free pixels). From an examination of these figures it is evident that in the annual mean, the meridional gradient of the downward solar ("Absorbed") flux is, indeed, much steeper than that of the upward "Longwave" flux, and as a result, the net radiation is downward equatorward of ~36° and upward poleward of that latitude. Local imbalances of net radiation in excess of 80 W m^{-2} (30% of the globally averaged absorbed solar radiation) are observed over large regions of the tropics and the polar caps.

The geographical distribution of the Clear Sky contributions is almost zonally symmetric, but for (1) the higher albedo of the land masses (the deserts, in particular); (2) slightly reduced OLR over parts of equatorial South America, Africa and Indonesia relative to the remainder of the tropics and (3) an east-west gradient in OLR across the North Atlantic, where the OLR contours parallel the annual mean sea-surface temperature contours The signature of the deserts is clearly evident even in the net radiation.

The "Cloud Forcing" contributes to the zonally averaged meridional gradient of net radiation and it introduces minor asymmetries such as the reduction of the downward net radiation in the regions of persistent stratus clouds off the coasts of Peru, Angola and California. There is a considerable amount of cancellation between the shortwave and longwave "Cloud Forcing"associated with the monsoons over the tropical continents and the ITCZ's over the tropical Atlantic and Pacific, and therefore, the signature of these cloud masses does not show up clearly evident in the distribution of net radiation. The signature of the ITCZ along 7°N is evident in zonally averaged values of both absorbed solar radiation and OLR in Fig. 6.

Figs. 5,7 and 8 document the large equatorial asymmetries in net radiation during summer and winter. The earth system is losing energy at a rate of ~160 W m^{-2} in the winter polar cap region, and gaining it at almost 100 W m^{-2} over a larger region in the subtropics of the summer hemisphere. Figs. 7 and 8 show that these asymmetries are mainly due associated with the absorbed solar radiation.

Questions

3.8 On the basis of the data presented in Fig. 6 of Appendix 3.2, roughly (to within 25%) estimate the poleward energy flux across 30° latitude in each hemisphere in the earth system.

3.9 Why would it be improper to pose the previous problem in terms of seasonal data such as those presented in Figs. 7 and 8?

3.10 From a careful examination of Fig. 1 it is evident that the cloud forcing over the polar icecaps and over the deserts tends to warm, rather than cool. Why is the observed?

3.11 It is possible to pose balance requirements for horizontal energy transports into or out of a local region such as a continent or a desert. Evaluating such transports tends to be more difficult than evaluating those into a polar cap region bounded by a latitude circle. Explain.

3.5 Horizontal transport of moist static energy within the atmosphere

The poleward transport of moist static energy across a latitude can be expressed in the form

$$\frac{1}{g}\int_0^{p_0}\left[\overline{ve}\right]dp = \frac{c_p}{g}\int_0^{p_0}\left[\overline{vT}\right]dp + \frac{L}{g}\int_0^{p_0}\left[\overline{vq}\right]dp + \frac{1}{g}\int_0^{p_0}\left[\overline{v\Phi}\right]dp \qquad (3.2)$$

where each of the terms on the right-hand-side can be expanded in terms of the conventional space-time formalism. We will discuss the transports in terms of the same three-term expansion as was used in the previous chapter for the poleward transport of zonal momentum.

The transport of moist static energy (e) in the mean meridional circulations depends upon the difference between typical values of e in the upper and lower branches. The air in the upper branch generally exhibits smaller sensible and latent heat, but much larger values of geopotential. Because of this compensation, the difference in e between the upper and lower branches is quite sensitive to the mean tropospheric lapse-rate. For example, in the middle of the Hadley cell, at 15° latitude, temperatures at mid-depth in the PBL (925 mb) are ~ +20°C, the specific humidities are ~12 g kg^{-1} (80% relative humidity) and the height above sea level is ~0.75 km. The upper branch is centered ~12.25 km (200 mb) where T ~ –55°C and the specific humidity is negligible. The difference in e (upper branch minus lower branch) is

$$(-55-20)\,c_p \;-\; 0.012\,L \;+\; 11{,}500\,g$$

$$-75{,}000 \;-\; 30{,}000 \;+\; 112{,}700 \;=\; 7{,}700 \text{ J kg}^{-1}$$

Despite this strong compensation, it is clear that the troposphere as a whole is stably stratified, even in the tropics. It follows that the mean meridional circulations transport in the direction of the flow in the upper branch, where e is larger. The Hadley cell contributes to the required poleward transport of energy in the earth system and the Ferrel cell works against it. In general, the ageostrophic flow associated with thermally direct circulations transports energy horizontally from the heat source to the heat sink, and thermally indirect circulations transport it in the opposite direction (see Wallace and Hobbs, §. 9.2.2).

Data on the poleward fluxes of sensible heat, moisture and geopotential by the transients and the standing eddies are presented in the last two pages of Appendix 3.2. They were calculated by Schubert et al. (1990), based upon 8 years of operational analyses by the European Centre. Note that the vertical scale in these figures is proportional to log of pressure, rather than pressure itself, so that care needs to be taken in inferring mass-weighted vertical integrals from the data in the figures. Units are given at the top of each figure. If one wishes to compare the contributions of the transports of latent and sensible heat, the transport of specific humidity, expressed in g kg^{-1} should be multiplied by $L/c_p \times 10^{-3} = 2.5$.

In the winter hemisphere, the poleward transport of moist static energy is dominated by the sensible heat term, which is poleward at all levels. The largest transports are observed ~50°, latitude, well poleward of the largest transports of zonal momentum. Near that latitude, the vertical profile of the transport is quite distinctive and reproducible, with prominent maxima near the 850 mb level and in the lower stratosphere. In the Northern winter, the transients and the standing eddies make roughly comparable contributions to the poleward heat transport, whereas in the Northern summer and in the Southern Hemisphere during both seasons the transients account for most of the transport.

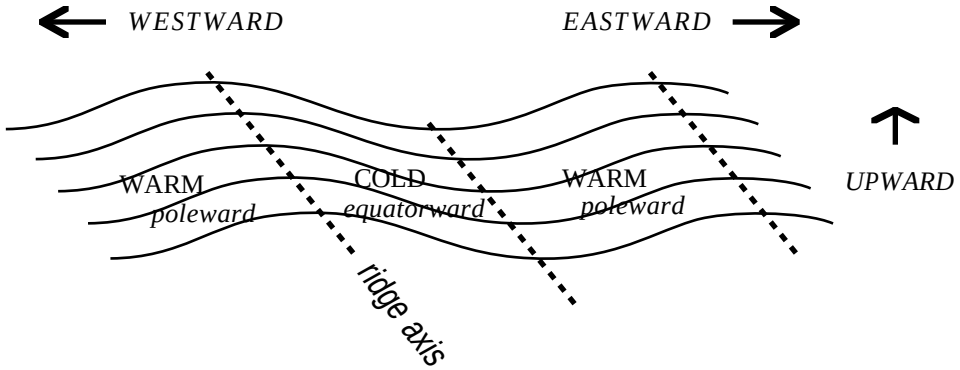

Fig. 3.6 Idealized longitude-height section through waves that transport heat poleward, showing pressure surfaces and axes of coldest and warmest air and poleward and equatorward flow.

The axes of eddies or waves that transport heat poleward tilt westward with height for the same reasons that the axes of eddies or waves that transport westerly momentum poleward tilt eastward with increasing latitude. Fig. 3.6 was constructed by flipping Fig. 2.11 horizontally rescaling it to compress it vertically and stretch it horizontally, relabeling "POLEWARD" as "UPWARD", and replacing the arrow denoting light zonal winds in Fig. 2.11 with "WARM" and the arrow denoting strong zonal winds by "COLD". The latter transformation is justified by the fact that *zonal momentum* is inversely proportional to the *meridional distance* between

pressure surfaces (through the geostrophic equation), while *temperature* is directly proportional to the *vertical distance* between pressure surfaces through the hypsometric equation. The meridional profile of $\left[\overline{v}^{*}\overline{T}^{*}\right]$ for DJF (Appendix 3.2, Fig. 7), with strong poleward transports across 60°N and almost no transport across 25°N is qualitatively consistent with the vertical tilts of the stationary waves on those latitude circles, as shown in Fig. 3.7.

Fig. 3.7 Longitude-height sections of the eddy component of the climatological mean streamfunction field for DJF along 60°N, where the poleward standing eddy heat transport is strong, and along 25°N, where it is almost zero. After Hoskins et al., 1989.

The latent heat transports tend to be concentrated in the lower troposphere and to peak at somewhat lower latitudes than the heat transports. It is evident that they make a substantial contribution to the transport of moist static energy, particularly during summer. The strong poleward transport of moisture by the standing eddies during JJA is a reflection of the strong influence of the subtropical oceanic anticyclones in the lower tropospheric flow, which carry warm, moist air northward over the western Pacific, much of East Asia, the western Atlantic and the eastern United States, while they carry cooler, much drier air southward over the eastern Pacific and Atlantic, as shown in Figs. 3.8 and 3.9.

Fig. 3.8 Climatological mean sea-level pressure field for JJA, after Schubert et al., 1990

Fig. 3.9 Climatological mean 850 mb specific humidity fields for JJA, after Schubert et al., 1990

The transports of geopotential are a full order of magnitude smaller than the sensible heat transports. We might have anticipated that result on the basis of scaling arguments, since it is

easily shown that the geostrophic wind does not contribute to the meridional transport of geopotential (see Problem 3.20). Yet despite their small size, they exhibit a coherent spatial pattern. For example, both the transients and the standing eddies transport geopotential equatorward across 30° at the jetstream level in DJF. In general, the geopotential transports by the transients and standing eddies tend to be large where the zonal momentum transports exhibit their primary maximum and they are in the opposite direction from the momentum transports. This relationship can be understood qualitatively in terms of the relationships illustrated schematically in Fig. 3.10. For simplicity, let us assume that the wave pattern is stationary, and that air parcels are moving through it from west to east, with mean speed $[u]>0$. It is clear that air parcels moving through the wave exhibit large zonal accelerations in association with the undulations in u^* imposed by the meridional tilt of the wave axes. Air parcels passing through the troughs of the waves are accelerating as they enter the region of positive u^* in the poleward flow, and air parcels passing through the ridges are decelerating as they enter the region of negative u^* in the equatorward flow. These accelerations must be accompanied by poleward cross-isobar flow in the wave troughs and equatorward cross-isobar flow in the ridges, as indicated in the figure. Hence, $[v_a^*\Phi^*] = [v^*\Phi^*] < 0$. The same argument holds if the wave is propagating zonally with phase speed c, provided that $[u]>c$, so that air parcels move through the waves from west to east. The larger the value of $([u] - c)$, the stronger the accelerations in the ridges and troughs of the waves and the larger the equatorward transport of geopotential.

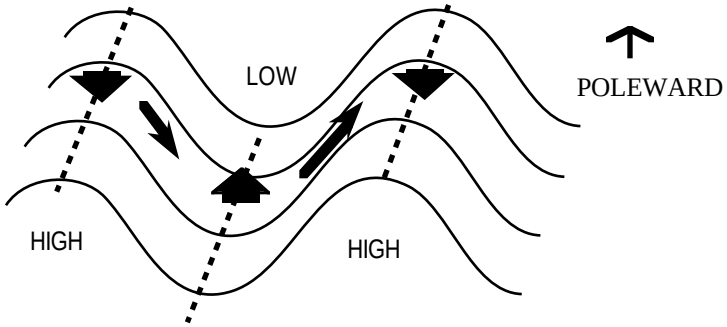

Fig. 3.10 Schematic illustration of a wave which transports zonal momentum poleward and geopotential equatorward. The wave pattern is identical to the one in Fig. 2.11. Note that the geopotential height contours are sinusoidal. The short arrows indicate the sense of the cross-isobar flow required to account for the zonal accelerations of air parcels passing through the waves.

The above argument can be made more quantitative by writing the zonal momentum equation for the stationary waves in Lagrangian form

$$\frac{Du^*}{Dt} = [u]\frac{\partial u^*}{\partial x} = fv_a^* \tag{3.3}$$

multiplying by Φ*, zonally averaging, and using the identity

$$\left[\Phi^* \frac{\partial u^*}{\partial x}\right] = -\left[u^* \frac{\partial \Phi^*}{\partial x}\right] = -f[u^* v^*] \tag{3.4}$$

we obtain

$$[v_a^* \Phi^*] = -[u][u^* v^*] \tag{3.5}$$

This derivation is easily extended to a zonally propagating wave with eastward phase velocity c, in which case, $[u]$ is replaced by $([u] - c)$. Since the phase speed of the transient eddies in the extratropics is generally eastward, the ratio $[\Phi^* v^*] / [u^* v^*]$ tends to be somewhat larger for the standing eddies than the transients.

Questions

3.12 At 15°N during wintertime $\int_0^{p_0} [\overline{qv}]dp$ and $\int_0^{p_0} [\overline{vT}]dp$ are equatorward, yet the mass weighted transport of moist static energy is poleward. Explain.

3.13 Estimate *e* in the upper and lower branches of the Ferrel cell at 45°N during DJF. Is the meridional transport of moist static energy larger, in absolute value, for the Hadley cell or the Ferrel cell? Explain.

3.14 At 15° latitude the mean meridional motions associated with the Hadley cell are ~2 m s^{-1} during DJF and they extend through a depth of ~150 mb (1.5×10^4 Pa). Using the estimates of the moist static energy in the upper and lower branches given in the text, estimate the transport of moist static energy (in units of W) across 15° latitude.

3.15 On the basis of the data given in Fig. 7 of Appendix 3.2, roughly estimate the poleward transport of moist static energy across 30°N (in between the Hadley and Ferrel cells) during DJF. [Hint: Ignore the contribution from the geopotential.]

3.16 Compare the transports in the two previous problems. If we assume that the eddy transports across 15°N are of secondary importance are the two estimates consistent?

3.17 On the basis of the results of in Problem 3.15 and a cursory inspection of the JJA eddy fluxes in Fig.8 of Appendix 3.2, make a rough estimate of the annual average poleward

transport of moist static energy across 30°N and compare it with the balance requirement in Problem 3.8. If the two estimates were highly accurate, should they necessarily work out to be the same?

3.18 What kind of processes have we ignored in not taking into account the phase changes between liquid water and ice in estimating the meridional transport of moist static energy? Are they likely to be important?

3.19 At the 850 mb level at 50°N during wintertime, the temporal variance of v is 40 $m^2 s^{-2}$ and the temporal variance of T is 20 K^2. Estimate the temporal correlation between v and T in the transients and compare it with the corresponding statistic for u and v, as computed in Problem (2.7).

3.20 Prove the identity (3.4)

3.21 Prove that $[v^*\Phi^*] = [v_a^*\Phi^*]$ (Hint: Prove that $[v_g^*\Phi^*] = 0$.)

3.22 Using a diagram and a mathematical derivation closely paralleling (3.3–3.5), prove that in the absence of diabatic heating,

$$[\omega^*\Phi^*] = -(f / \sigma)\,([u] - c)[v^*T^*].$$

3.6 Meridional transport of heat within the ocean

As noted in §3.4, it is possible to infer the meridional heat transports by the ocean circulation as a residual in the global energy balance. Since the atmospheric energy transports can be determined to a higher level of accuracy in the Northern Hemisphere, we have more confidence in the transports in the northern oceans. The residual estimates based on the zonally averaged atmospheric transports do not tell us how the transports are partitioned between the individual ocean basins, but they indicate that the transport should be northward in the Northern Hemisphere and that it should account for ~25% of the energy transport required to balance the meridional profile of net radiation through the top of the atmosphere.

As in the atmosphere, the ocean transports can be partitioned into components from transients, from basin-wide, wind-driven gyre circulations in the horizontal plane analogous to the atmospheric stationary waves, and overturning in the longitude-height plane associated with the deep "thermohaline circulation", which may be viewed as the counterpart of the atmospheric mean meridional circulation, although it is dependent upon longitude and it exhibits a more complicated vertical structure than the tropospheric mean meridional circulations because of the formation of layers of water with temperatures and densities intermediate between those of surface and bottom waters through air-sea interaction in middle latitudes. The transient

component of the transport is difficult to determine directly from observations, since much of the transient variability in the ocean occurs on space scales of 10-100 km, which corresponds to the oceanic radius of deformation. Such small eddies might not be very effective at transporting heat over large distances. The gyres definitely contribute to the required poleward heat transport. The Gulfstream and the Kuroshio current carry large masses of warm water poleward, and cooler currents on the eastern side of the basin return it to the tropics after it has lost large amounts of its energy by upward fluxes through the air-sea interface. However the gyres are not the whole story: the thermohaline circulation plays an important role which has appears to be quite different in different ocean basins.

As anticipated by Stommel (194xx), the formation of "bottom water" in the oceanic thermohaline circulation takes place in localized regions at the edge of the sea-ice where the surfaces water become sufficiently cold and salty to achieve the density required to break through the thermocline[12]. The process is somewhat analogous to deep convection in the tropical atmosphere, only upside down: plumes of negatively buoyant water sink to the bottom and flow equatorward as part of a large circulation cell in which water parcels may take centuries to make a complete circuit. The existence of such a circulation has been confirmed by the measurement of freons of recent anthropogenic origin in the bottom waters of the North Atlantic, which have been observed to spread southward over the past few decades from a source in the Greenland Sea. A similar sinking region has been observed in the Weddell Sea in the Antarctic. The thermohaline circulation in the Atlantic carries warm, surface water northward and much colder bottom water southward. It is believed to extend from the Greenland Sea across the equator into the Southern Hemisphere, and to be connected to the other oceans via the Antarctic to form a giant "conveyor belt" (Broecker reference). The oceanic heat transport by this circulation is northward (i.e., equatorward) in the South Atlantic and southward in the other ocean basins.

Bottom water does not form in the North Pacific, apparently because the surface waters at the edge of the sea-ice in the Gulf of Alaska and the Bering Sea are too fresh to become dense enough to sink. Broecker has proposed that a similar situation might have existed in the North Atlantic during the "Younger Dryas" period ~15,000 years ago, when the Atlantic sector of the hemisphere suffered a rather sudden relapse into ice age conditions which lasted ~x,000 years. Without the northward heat transport associated with the thermohaline circulation, the North Atlantic would have become much colder, allowing the ice edge and the adjacent continental ice sheets to advance. Broecker proposed that the shutoff of the circulation might have been due to a decrease in precipitation over the North Atlantic and the drainage basins of the rivers that flow

[12] The salinity of the surface water is increased by the rejection of salt during ice formation.

into it, or to a temporary diversion of one of the major rivers.[13]

3.7 Energy fluxes at the earth's surface

Distribution; Land vs. ocean; concentration in areas of cold advection, such as the western boundary currents. Role in modulating SST. Influence upon boundary layer structure (cloudiness, humidity..) To be added. For this year, it is recommended that the student read Wallace and Hobbs, § 7.3 – 7.5.

3.8 Further comments on the hydrologic cycle

From the foregoing discussion it is evident that the atmospheric transport of water vapor influences the salt budget of the oceans. It also influences the storage and flow of liquid water and ice on land. These relationships can be expressed in the form

$$\int_0^{p_0} \left[\overline{q\vec{V}}\right] dp = E - P = X \qquad (3.6)$$

where E and P are the rates of precipitation and evaporation per unit area, and X represents the appropriate water balance quantities on the underlying surface. Over the oceans X is a source term on the equation for the time-rate of change of salinity. Over land it represents the (negative) rate of change of storage in lakes and soils plus the convergence of the transport by rivers and subsurface aquifers. For the special case of a landlocked basin, it reduces to the rate of change of the storage. It is evident from the large interdecadal changes in the levels of lakes such as the Great Salt Lake in the western U.S. and the Caspian Sea in the U.S.S.R. that the storage, which represents the time integral of the convergence of the atmospheric transport of water vapor into the basin, exhibits behavior suggestive of a "random walk" process. Over the continental ice sheets, X represents (negative) changes in storage plus the convergence of the horizontal transport of ice. For example, in the center of a steady-state ice cap, the mass acquired from the excess of precipitation over evaporation is balanced by a divergence of ice toward the edges of the cap.

---

[13] Broecker suggested that the deposit of sediments by the retreating continental ice sheets might have temporarily diverted the Mississippi river into the St. Lawrence, thereby increasing the influx of fresh water into the North Atlantic.

The quality of the atmospheric data has reached the point where it is often possible to estimate the atmospheric water vapor transport divergence $\int_0^{p_0}\left[\overline{q\vec{V}}\right]dp$ more accurately than either $(E - P)$ or X. In this sense, the atmospheric water balance can provide useful constraints on the oceanic salinity budget, the land surface hydrology, and the mass balance of the ice sheets (e.g., see Rasmusson, 1968)). Accurate evaluation of the atmospheric transports requires at least twice daily data because of the large diurnal variability in the surface winds in the planetary boundary layer. For example, a moisture budget based on afternoon observations alone would tend to overemphasize the role of seabreezes and upslope mountain-valley wind systems.

Fig. 3.11 The annual average, zonally averaged distribution of evaporation (——) and precipitation (-----) per unit area expressed in meters per year. Arrows represent the sense of the required atmospheric water vapor transport, [Adapted from W.D. Sellers, *Physical Climatology*, Univ. of Chicago Press, 1965, p.84.]

Fig. 3.11 shows the balance requirements for the annual mean, zonally averaged atmospheric water vapor transport. The tropical monsoons and the ITCZ are responsible for the primary maximum in precipitation and the mid-latitude storm tracks are responsible for the secondary maxima ~50°N and 50°S. Evaporation tends to be largest in the relatively cloud-free regions of the subtropical anticyclones and the trades. As indicated in the figure, local imbalances in $E–P$ are associated with convergence or divergence in the meridional transport of water vapor. The tradewinds which are, in effect, the lower branch of the Hadley cell, account for much of the convergence of water vapor into the tropics. The poleward transport at higher latitudes is primarily associated with the eddies.

The hydrological cycle is the focus of the Global Energetics and Water Cycle Experiment (GEWEX), which is one of the major components of the International Geosphere Biosphere Program (IGBP).

Questions

3.23 On average over land, $P>E$. How do we know?

3.24 At 15° latitude the mean meridional motions associated with the Hadley cell are ~2 m s^{-1} during DJF and they extend from the 1000 mb level up to ~850 mb. The mean specific humidity within this layer is 12 g kg^{-1}. Assume that there is no moisture flux across the equator. Calculate the mean value of $E–P$ in the belt between the equator and 15°N, expressed in mm day-^{1} of liquid water.

3.25 It has been suggested that a global warming might result in an expansion of the Antarctic sheet. Explain, in terms of Eqn. 3.3 how this could occur.

3.26 Show that the low-level structure of baroclinic waves is conducive to the poleward transport of water vapor.

3.9 The local, zonally averaged thermodynamic energy balance

In Appendix 3.1 it is shown that the zonally averaged thermodynamic energy equation can be written in the form

$$\frac{\partial [T]}{\partial t} = [\omega]\left(\frac{\kappa [T]}{p} - \frac{\partial [T]}{\partial p}\right) - \frac{[v]}{\cos\phi}\frac{\partial}{\partial y}[T]\cos\phi - \frac{1}{\cos\phi}\frac{\partial}{\partial y}[v^* T^*]\cos\phi - \frac{\partial}{\partial p}[\omega^* T^*] + [\mathrm{Q}] \tag{3.7}$$

in spherical coordinates or in the approximate form

$$\frac{\partial [T]}{\partial t} = [\omega]\left(\frac{\kappa [T]}{p} - \frac{\partial [T]}{\partial p}\right) - [v]\frac{\partial [T]}{\partial y} - \frac{\partial}{\partial y}[v^* T^*] - \frac{\partial}{\partial p}[\omega^* T^*] + [\mathrm{Q}] \tag{3.8}$$

in Cartesian coordinates. If we neglect the advection of zonally averaged temperature by the mean meridional motions and the vertical heat fluxes on the basis of scaling arguments, we can write

$$\frac{\partial [T]}{\partial t} = [\omega]\left(\frac{\kappa [T]}{p} - \frac{\partial [T]}{\partial p}\right) + \mathrm{P} + [\mathrm{Q}] \tag{3.9}$$

These expressions are similar in form to Eqn's.2.8–10. The time derivative term on the left-

hand-side can be related to the time rate of change in the vertical distance between zonally averaged pressure surfaces, whereas in (2.8-10) it can be related to the meridional distance between pressure surfaces. In place of the inertial stability times $[v]$ we have the static stability times $[\omega]$. Diabatic heating takes the place of friction and the eddy heat flux convergence term P is similar in form to the expression for *G* in the zonal momentum equation.

In the average over a year, the time derivative term on the left-hand-side is virtually identical to zero so that the three terms on the right-hand-side must balance. Since the distributions of P and Q are known, at least qualitatively, $[\omega]$ can be determined as a residual. in the same way that $[v]$ was determined as a residual in (2.10). Fig. 3.12 shows the resulting balance in the meridional plane.

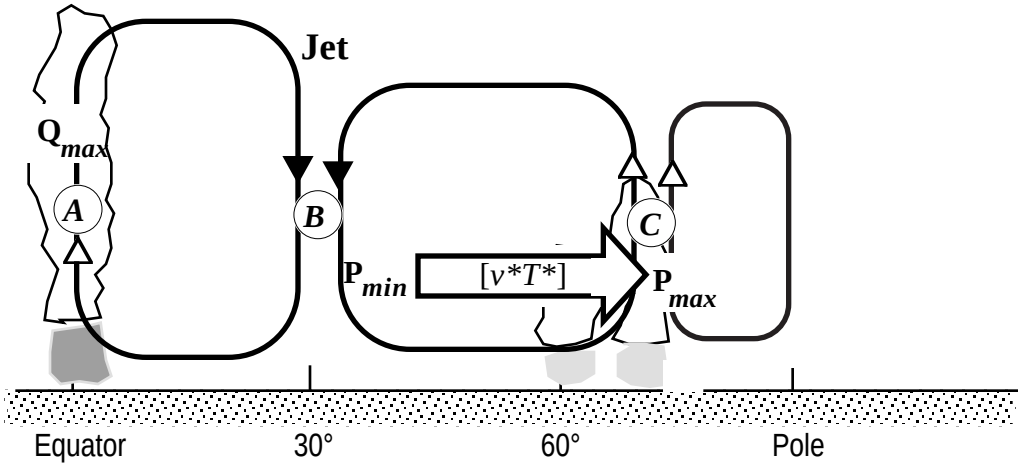

Fig. 3.12 See text for explanation.

Ascent is required at *A* to balance the large diabatic heat source associated with convection along the ITCZ and in the monsoon areas over the tropical continents and Indonesia, and descent is required at *B (*ascent at *C)* to balance the divergence (convergence) of eddy heat transport. The corresponding mean meridional circulation, which can be inferred from the continuity equation, are consistent with the analysis in §2.5.

3.10 Heat transports and Lagrangian mean meridional circulations

From the foregoing section it is evident that the temperature changes induced by the eddy heat transports in middle latitudes are partially compensated by the Ferrel cell. The compensation cannot be complete because $[\omega] \approx 0$ at the earth's surface, whereas $[v^*T^*]$ remains quite large. There are only two processes that can cool an air parcel while it resides poleward of a given latitude circle so that it is cooler when it crosses the circle going

equatorward than it was going poleward: adiabatic ascent and diabatic heat loss. Figures. 3.13 and 3.14 illustrate how these processes are reflected in the parcel trajectories. In this discussion we will assume that the eddies are wavelike and restricted to a channel of finite width, with wave amplitude decreasing as one approaches the northern and southern walls of the channel. The poleward wall represents the pole and the equatorward wall represents the outer edge of the tropics near 30°latitude.

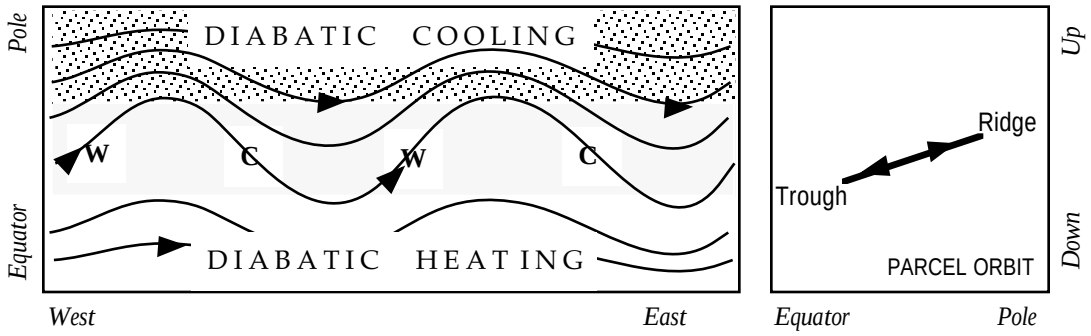

Fig. 3.13 Heat transport associated with a meridional gradient of diabatic heating. Left panel show streamlines on a map and the maxima and minima in T^*. Right panel shows the orbit of an air parcel moving through the wave, projected onto the longitude-height plane. Whether the parcel trajectories tilt upward toward the pole or not does not matter for the purposes of this discussion.

The component of the heat transport associated with diabatic heating is characterized by air parcels moving poleward and equatorward along the same trajectories in the meridional plane, which may either be sloping, as pictured in Fig. 3.13, or perfectly flat. In either case, the temperature differences between poleward and equatorward moving air must be a consequence of the diabatic heating and cooling that takes place while air parcels are displaced from their equilibrium latitude. Furthermore, it can be argued that the meridional gradient of diabatic heating is a consequence of the presence of the eddies. In the absence of eddies, the high latitudes would cool and the tropics would warm until some equilibrium temperature profile was reached. However, the mixing associated with the eddies prevents the atmosphere from reaching that equilibrium state. Tropical air is continually being carried poleward into high latitudes where it experiences strong diabatic cooling, and polar air is continually being advected into lower latitudes, where it rapidly warms up. In a steady state situation in which the diabatic heating is entirely due to the eddy mixing of sensible heat, (3.9) reduces to the statement that $P = -[Q]$. In the climatological mean, such a balance must exist close to the earth's surface, where the vertical velocities are very small in both the mean meridional circulations and in the eddies.

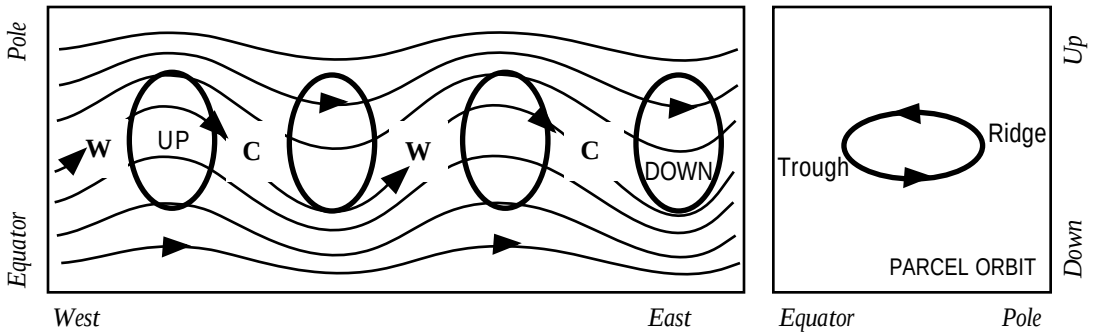

Fig. 3.14 As in the previous figure but for meridional heat transport induced by vertical velocities in the waves in the absence of diabatic heating. Ellipses in the left panel indicate the axes of the vertical motion field.

In the adiabatic case, the temperature differences between equatorward and poleward moving air are induced by vertical velocities in the ridges and troughs of the waves as pictured in Fig. 3.14. Any air parcel moving through the equatorward segment of its "orbit" in the wave is cooler than it was while in the poleward segment of its orbit, but it possesses more potential energy because it rose to a higher level in the atmosphere while ascending in its passage through the ridge (see Problem 3.22). Air parcels conserve static energy $c_p T + \Phi$ as they move around their elliptical orbits in the meridional plane, so there can be no net transport of static energy.

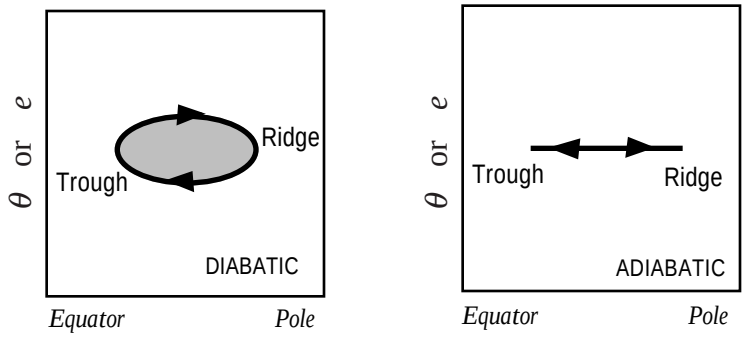

Fig 3.15 The orbits of the air parcels, projected onto the latitude vs. potential temperature (or static energy) plane. *Left panel:* heat transports associated with the meridional gradient of diabatic heating. *Right panel:* adiabatic case.

When the same orbits are viewed in the latitude–potential temperature (or static energy)

plane (Fig. 3.15),the transport associated with diabatic heating traces out an elliptical trajectory, with θ or e increasing while the air parcel is residing in low latitudes and decreasing while it is residing in high latitudes. It is readily verified that the poleward energy transport by the air parcel is proportional to the area enclosed by the ellipse divided by the time required for the parcel to execute a complete circuit around it. For the adiabatic case the area enclosed by the ellipse is zero.

Since the adiabatic component of the heat transport does not contribute to the poleward transport of static energy, it cannot change the zonally averaged temperature field. Hence, it must be exactly balanced by the vertical motion term in (3.9). The left-hand panel of Fig. 3.16 provides a geometrical perspective on the relationship between the eddies and the mean meridional circulation. It shows the orbits of the oscillatory component of the motion for selected air parcels moving through the waves. The vertical scale of the orbits is expanded in order to make the figure more readable. Near the middle of the channel, where the poleward heat transports are largest, the orbits of individual air parcels are quite large, but as one moves towards the side walls or the top and bottom they are increasingly constrained by the presence of the boundaries. Because of these geometrical constraints most of the air parcels near the bottom boundary are in the poleward segment of their orbits and hence the Eulerian flow (as would be measured by a fixed current meter) is poleward. For similar reasons, the Eulerian flow near the poleward boundary it is upward, etc. Hence, the counterclockwise "orbital" motion of the air parcels as they move through the waves gives rise to a mean meridional circulation in the same sense as the Ferrel cell. The adiabatic temperature changes induced by this cell exactly cancel the eddy forcing as represented by the P term in (3.9) and the equatorward transport of static energy by the cell exactly balances the poleward eddy transport of static energy.

But individual air parcels do not experience the mean meridional circulation pictured in the left panel of Fig. 3.16. If they did so (adiabatically) they would carry the zonally averaged isentropes with them and the meridional temperature gradient would steepen. The Lagrangian motion of individual air parcels must be purely oscillatory, as pictured in the right-hand panel of Fig. 3.14. Hence, the Eulerian mean meridional circulation must somehow be accompanied by a systematic "drift" of individual air parcels in the opposite direction, relative to the background flow.

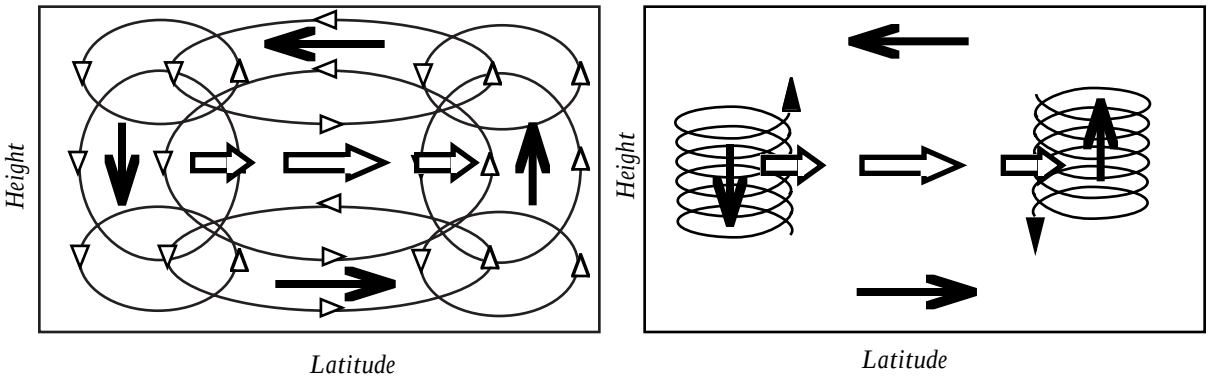

Fig. 3.16. *Left Panel:* The oscillatory component of orbits of air parcels moving through waves in the adiabatic case (ellipses); Meridional heat transports are indicated by large white arrows pointing toward the right and the induced Eulerian mean meridional circulation by black arrows. The vertical scale of the orbits is exaggerated. *Right panel:* The nonlinear "Stokes drift" associated with the meridional gradient in the amplitude of the vertical velocity field in the waves.

The right-hand panel of Fig.3.16 shows part of this so-called "Stokes drift"[14] superimposed the Eulerian mean meridional circulation. It may be viewed as a small (nonlinear) correction to the pure oscillatory motion discussed in the previous paragraph that owes its existence to the meridional gradient of the amplitude of orbital motion pictured in the left-hand panel of Fig. 3.14. Air parcels in high latitudes undergo descent in that segment of their orbits in which they are closest to the 'stormtrack' and they undergo ascent when they are farthest poleward and most distant from the stormtrack. Hence, in their passage through one complete wave or eddy, they experience somewhat more descent than ascent, so they end up lower than they started. The projection of the orbits of individual air parcels onto the meridional plane take the form of downward spirals. For analogous reasons, the "Stokes drift" of individual air parcels on the equatorward side of the stormtrack is upward. In steady-state, adiabatic flow, the Stokes drift and the Eulerian mean meridional circulation exactly cancel so that the Lagrangian mean meridional circulation is exactly zero and the motion of individual air parcels is purely oscillatory. If it were not purely oscillatory, the zonally averaged isentropes would be advected by the Lagrangian circulation in the meridional plane and a steady state could not be maintained.

[14] After Stokes (1847) who pointed out this phenomenon in connection with deep water waves. Water parcels in such waves drift in the direction of the waves by virtue of the vertical gradient of the amplitude of the oscillatory (orbital) motion that parcels experience as a wave passes. This wave induced drift exists independently of any Eulerian current thta might be present. If, and only if. the Eulerian current just happens to be equal and opposite to this 'Stokes drift', the Lagrangian parcel motion will be purely oscillatory and a passive tracer like the edge of a blob of dye will not move systematically in either direction.

In symbolic form we have, for the Eulerian motions (3.10)

$$\frac{\partial[T]}{\partial t} = s[\omega] + \mathrm{P} + [\mathrm{Q}] \tag{3.11}$$

whereas for the Lagrangian motions

$$\frac{\partial[T]}{\partial t} = s[\omega_L] + [\mathrm{Q}] = s[\omega] + s[\omega_S] + [\mathrm{Q}] \tag{3.12}$$

where the *L* subscript denotes Lagrangian and the *S* subscript denotes the Stokes drift. Note that in the Lagrangian formulation the 'Stokes correction' to the mean meridional motion replaces the eddy heat transport term P in the Eulerian formulation. Under adiabatic, steady state conditions $[\omega] = -[\omega_S]$ and $[\omega_L] = 0$. In the extratropical upper troposphere and stratosphere we observe a strong compensation between the Eulerian mean meridional circulations and the Stokes drift.

The distinction between Lagrangian and conventional Eulerian mean meridional circulations is illustrated in the following thought experiment. Suppose that we identify a large number of air parcels, equally spaced along a particular latitude circle, on a particular pressure level, and follow the subsequent motion of these marked parcels, as projected onto the meridional plane. Initially all the parcels occupy the same point in the plane, but they will instantly disperse into a cloud which gradually spreads until it occupies the whole domain. Beyond some characteristic "memory time", clouds of marked parcels emanating from different points in the meridional plane are no longer distinguishable from one another. For time intervals much shorter than this "memory time" is it meaningful to identify the "center of mass" of the cloud of air parcels and follow it as it moves in the meridional plane. The Lagrangian mean meridional circulation is defined as the vectorial time rate of change of the position of this cloud. In the presence of eddies the Lagrangian mean meridional motions need not be the same as the Eulerian mean meridional motions.

Kida (1977) performed such an experiment with a simple general circulation which was capable of simulating, at least qualitatively, the Eulerian mean meridional circulations including the thermally indirect Ferrel cell. Centroids of clouds of marked particles were tracked as they dispersed. The results are summarized schematically in Fig. 3.17. A well defined thermally direct circulation extending virtually from equator to pole emerged in the upper troposphere and lower stratosphere. At lower levels where the mean zonal winds were comparable to the phase speeds of the waves the clouds of tracers dispersed so rapidly that their centroids could not be reliably tracked. In low latitudes, where the eddies in the model simulation were quite weak, the Eulerian and Lagrangian mean meridional motions were found to be similar but in higher latitudes they were found to be in the opposite sense.

Fig. 3.17 Schematic illustration of the Lagrangian mean meridional motion as deduced from the motions of the of tracers inserted into the flow in a simple general circulation model. Looping arrows show tracks of individual tracers and heavy arrows show tracks of centroids of clouds of tracers emanating from points in the meridional plane. After Kida (1977).

The existence of such a circulation is confirmed by the remarkable dryness of the stratosphere where dew-points are on the order of –80°C throughout the year. The parts of the stratosphere in which temperatures as low as –80°C are observed are the equatorial tropopause and, for a few midwinter months, the polar night region. The Lagrangian circulation pictured in Fig. 3.17 is consistent with the idea, first suggested by Brewer (1949) that the equatorial tropopause acts as a "cold trap" for most of the air parcels entering the stratosphere in the ascending branch of the Hadley cell.[15]

Questions

(3.27) Consider a wave analogous to the one pictured in Fig. 3.14, but with an arbitrary phase angle between the ridges and the peak of the upward motion. Describe how the shape of the orbits of air parcels moving through the waves (as projected onto the meridional plane) depends upon this angle.

(3.28) Discuss how the orbit in Fig. 3.14 depends upon the doppler-shifted phase velocity of the wave $[u] - c$.

References

[15] The so-called Brewer-Dobson model of the stratospheric circulation (Brewer was responsible for the first definitive measurements of stratospheric water vapor) was rejected for many years because it appeared to be inconsistent with the Eulerian mean meridional circulation and it did not explicitly take into account the role of the eddy transports. It was not until the late 1970's that Brewer-Dobson model was reconciled with evidence concering the mean meridional circulations based upon Eulerian measurements.

Brewer, A.W., 1949: Evidence for a world circulation provided by the measurements of the helium and water vapor distributions in the stratosphere. *Quart. J. Roy. Meteorol. Soc.,* **75**, 351-363.

Bryden, H.L. and M.M. Hall, 1980: Heat transport by ocean currents across 25°N latitude in the Atlantic Ocean. *Science,* **207**, 884-886.

Dobson, G.M.B., 1951: Recent work on the stratosphere. *Quart. J. Roy. Meteorol. Soc.,* **77**, 488-494.

Kida, H. 1977: A numerical investigation of the atmospheric general circulation and stratoapheric-tropospheric mass exchange: II Lagrangian motion of the atmosphere. *J. Meteorol. Soc. Japan.,* **55**, 71-88.

Matsuno, T., Lagrangian motion of air parcels in the stratosphere in the presence of planetary waves. *Pure and Appl. Geophys.,* **118**, 189-216.

Oort, A.H. and T.H. Vonder Haar, On the observed annual cycle in the ocean-atmosphere heat balance over the Northern Hemisphere. *J. Phys. Oceanogr.,* **6**, 781-800.

Rasmusson, E.M., 1968: Atmospheric water vapor transport in the water balance of North America. II Large-scale water balance investigations. *Mon. Wea. Rev.,* **96**, 720-734.

Schubert, S., C.-K. Park, W. Higgins, S. Moorthi and M. Suarez, 1990: *An Atlas of ECMWF Analyses (1980-87). Part I– First Moment Quantities.* NASA Technical Memorandum 100747.

Schubert, S., W. Higgins, C.-K. Park, S. Moorthi and M. Suarez, 1990: *An Atlas of ECMWF Analyses (1980-87). Part II– Second Moment Quantities.* NASA Technical Memorandum 100762.

Stokes, G.G., 1847: On the theory of oscillating waves. *Trans. Cambridge Phil. Soc.,* **8**.

Trenberth, K.E., 1979: Mean annual poleward energy transports by the oceans in the Southern Hemisphere. *Dyn. Atmos. Oceans,* **4**, 57-64.

Vonder Haar, T. and A.H. Oort, 1973: New estimate of the annual poleward energy transport by Northern Hemisphere oceans *J. Phys. Oceanogr.,* **3**, 169-172.

4. DYNAMICS OF A GEOSTROPHICALLY BALANCED VORTEX

4.1 The governing equations

The zonally averaged versions of (1) the zonal momentum equation, (2) the thermodynamic energy equation, (3) the thermal wind equation, and (4) the continuity equation together form a closed system of prognostic equations which can be solved as an initial value problem in order to forecast the future evolution of the zonally averaged zonal wind and temperature fields in response to time dependent distributions of diabatic heating, sources or sinks of zonal momentum, and eddy fluxes of heat and zonal momentum. At each time step, the distribution of mean meridional circulations is derived as a by-product. The system of equations is, in fact, a specialized form of the quasi-geostrophic equations in which zonal momentum plays a role analogous to vorticity and the mean meridional circulations are the ageostrophic motions that maintain the zonally averaged zonal wind and temperature fields in a state of thermal wind balance, and the eddy fluxes play a role analogous to the vorticity and temperature advection which act to drive the zonal wind and temperature fields out of geostrophic balance.

The dynamics of a geostrophically balanced vortex were first discussed by Eliassen (1952) and applied more extensively to the diagnosis of mean meridional circulations in the earth's atmosphere by Kuo (1956). More recent reviews of this material can be found in Holton (1979: Section 10.4), Charney (1973), and Holton (1975), where these references are listed in order of increasing complexity of the treatment. This system of equations has been applied to the study of the annual cycle in the mesospheric jetstreams by Leovy (1964), the quasi-biennial oscillation by Wallace and Holton (1968) and the zonally symmetric component of the Martian circulation by Haberle (19xx).

The full system of equations governing the time evolution of geostrophic, zonally symmetric motions on a spherical earth is derived in the Appendices (not yet available). In this section we will deal with a simplified set based on Cartesian geometry, which retains only the leading terms.

Q the diabatic heating rate in deg K per unit time.

F the frictional source or sink of zonal momentum/unit mass.

G $-\partial[u^*v^*]/\partial y = [v^*\zeta^*]$: the source or sink of zonal momentum/unit mass due to meridional eddy transports.

P $-\partial[v^*T^*]/\partial y$: the time rate of change of temperature due to meridional eddy transports.

With these assumptions the set of equations that we will be discussing is analogous to the quasi-geostrophic equations except that we will retain the latitudinal variation of the Coriolis parameter. It is a tedious, but straightforward task to derive analogues of all the results that we

will present here for the primitive equations with spherical geometry, including vertical as well as horizontal fluxes. The simplified equations that will be our starting point are

$$\frac{\partial[u]}{\partial t} = f[v] + G + F \tag{4.1}$$

$$\frac{\partial[T]}{\partial t} = \mathrm{s}[\omega] + \mathrm{P} + [\mathrm{Q}] \tag{4.2}$$

$$\frac{\partial[u]}{\partial p} = \frac{R}{fp}\frac{\partial[T]}{\partial y} \tag{4.3}$$

$$\frac{\partial[v]}{\partial y} + \frac{\partial[\omega]}{\partial p} = 0 \tag{4.4}$$

This set of equations involves four unknowns: $[u]$, $[T]$, $[v]$ and $[\omega]$. We can reduce it to three equations in three unknowns by expressing the mean meridional motions in terms of the gradient of a streamfunction Ψ; that is

$$[\omega] = \frac{\partial \psi}{\partial y} \quad \text{and} \quad [v] = -\frac{\partial \psi}{\partial p} \tag{4.5}$$

Use of the streamfunction insures that (4.4) is satisfied. We can achieve some further simplification by making use of the equation of state in the form $T = p\alpha/R$ to transform (4.3) into an expression for the time rate of change of specific volume or thickness ($-\partial\Phi / \partial p$). In the transformed equation $\sigma = (R/p)s$, $P = (R/p)\mathrm{P}$ and $Q = (R/p)\mathrm{Q}$. Since all the terms in (4.1)-(4.4) are zonally averaged anyway, we can drop the brackets notation and write

$$\frac{\partial u}{\partial t} = -f\frac{\partial \psi}{\partial p} + G + F \tag{4.6}$$

$$\frac{\partial \alpha}{\partial t} = \sigma\frac{\partial \psi}{\partial y} + P + Q \tag{4.7}$$

and

$$\frac{\partial u}{\partial p} = \frac{1}{f}\frac{\partial \alpha}{\partial y} \tag{4.8}$$

Before proceeding any farther, let us reflect upon the nature of time dependent solutions of (4.6)-(4.8). At any instant in time, u is changing in response to the distributions of F and G, while α is changing in response to the distribution of P and Q which, for all we know, are entirely unrelated to those of F and G. Yet despite the lack of any dependable relation between G, F, P and Q, we know that α and u are changing in a manner consistent with the thermal wind equation: i.e., the meridional temperature gradient can't change unless the vertical wind shear changes, and vice versa. How does the temperature field know how the wind field is

changing, and vice versa? Any change in one field without a compensating change in the other immediately creates a small departure from geostropic balance (that is, the zonal wind suddenly finds itself subgeostrophic or supergeostrophic). The resulting imbalance between the meridional components of the pressure gradient force and the Coriolis force gives rise to an acceleration in the meridional direction and hence to mean meridional motions, together with the corresponding vertical velocities as required by the continuity equation. Hence it is the terms involving mean meridional motions (the ψ terms) in (4.6) and (4.7) which keep the zonal wind and temperature fields in thermal wind balance. The ageostrophic flow plays an analogous role in the quasi-geostrophic system.

Fig. 4.1 Zonally averaged zonal wind and temperature at the solstice seasons. Courtesy of R.J. Reed.

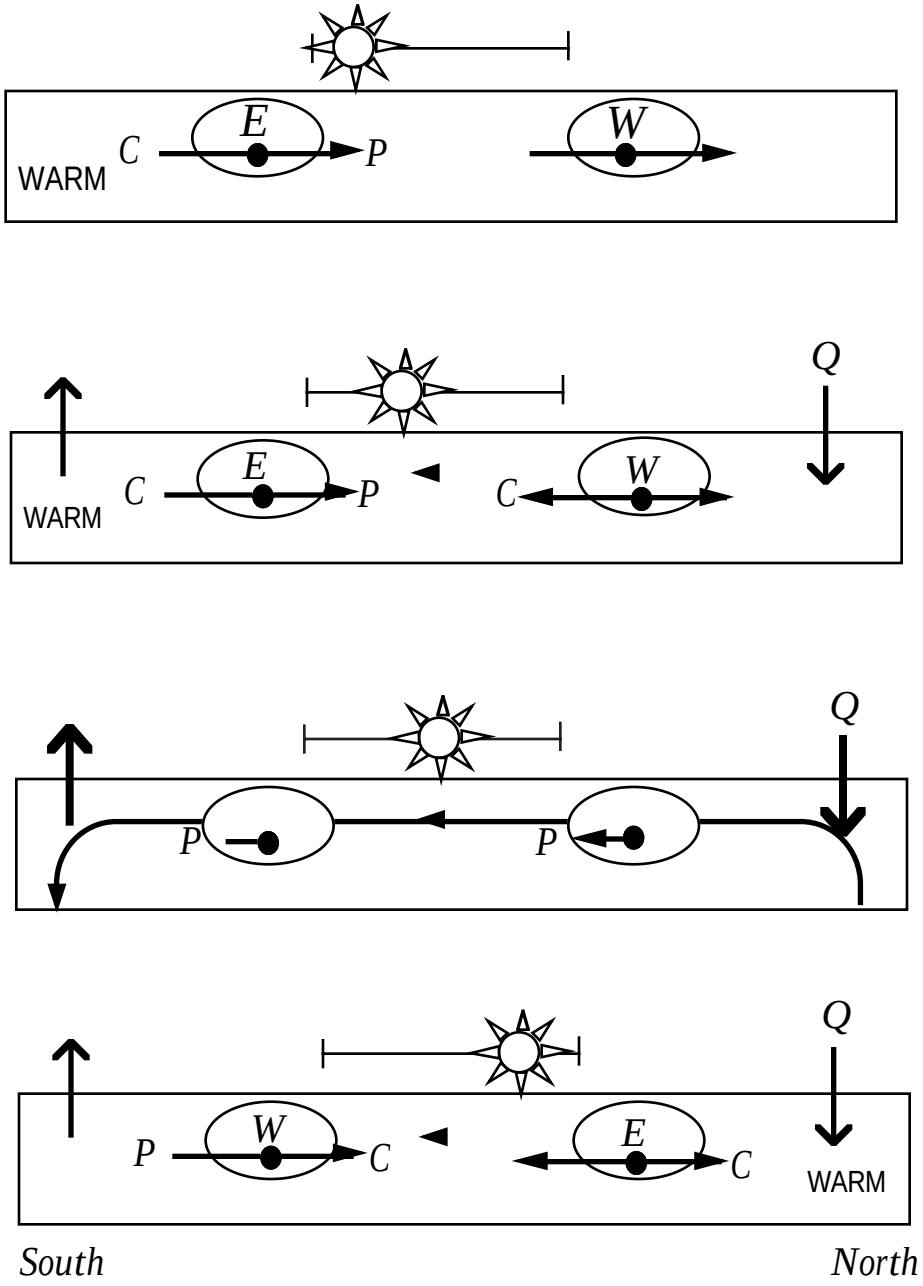

Fig. 4.2 Schematic of the seasonal evolution of the zonally averaged circulation in the mesosphere showing the jets (W, E), the pressure gradient (P) and Coriolis (C) forces, the diabatic heating (*Q*), the latitude at which the sun is overhead, and the mean meridional circulations, indicated by the cell. Intensity is indicated by line width and the thickness of the labels. The sections extend from ploe to pole and from 30 to 80 km.

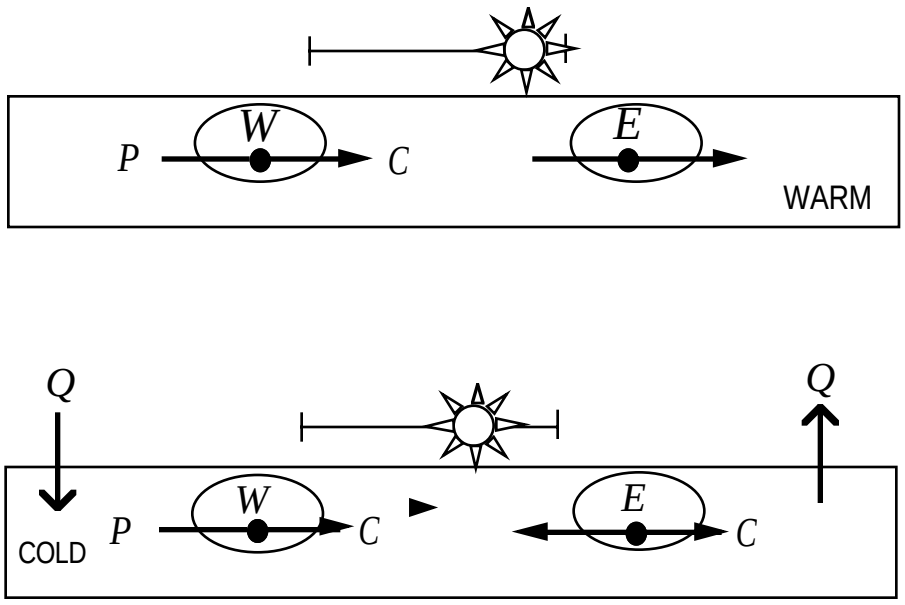

Fig. 4.2 Concluded

4.2 Some examples of geostrophic adjustment

In order to better understand how the mean meridional motions perform this "balancing act", let us consider a few specific examples:

a) the annual cycle in the mesosphere:

At the times of the solstices the zonal flow at mesospheric levels is characterized by a matched pair of mid-latitude jetstreams with westerlies in the winter hemisphere, as described in Figs. 4.1 and 4.2. With the approach of the equinoxes, temperatures at the stratopause level begin to warm over the pole which is experiencing late winter. The warming is reflected in the thickness field, so that geopotential height in polar latitudes at mesospheric levels must rise. As the heights over the polar region rise, the meridional pressure gradient weakens and the westerly jet in middle latitudes finds itself supergeostrophic. (Its supporting temperature gradient is literally being cut out from underneath it by the radiative warming at the polar stratopause). In response to this supergeostrophic flow the unbalanced equatorward Coriolis force induces a meridional circulation up the pressure gradient toward lower latitudes. This equatorward flow is accompanied by ascent over the pole at the stratopause level whose adiabatic cooling counteracts but doesn't completely cancel the radiative warming. Meanwhile, in the late summer hemisphere

the easterly jet is also finding itself in a supergeostrophic state as the polar regions begin to cool off at the stratopause level. The unbalanced Coriolis force induces a flow toward the pole which is accompanied by subsidence over the pole, whose adiabatic warming counteracts but doesn't completely cancel the radiative cooling. These relationships are illustrated in the second (February 15) panel of Fig. 4.2.

Note that the mean meridional circulation takes the form of a single cell extending from pole to pole. It is thermally indirect, with rising over the colder pole and sinking over the warmer pole and cross-isobar flow toward higher pressure. In effect, the mean meridional circulation is trying (without complete success) to maintain the existing meridional temperature gradient at the stratopause level, but in so doing, it is destroying the jetstreams. Kinetic energy is being converted into available potential energy which, in turn, is being destroyed by radiative heating over the cold pole and radiative cooling over the warm pole. The mesospheric jetstreams and the meridional temperature gradients at the stratopause level are both weakening at rates just sufficient to keep them in thermal wind balance. If the decrease in the temperature gradient gets a little bit ahead of the decrease in the strength of the jets, the winds will become more supergeostrophic and the mean meridional circulation will speed up a little so that the balance is restored.

Shortly after the time of the equinox (indicated by the April 1 panel in Fig. 4.2), the mesospheric jets in Fig. 4.1 completely disappear at precisely the same time that the pole-to-pole temperature gradient at the stratopause level reverses so that the springtime pole becomes warmer than the autumn pole. The mean meridional circulation continues in the same sense as in later winter, only from this point on it is thermally direct, with rising over the warmer pole, sinking over the colder pole, etc. This continuing mean meridional circulation gives rise to a new pair of jets whose polarity is the opposite of those that existed previously, as indicated in the next three panels.

Soon after the equinox (the July 15 panel), temperatures at the stratopause level eventually attain equilibrium with the thermal forcing and the radiative heating and cooling stop. In the absence of other forcing the mean meridional circulation would also grind to a halt and the zonal wind and temperature fields would remain in thermal wind equilibrium. But soon radiative heating and cooling resume with the opposite polarity, which leads to the development of a mean circulation in the opposite sense as indicated in the final panel.

In the situation considered above the only forcing was in the diabatic heating field Q. Although the Q term appears only in the Thermodynamic Energy Equations (4.7), the forcing was felt by the zonal wind through the $-\partial\psi/\partial p$ term in (4.6). Now let us consider a situation in which the forcing comes from the eddy flux terms P and G.

b) eddy transports in the mid-latitude troposphere

In the mid-latitude troposphere during winter, the eddies produce strong poleward transports of heat and zonal momentum. At 50°N, 500 mb the momentum forcing G is positive and increasing with height. Hence, the eddies are acting to increase the existing vertical wind shear, making the westerlies increase more rapidly with height. The poleward eddy heat transport is near its maximum at 50°N, so that P is increasing with latitude; from negative values to the south, to positive values to the north. Hence $\partial P/\partial y > 0$ and P is acting to reduce the existing mean temperature gradient; producing cooling to the south and warming to the north. These relationships are illustrated in Fig. 4.3.

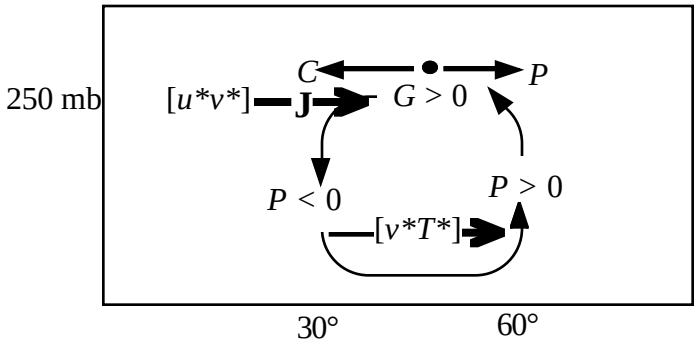

Fig. 4.3 Effect of eddy transports of heat and zonal momentum in making the zonal wind supergeostrophic poleward of the jetstream.

From the standpoint of the acceleration of the zonal flow, it is evident that the eddy transports of zonal momentum and heat are working at cross purposes: the former are acting directly to accelerate the westerly flow at 50°N at the jetstream level while the latter are acting indirectly, through their induced mean meridional motions, to decelerate it. The net result, to first order, is zero acceleration. However, from the standpoint of the induction of mean meridional circulations, it is evident that the two kinds of transports are both contributing to make the westerlies supergeostrophic at the jetstream level, thus inducing an equatorward flow which constitutes the upper branch of the Ferrel cell. The Coriolis force associated with this equatorward flow cancels the momentum forcing G, while the adiabatic heating and cooling associated with the corresponding vertical motions cancels the thermal forcing P. If there were no eddy transports, there would be no need for a Ferrel cell as a mechanism for keeping the mean zonal wind and temperature fields in thermal wind balance. In this sense we can think of the Ferrel cell as being driven by the eddies.

In the two examples considered with this section, some rather general conclusions can be drawn. If one type of forcing (G, F, P or Q) is considered in isolation, it must contribute to

inducing mean meridional circulations, which will always act so as to oppose the forcing. Despite this opposition, the zonal flow and its associated temperature field will change in the sense in which the forcing is acting. The changes will occur in such a way that the zonal wind and temperature fields remain in thermal wind balance. The particular example that we considered in detail involved forcing through the *Q* term. However, it is easily verified that these conclusions are valid for any of the forcing terms.

The combined effect of forcing from eddy fluxes *P* and *G* is inherently more complex. In the particular example that we considered, *P* and *G* were distributed in such a way as to produce little or no net forcing of the zonal flow ($\partial u/\partial t = 0$), but they worked together to force a strong mean meridional circulation. One can imagine other distributions (hypothetical ones, at least) which might produce a strong forcing of the zonal flow and little or no mean meridional circulations, or some of both. It remains to be seen whether, in the climatological mean, *P* and *G* just happen to be distributed so as to produce no net forcing of the mean zonal flow or whether there is some fundamental reason why they oppose one another.

Questions

4.1 Complete the series of sketches in Fig. 4.2.

4.2 Show that the energy in the A_Z and K_Z reservoirs in the middle atmosphere and the conversions between them undergo a semiannual cycle

4.3 If the tropospheric circulation were "started up" from a state of rest by imposing an equator to pole diabatic heating gradient, describe the first stages in its development.

4.3 A vectorial representation of the governing equations

We will now define a set of vectors which represent zonally averaged quantities in the meridional plane in which $\boldsymbol{j}$ is the unit vector in the meridional direction (positive poleward in the Northern Hemisphere) and $\boldsymbol{k}$ is the unit vector in the vertical (positive downward, toward increasing pressure). The zonally averaged *pressure gradient force vector* in the meridional plane is given by

$$\vec{\Sigma} \equiv -\nabla\Phi^{\prime} = (-\partial\Phi^{\prime}/\partial y\,\vec{j},\ -\partial\Phi^{\prime}/\partial p\,\vec{k}) = (fu\,\vec{j},\ \alpha^{\prime}\vec{k}) \qquad (4.9)$$

where $\Phi^{\prime}$ and $\alpha^{\prime}$ represent departures from the respective globally averaged profiles $\overline{\Phi}(p)$ and $\overline{\alpha}(p)$ for which the pressure gradient force is balanced by effective gravity. In regions of zonally averaged westerlies, $\vec{\Sigma}$ has a poleward component which is balanced by the Coriolis

force. In regions of the meridional plane that are warmer (i.e., exhibit larger thickness) than the global mean temperature (thickness) at that level, pressure tends to be high above and low below, in comparison to global means at the same levels, and so $\vec{\Sigma}$ exhibits a downward component. Note that the thermal wind equation (4.8) follows directly from the fact that $\vec{\Sigma}$ is the gradient of a potential function: i.e., it is equivalent to the vectorial identity

$$\vec{i} \cdot \left(\nabla \times \vec{\Sigma} \right) = 0 \tag{4.10}$$

where ***i*** is the unit vector in the zonal direction.

The *displacement vector* defined as

$$\vec{S} \equiv \left(\frac{u}{f} \vec{j}, \frac{\alpha'}{\sigma} \vec{k} \right) \tag{4.11}$$

may be interpreted as follows. We start with an atmosphere at rest relative to the rotating earth, and displace zonally symmetric rings of air meridionally letting $Du/Dt = fv$ and vertically letting $D\alpha/Dt = \sigma\omega$ until u and α' attain the observed values. It may be helpful to think of these displacements as relating to an imaginary membrane in the meridional plane which is of uniform thickness when the atmosphere is at rest but becomes stretched out in some places and thickened in others as zonal rings of air are displaced from their original positions The required displacements are the meridional and vertical components of $\vec{S}$. As illustrated schematically in Fig. 4.4, the displacement vectors tend to be pinched together in both the meridional and vertical directions poleward of the jetstream and stretched apart in both directions equatorward of the jetstream. The amount of pinching or stretching in the vertical is directly related to the local static stability and the amount in the horizontal is directly related to the local relative vorticity of the zonally symmetric flow. The amount of pinching in two dimensions is given by

$$-\nabla \cdot S = -\frac{\partial}{\partial y}\frac{u}{f} - \frac{\partial}{\partial p}\frac{\alpha'}{\sigma} \tag{4.12}$$

If the latitudinal variation of f is ignored, the expression on the right-hand-side may be recognized as the variable part of the quasi-geostrophic potential vorticity divided by f.[16] Hence, the thickness of the imaginary membrane is a measure of the potential vorticity.

---

[16] It is not necessary to ignore the latitudinal variation of f. In a more exact treatment with full spherical geometry, f in (4.11) is replaced by the inertial stability term in (2.8), which is equal to the meridional gradient of angular momentum per unit mass divided by $R_E \cos\phi$ and σ is replaced by $-\partial\theta/\partial p$. The area of distorted "grid squares" bounded by contours of constant m in the meridional direction and isentropes in the vertical is inversely proportional to the isentropic potential vorticity (IPV) times the factor $R_E \cos\phi$.

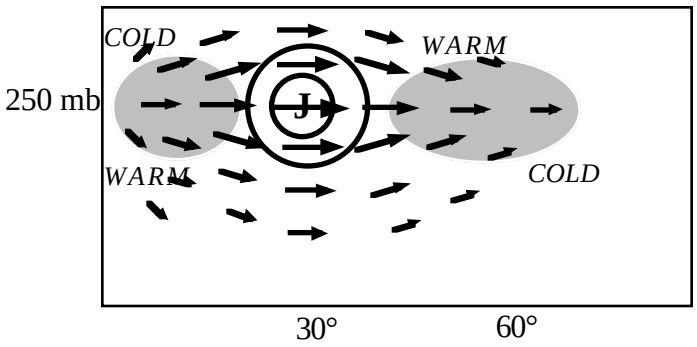

Fig. 4.4 Idealized displacement vectors for the observed tropospheric circulation showing stretching and pinching on the flanks of the jetstream.

Note that the pressure gradient force vector and the displacement vector are similar in form, and that

$$\vec{\Sigma} = \left(f^2, \sigma \right) \vec{S} \tag{4.13}$$

where the factor $\left(f^2, \sigma \right)$ is like a two-dimensional "stiffness": i.e., the force required to maintain a unit displacement of an element within the imaginary membrane[17]. The meridional stiffness of the membrane increases with latitude and the vertical stiffness is much larger in the stratosphere than in the troposphere.

The energy required to displace a zonal ring of air to its "observed position" in the distorted membrane is simply one half the force times the displacement

$$\frac{1}{2} \vec{\Sigma} \cdot \vec{S} = \frac{u^2}{2} + \frac{\alpha'^2}{2\sigma} \tag{4.14}$$

It is readily verified that when this expression is integrated over the mass of the atmosphere, the result is

$$\frac{1}{2g} \int_0^{p_0} \overline{\vec{\Sigma} \cdot \vec{S}} \, dp = \overline{K} + \overline{A} \tag{4.15}$$

It follows that *K* is the energy associated with the meridional stretching of the membrane and *A* is the energy associated with the vertical stretching.

Finally let us define the mean meridional motion vector

$$\vec{\Psi} \equiv \vec{i} \times \nabla \psi = \left(v \vec{j}, \omega \vec{k} \right) \tag{4.16}$$

and the forcing vector

$$\vec{\Gamma} = \left(\frac{G + F}{f} \vec{j}, \frac{P + Q}{\sigma} \vec{k} \right) \tag{4.17}$$

which incorporates the eddy forcing together with diabatic heating and friction.

---

[17] Note that σ is equivalent to N^2, the square of the Brunt-Vaisälä frequency.

It is readily verified that (4.6) and (4.7) can be written in condensed vectorial form

$$\frac{\partial \vec{S}}{\partial t} = \vec{\Gamma} + \vec{\Psi} \tag{4.18}$$

It follows that for climatological mean (steady state) conditions

$$\vec{\Psi} = -\vec{\Gamma} \tag{4.19}$$

Figure 4.5 illustrates the application of this identity to the observed tropospheric flow. It is a vectorial representation of the information in Figs. 2.19 and 3.12.

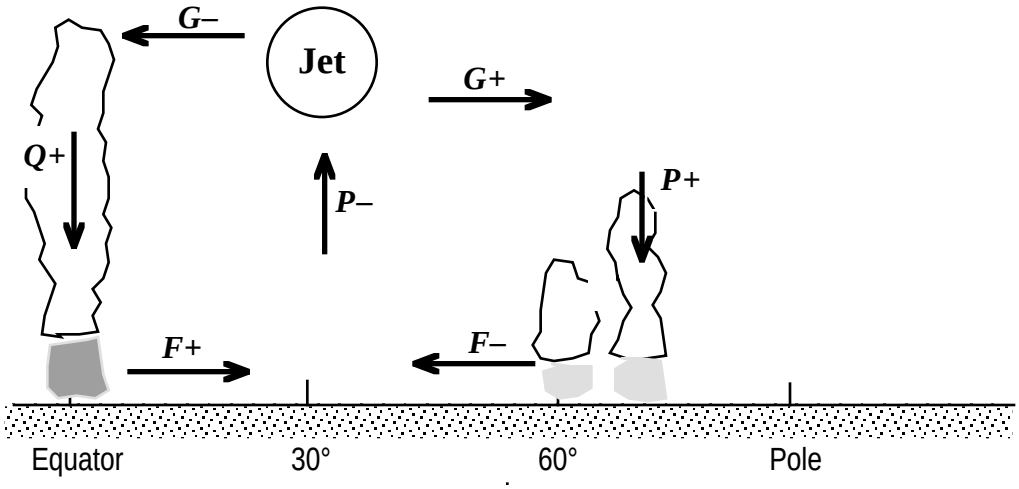

Fig. 4.5 A vectorial representation of the forcing vector in the meridional plane.

It follows from (4.17) that for the climatological mean flow, the forcing vector $\vec{\Gamma}$ must be nondivergent in the meridional plane and it is subject to the same bottom and lateral boundary conditions as the mean meridional circulations. If, at some point in time, the forcing vector does not satisfy these conditions, displacements (i.e., changes in zonal wind and temperature) must occur, and $\vec{\Gamma}$ will evolve in response to those displacements.

Problems

4.4 (a) Prove that

$$\frac{1}{g}\int_0^{p_0} \overline{\vec{\Psi} \cdot \vec{\Sigma}}\ dp = 0 \tag{4.20}$$

where the overbar represents a global average as in Chapter 1. (b) Show that a similar identity holds for the region of the meridional plane within any closed circulation cell such as the Hadley cell. Interpret this result in terms of (1.28).

4.4 The omega equation

We can gain a clearer understanding of the forcing of mean meridional motions by diabatic heating, friction, or eddy fluxes if we eliminate the time dependent terms in (4.6) and (4.7) and solve directly for Ψ in terms of *G, F, B,* and *Q*. To this end we differentiate (4.6) with respect to pressure, and (4.7) with respect to latitude and substitute the right hand sides of both equations into (4.8) to obtain, after some minor rearranging,

$$A(\psi) \equiv \sigma \frac{\partial^2 \psi}{\partial y^2} + f^2 \frac{\partial^2 \psi}{\partial p^2} = -f \frac{\partial}{\partial p}(G + F) + \frac{\partial}{\partial y}(P + Q) \qquad (4.21)$$

where $A(\ )$ is an elliptic operator. The distributions of $A(\psi)$ and ψ in the meridional plane should be qualitatively similar but of opposite sign, with the ψ distribution being smoother. Hence, distinct maxima and minima in ψ should correspond roughly to centers of circulation cells in the meridional plane. By our definition, the Hadley cell should circulate around a minimum in the ψ field and the Ferrel cell around a maximum.

In the middle of the Ferrel cell *G* is increasing with height (decreasing with pressure) and *P* is increasing with latitude from negative values to the south of the maximum in [v^*T^*] to positive values to the north of it, as summarized in Fig. 4.5. Hence, both terms in (4.21) are contributing to producing negative values of $A(\psi)$ which results in a local minimum and maximum in ψ itself. *F* also contributes to producing negative values of $A(\psi)$ near the top of the planetary boundary layer in middle latitudes because of the presence of surface westerlies. The reader is invited to verify that the *F, G,* and *Q* terms all contribute to positive values of $A(\psi)$ in the vicinity of the Hadley cell.

In Problem 2.18 the reader was asked to show that *G* can be interpreted as the poleward eddy transport of relative vorticity. Hence, the forcing term in (4.21) is quite analogous to its counterpart in the conventional, three-dimensional omega equation. It involves the vertical derivative of the (eddy induced) vorticity advection. The meridional gradient of *P* may be recognized as being equivalent to the Laplacian of the zonally averaged heat transport by the eddies.

Equation (4.21) has a simple vectorial intepretation. The right-hand side resembles the curl of the forcing vector $\vec{\Gamma}$, but the meridional component is scaled by f^2 and the vertical component by σ. Hence, it represents the curl of the tendency in the pressure gradient force $\vec{\Sigma}$ induced by the forcing vector $\vec{\Gamma}$. In a similar manner, the left-hand-side may be recognized as the curl of the tendency in the pressure gradient force induced by the mean meridional motion vector $\vec{\Psi} = \vec{i} \times \nabla\psi$. In order to assure that $\vec{\Sigma}$ remains irrotational as the flow evolves, the mean meridional circulations must cancel the effects of the forcing.

A more exact equation analogous to (4.21) can be derived from the complete zonally averaged versions of the zonal momentum equation and the First Law. The resulting equation contains a $\partial^2\psi / \partial y \partial p$ term and first order derivatives, but it is still elliptic, provided that angular momentum per unit mass decreases with latitude on isentropes, which corresponds to the criterion for stability with respect to zonally symmetric disturbances. If this criterion is satisfied, isentropic potential vorticity (IPV) will be positive everywhere, grid boxes bounded by m and θ contours will not double back upon themselves, and the imaginary membrane will not tear. Given suitable boundary conditions (e.g., $\psi = 0$ at the earth's surface and at the poles), (4.21) or its more exact counterpart can be solved by conventional numerical methods. For an example in which the complete equation is derived and solved numerically, see Wallace and Holton (1968).

We have now considered four different methods of inferring the mean meridional motions:

(1) Direct estimates of $[v]$ on the basis of wind data, and inference of $[\omega]$ from the continuity equation, given suitable top or bottom boundary conditions. This method is the most straightforward in principle, but it is difficult because $[v]$ is one or two orders smaller than v at individual longitudes, so that sampling errors may be larger than $[v]$ itself.

(2) Inference of $[v]$ from the zonally averaged zonal momentum equation (2.8-10), where $\partial[u]/\partial t$, and G are estimated on the basis of observational data and frictional drag F and the meridional advection terms $-[v]\partial[u]/\partial y$ and $-[\omega]\partial[u]/\partial p$ are assumed to be negligible. For seasonal mean statistics the time rate of change term can often be neglected. As in (1), $[\omega]$ can be inferred from $[v]$ on the basis of the continuity equation. This method yields results to within ~20% accuracy for the strength of the Ferrel cell. This method is difficult to apply in the planetary boundary layer where frictional drag is of first order importance.

(3) Use of the First Law to estimate $[\omega]$, from which $[v]$ is inferred through the use of the continuity equation. As in (2), the time rate of change term can often be neglected. This method is capable of defining the Hadley cell. Diabatic heating must either be neglected or somehow estimated and the meridional advection term $-[v]\partial[T]/\partial y$ is normally ignored.

(4) Use of the diagnostic equation (4.21) which, in effect, represents a combination of (2) and (3) to eliminate the time-dependent terms.

If the zonal flow is changing with time and if its future evolution is not known, the $\partial/\partial t$ terms will be difficult to estimate accurately, so that methods (2) and (3) will not be reliable. In this situation, (4) will give a better of the mean meridional motions.

It is of interest to compare these four methods of inferring the mean meridional motions to the four methods of estimating synoptic-scale vertical velocity at a fixed point in space and time. Method (1) is analogous to the kinematic method and it is subject to similar limitations with regard to sampling errors because of the smallness of the divergent component of the wind, which tends to be almost an order of magnitude smaller than the total wind. Hence, whatever method one uses to estimate the divergence, one is faced with the problem of evaluating small differences between large numbers Method (2) is analogous to the vorticity budget approach, in which one infers divergence as a residual from the vorticity equation and integrates vertically (usually downward from a "top" boundary condition) to obtain vertical velocity. Method (3) is the zonally averaged version of the "adiabatic method" (see Problem 8.7 of Wallace and Hobbs 1977)) in which the local vertical velocity is estimated as a residual from the First Law. Method (4) is analogous to family of diagnostic equations for ω, from which the time dependent terms have been eliminated. The simplest of these diagnostic equations is the quasi-geostrophic omega equation, analogous to (4.21) and the most complete is based on numerical solution of the primitive equations without any simplifications.

4.5 The potential vorticity equation

In order to deduce the changes in the zonally averaged wind and temperature fields which should occur in response to forcing from the *G*, *F*, *P* and *Q* fields it is necessary to eliminate the terms involving mean meridional circulations from (4.6) and (4.7). To this end we (1) divide (4.6) by *f* and differentiate it with respect to latitude,[18] and (2) divide (4.7) by σ and then differentiate it with respect to pressure, (3) add the two equations, and (4) reverse all the signs to obtain

$$\frac{\partial}{\partial t}\left(-\frac{\partial}{\partial y}\frac{u}{f}-\frac{\partial}{\partial p}\frac{\alpha'}{\sigma}\right)=-\frac{\partial}{\partial y}\left(\frac{G+F}{f}\right)-\frac{\partial}{\partial p}\left(\frac{P+Q}{\sigma}\right) \qquad (4.22)$$

[18] In accordance with the quasigeostrophic formulation we ignore the latitudinal variation of *f*. This approximation simplifies the algebra somewhat, but it is not necessary.

As in (4.12), the left-hand side may be identified with potential vorticity and is directly proportional to quasi-geostrophic potential vorticity if *f* is held fixed. This equation can also be expressed in the form

$$\frac{\partial}{\partial t}\left(\frac{1}{f^2}\frac{\partial^2\Phi}{\partial y^2}+\frac{1}{\sigma}\frac{\partial^2\Phi}{\partial p^2}\right)=-\frac{\partial}{\partial y}\left(\frac{G+F}{f}\right)-\frac{\partial}{\partial p}\left(\frac{P+Q}{\sigma}\right) \tag{4.23}$$

and the field of $\partial\Phi/\partial t$ can be recovered by numerical relaxation if the forcing function on the right-hand-side is known. It is easily shown that the eddy forcing terms on the right-hand-side are analogous to the vorticity and temperature advection terms in the quasigeostrophic geopotential tendency equation.

Note that (4.22) can be derived simply by applying the divergence operator to (4.18). The right-hand-side of (4.22) may be recognized as the convergence (in the meridional plane) of the forcing vector $\vec{\Gamma}$, which controls the thickening or thinning of the imaginary membrane. (The mean meridional circulations have no effect upon the thickness of the membrane, since they are nondivergent.) For quasigeostrophic scaling,with *f* and σ independent of latitude, (4.22) reduces to

$$\frac{\partial q}{\partial t}=-f\nabla\cdot\vec{\Gamma} \tag{4.23}$$

where *q* is the quasigeostrophic potential vorticity.

A forcing comprised of only one component of $\vec{\Gamma}$ will inevitably involve nondivergent and irrotational components of comparable magnitude. For example, if diabatic heating were the only forcing, as in the example discussed in §4.2, the nondivergent component would be $\sigma^{-1}\partial Q/\partial y$ and the irrotational component would be $\sigma^{-1}\partial Q/\partial p$. The former would drive a compensating mean meridional circulation, (perfectly compensating, if that is not precluded by the boundary conditions) while the latter changed the distribution of potential vorticity which reflects changes the distribution of *u* and α. Hence the forcing is compensated by the effects of the mean meridional circulations, but not completely. The zonal wind and temperature distribution change in a manner qualitatively consistent with the forcing, but the change is not as large as it would have been if the forcing had not been opposed by the mean meridional circulations.

From Fig. 4.4 it is evident that westerly jets lie in regions of strong potential vorticity gradient with high potential vorticity (a thickening of the membrane) on the poleward flank and low potential vorticity (a thinning of the membrane) on the equatorward flank. It follows that at any point in the meridional plane, a westerly acceleration is characterized by a poleward eddy transport of potential vorticity (mass of the membrane), which is given by

$$\left[q^* v^*\right] = \left[\zeta^* - f\frac{\partial}{\partial p}\frac{\alpha^*}{\sigma}\right]v^* = G - f\frac{\partial}{\partial p}\frac{\left[v^*\alpha^*\right]}{\sigma} \tag{4.24}$$

G may be recognized as the meridional component of the forcing vector, which is related to the acceleration of the zonal wind component. The interpretation of the other term will be discussed in the context of the following example.

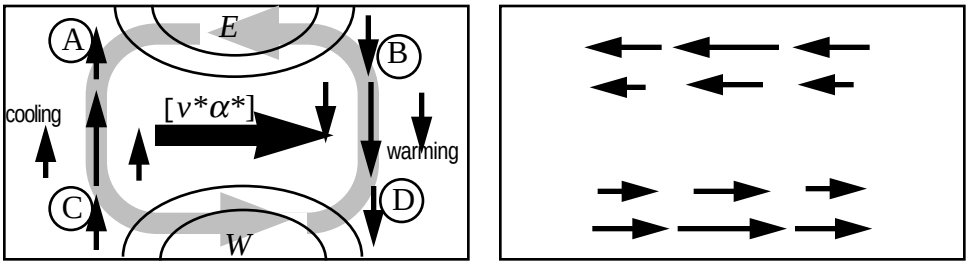

Fig. 4.6 *Left panel:* hypothetical distribution of eddy heat transports (heavy arrow) and resulting *P* field (vertical arrows) and induced mean meridional circulation (shaded arrows) which induces an easterly acceleration (upper ellipse) and a westerly acceleration (lower ellipse). Alternatively, the vertical arrows can be viewed as the diabatic heating *Q* field. Right panel: meridional transport of potential vorticity (membrane mass) that would produce the same net result. Latitude increases toward the right.

Fig. 4.6 depicts a localized region of poleward heat flux confined to the central part of the meridional plane so that $\vec{\Gamma}$ is convergent at A and D where it acts to increase the local static stability, and divergent at B and C, where it acts to decrease the static stability. Since the mean meridional circulations have no effect upon the distribution of potential vorticity, the potential vorticity must be increasing at A and D and decreasing at B and C. The forcing also contains a substantial nondivergent component, which (in accordance with (4.21) will be opposed by the mean meridional circulation shown in the figure. The Coriolis forces induced by this circulation cause an easterly acceleration in the upper branch and a westerly acceleration in the lower branch. These changes in zonal wind are consistent with the changes in potential vorticity. In summary then, the response to the forcing consists of geostrophically consistent changes in the meridional temperature gradient and the vertical shear of the zonal wind, in the direction implied by the forcing (e.g., a net warming occurs poleward of the strongest heat transports, where $P > 0$). The tendencies in both fields are implicit in the potential vorticity tendency, which can be inferred from a knowledge of the forcing, without reference to the mean meridional circulations.

The forcing in Fig. 4.6 can be related to the meridional transport of potential vorticity through the following argument. At lower levels, where $[v^*\alpha^*]$ is increasing with height, we

can write

$$\frac{\partial}{\partial p}\left[v^*\alpha^*\right]=\left[v^*\frac{\partial\alpha^*}{\partial p}\right]+\left[\alpha^*\frac{\partial v^*}{\partial p}\right]<0 \tag{4.25}$$

If we approximate v^* by v_g^*, and use the thermal wind equation, the second term on the right-hand-side vanishes. The remaining term, with sign reversed, may be recognized as the poleward transport of static stability, which is a component of the potential vorticity.

The change in the zonal wind field can be related to the change in the distribution of potential vorticity by the following argument.. Let us define the field G^*, a hypothetical momentum forcing that would change the distribution of potential vorticity (i.e., membrane thickness) at exactly the same rate within the atmosphere as the observed distrbution of eddy heat transports). For example, the stretching and pinching of the membrane induced by the P field forcing in Fig. 4.6 is equivalent to pulling the membrane poleward below the level of the strongest heat fluxes and pulling it equatorward above that level. Formally, we can write

$$\begin{aligned}\frac{\partial}{\partial y}\left(\frac{G^*}{f}\right)&\equiv\frac{\partial}{\partial p}\left(\frac{P}{\sigma}\right)\\&=-\frac{\partial}{\partial p}\frac{1}{\sigma}\frac{\partial}{\partial y}\left[v^*\alpha^*\right]\end{aligned} \tag{4.26}$$

And since σ is independent of latitude, it follows that

$$G^*=-f\frac{\partial}{\partial p}\frac{\left[v^*\alpha^*\right]}{\sigma} \tag{4.27}$$

Now provided that the eddy contribution to the forcing $\vec{\Gamma}$ vanishes on the boundaries, as in the situation pictured in Fig. 4.6, or that the point in question is sufficiently far away from the boundaries, the time rate of change of zonal wind should be completely determined by the time rate of change of potential vorticity within the fluid. Subject to these conditions, the zonal acceleration forced by the eddy transports, taking into account the eddy-induced mean meridional circulations is simply

$$\frac{\partial u}{\partial t}=G+G^*=\left[q^*v^*\right] \tag{4.28}$$

In order to complete the analysis we will need to consider the acceleration in the zonal wind induced by the eddy forcing at the boundaries of the domain. In order to illustrate the importance of this effect, let us assume that the eddy heat flux is independent of height and, for the sake of symmetry, let us assume that there is an upper boundary as well as a lower boundary on which $[\omega] = 0$, as shown in Fig. 4.7. In this case, the divergence of the forcing vector is concentrated at the upper and lower boundaries, along which the membrane material is being pulled out of or pushed into imaginary 'reservoirs'. Even though the eddies are not changing the distribution of potential vorticity within the fluid, we know that they must be

changing the temperature field because the eddy heat flux convergence *P* cannot possibly be cancelled by the eddy induced mean meridional circulations adjacent to the upper and lower boundaries, where the vertical velocity is vanishingly small. These changes will be induced by the boundary forcing in the elliptic equation (4.23). Segments of the boundary along which the storage of potential vorticity is increasing, will tend to 'attract' or 'pull' the neighboring part of the membrane through the boundary, and segments along which it is decreasing will tend to 'repel or push the neighboring membrane away. The smaller the "stiffness" σ, in the vertical the deeper the boundary effects will penetrate into the interior.

Within the affected layers the meridional gradient of thickness $\partial\alpha / \partial y$ is changing with time so we should expect to observe vertical shear in the zonal wind tendency. If the idealized atmosphere is deep enough, there may be layer in the interior that does not feel the effect of the potential vorticity changes in the reservoirs at the top and bottom. And since $\nabla \cdot \vec{\Gamma} = 0$ in the interior, it follows that the distribution of zonal wind and temperature cannot be changing there.

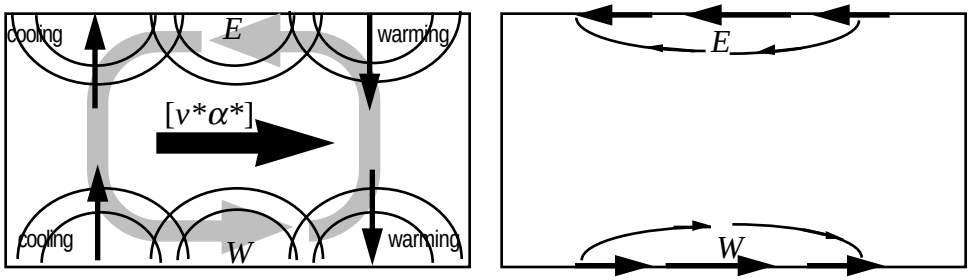

Fig. 4.7 As Fig. 4.6, but the poleward heat transport is independent of height. *Left panel:* the forcing vector is denoted by the vertical arrows. The induced mean meridional circulation is denoted by the thick, shaded ellipse. Contours at top and bottom give an indication of where the strongest net warming and cooling and zonal circulations are induced by the changes in potential vorticity in the top and bottom boundaries. *Right panel:* Net movement of potential vorticity (or membrane material) in the upper and lower boundaries due to the poleward heat fluxes, denoted by the heavier arrows. and the unduced (nondivergent) change in the state vector, denoted by the lighter arrows.

The resulting changes in zonal wind and temperature are shown in the left panel of Fig. 4.7. The poleward heat transports induce a mean meridional circulation which completely cancels their effect on the time rate of change of temperature at middle levels. Within that region, $\omega = -P/\sigma$ which is independent of height, $v = 0$, and u is not changing with time. Poleward of the strongest heat transports, the buildup of potential vorticity in the reservoir at the bottom may be viewed as pulling membrane material through the boundary. In terms of (4.23) the boundary

forcing is inducing height falls in the layer adjacent to the boundary, which become smaller with height as indicated by the contours.[19] In accordance with the hypsometric equation, thickness must be increasing within this layer. Equatorward of the largest poleward heat transports, changes in the opposite sense are occurring at the lower boundary and, by symmetry, there must be a sign reversal between the changes occurring along the top and bottom boundaries. Consistent with the pattern of induced membrane displacement and geopotential height tendencies, westerly accelerations occur along the bottom boundary and easterly accelerations along the top. The vertical shear of these accelerations is in thermal wind balance with the thickness changes described above: i.e., $\partial u / \partial p$ is positive in the lower layer, zero in the interior, and negative in the top layer.

Note that in the situation pictured in Fig. 4.7 the only changes in the distribution of potential vorticity that are taking place are within the reservoirs at the upper and lower boundaries. It is readily verified that the changes in potential vorticity along the boundaries are equivalent to what would be produced by a poleward transport of magnitude $[v^* \alpha^*] / \sigma_B$, concentrated in the boundaries, where σ_B is the value of static stability just inside the boundary. Hence,the poleward heat flux along the lower boundary has the effect of pulling membrane material poleward, inducing a westerly acceleration as indicated in the right-hand panel of Fig. 4.7. Note that the deformation of the membrane must be nondivergent, since potential vorticity is not changing, except on the boundaries.

The potential vorticity changes at the earth's surface play an important role in the tropospheric circulation. The poleward heat transport at the surface is about half as large as at the maximum in the vertical profile, near 850 mb. Since σ tends to be rather small in the troposphere, the induced changes in zonal wind and temperature extend through much of the lower troposphere.

Questions

4.5 Reinterpret the annual cycle in the zonally symmetric circulation of the middle atmosphere (Figs. 4.1 and 4.2) in terms of the changes in potential vorticity induced by the seasonally varying diabatic heating. [Hint: adapt the upper half of Fig. 4.6, where the vertical arrows are used to represent diabatic heating.]

4.6 Draw a diagram analogous to Fig. 4.6 to describe the response to a poleward transport of zonal momentum, centered in the middle of a rectangular domain and decreasing monotonically to zero on the boundaries.

---

[19] The induced height tendencies in (4.22) tend to be of opposite sense to the forcing term on the right-hand-side, just as Ψ in the omega equation (4.20) tends to be of opposite sense to the forcing on the right-hand side.

4.7 How could one estimate how much quasi-geostrophic potential vorticity is 'stored' in the reservoir at the lower boundary. [Hint: use as a reference value the potential vorticity of an atmosphere at rest. Assume that static stability is independent of height.]

4.8 Under what conditions can a forcing induce changes in the zonal flow in the absence of mean meridional circulations?

4.9 Write an expression for the convergence of the displacement vector $\left(-\nabla\cdot\vec{S}\right)$ in terms of the perturbation geopotential height field Φ'. This equation can be solved for Φ' if the distributions of $\left(-\nabla\cdot\vec{S}\right)$ in the interior and α' on the lower boundary are known. Relate this equation and the bottom boundary condition to potential vorticity. Specifically, show that the boundary condition can be viewed as the meridional distribution of potential vorticity in a reservoir along the bottom boundary.

4.10 Describe how the induced circulation in Fig. 4.7 depends upon the static stability. For example, suppose that the static stability along the upper boundary is much larger than along the lower boundary.

4.11 Prove that for quasi-geostrophic scaling, where $f = f_0$ and the heat and momentum transports are associated entirely with the geostrophic wind,

$$\frac{\partial[q]}{\partial t} = -f\nabla\cdot\vec{\Gamma} = -\frac{\partial}{\partial y}\left[q^* v^*\right] \qquad (4.25)$$

where q is the quasi-geostrophic potential vorticity. [Hint: expand q into components involving vorticity and static stability and make use of (4.23) and (4.24).] Note the similarity of (4.25) to the conventional quasi-geostrophic tendency equation.

4.12 Prove that the meridional heat fluxes by the eddies and the mean meridional circulations that they induce have no effect on the vertically integrated angular momentum.

4.6 Application to the winter stratospheric circulation

In §4.2 we considered the radiative forcing of the annual cycle in the zonally symmetric circulation of the middle atmosphere. In this section we will examine the northern wintertime circulation in more detail, with emphasis on the eddy forcing of the mean flow. Figure 4.8 shows zonally averaged wind and temperature fields for January based on four years of data compiled by Wu et al. (1984). The analysis relies heavily upon satellite radiances, which are used to infer the temperature distribution, from which the winds are computed from the thermal wind equation, using the operational tropospheric analyses as a lower boundary condition. The 'eddies' at this level are largely restricted to planetary waves with zonal wavenumbers 1, 2 and 3.

The 'polar night jet' with wind speeds in excess of 50 m s^{-1} is evident ~55°N at the 50 km level (6 scale heights). When midwinter warmings are not in progress, the speed of this jet often exceeds 65 m s^{-1}. Below the jet is a deep layer of relatively strong baroclinity extending from 2-6 scale heights. This region is characterized by strong poleward heat transports which reach peak values at the base of the jet. Note that these transports decrease rapidly with height within the jet itself. Large poleward momentum transports are also observed, with peak values at or above the top of the cross section, 5-10° equatorward of the jet and 10-15° equatorward of the strongest heat transports. Hence, westerly momentum is converging into the region directly above the strongest heat transports[20]. The situation in this region is somewhat analogous to conditions in the upper branch of the Ferrel cell where the eddy heat transport is also decreasing with height in the presence of strong positive values of *G*.

For both heat and momentum transports the standing eddy contribution is larger than the transient eddy contribution because the stationary waves account for most of the amplitude of zonal wavenumbers 1-3, not only in the stratosphere, but in the troposphere as well.

Questions:

4.13 Display the distribution of *P* and *G* in Fig. 4.8 in a format analogous to Fig. 4.5. Use this figure to infer the distribution of mean meridional circulations induced by the eddies.

4.14 Show that in the vicinity of the jet in Fig. 4.8 the heat and momentum transports make compensating contributions to the time rate of change of potential vorticity and to the poleward transport of quasi-geostrophic potential vorticity.

4.7 A world without eddies

A review of the Schneider / Lindzen / Hou zonally symmetric modeling results. [To be added]

---

[20] Since the strongest eddy transports of heat and westerly momentum are occurring at quite high latitudes in the stratosphere, it is worth keeping in mind that the convergence of the meridians makes a substantial contribution to the convergence of the transports. Because of this effect, the strongest convergence is not as far poleward of the peak transports as one might infer from a casual inspection of the diagrams.

Fig. 4.8 Meridional cross-sections of the zonally averaged Northern Hemisphere circulation during January based on four years of data, after Wu et al., 1984. The vertical coordinate is scale height, which may be taken as 8 km and the meridional scale extends from 10° ~to 85°N. *Top panels:* zonal wind (contour interval 10 m s^{-1}) and temperature (contour interval 10 K). *Middle panels:* transient and standing eddy heat transport (contour intervals 10 and 30 m s^{-1} K, respectively). *Lower panels:* transient and standing eddy transport of westerly momentum (contour intervals 50 and 20 m^2s^{-2}, respectively).

References

Eliassen, A., 1952: Slow thermally or frictionally controlled meridional circulation in a circular vortex. *Astrophys. Norv.,* **5**, 19-60.

Leovy, C.B., 1964: Simple models of the thermally driven mesospheric circulation. *J. Atmos. Sci.,* **21**, 327-341.

Holton, J.R., 1979: *An Introduction to Dynamic Meteorology*. 2nd Ed., Academic Press, 391pp.

Kuo, H.-L., 1956: Forced and free meridional circulations in the atmosphere. *J. Meteor*., **13**, 561-568.

Pfeffer, R.L., 1981: Wave-mean flow interactions in the atmosphere. .*J. Atmos Sci..,* **38**, 1340-1359

Wallace, J.M. and J.R. Holton, 1968: A diagnostic numerical model of the quasi-biennial oscillation.*J. Atmos Sci..,* **25**, 280-292.

Wu, M.F., M.A. Geller, J.G. Olson and M.E. Gelman, 1984: *Troposphere-stratosphere (surface-55 km) monthly general circulation statistics for the Northern Hemisphere—Four Year averages.* NASA Technical Memorandum 86182.

5. WAVE–MEAN-FLOW INTERACTION

5.1 Energetics of wave–mean-flow interaction

Let us now consider the role of the eddy transports in the exchange of kinetic and potential energy between the eddies and the zonally averaged flow. We begin by deriving an expression for the time rate of change of zonal kinetic energy. This is done simply by multiplying (2.10) by $[u]$ and integrating it over the mass of the atmosphere to obtain

$$\frac{\partial \overline{K}_Z}{\partial t} = \frac{1}{g}\int_0^{p_0} f\overline{[u][v]}dp + \frac{1}{g}\int_0^{p_0} \overline{[u]G}dp + \frac{1}{g}\int_0^{p_0} \overline{[u][F_x]}dp \qquad (5.1)$$

The first term on the right-hand side may be rewritten as $-[v]\dfrac{\partial[\Phi]}{\partial y}$, in which form it may be recognized as representing the down-gradient cross isobar flow. This term was related to the release of available potential energy through the $[\omega][\alpha]$ term in (1.28). This term is clearly positive in the Hadley cell, which is thermally direct with warm air rising in the deep tropics and slightly cooler air sinking in the subtropics, equatorward flow down the sea-level pressure gradient in the trades, and poleward flow down the pressure gradient in the westerlies in the upper troposphere. However, it is negative in the Ferrel cell which is thermally indirect with relatively warm air sinking in the subtropics and much cooler air rising near 60° latitude. The Hadley cell is 3-4 times as strong as the Ferrel cell, but the temperature gradient across the Ferrel cell is larger, by about the same factor, than that across the Hadley cell. Hence, there is a strong compensation between the energy conversions in the two cells: so strong, in fact, that one cannot say, with certainty, which way the net conversion goes. Most estimates favor a weak conversion in a thermally indirect sense, from kinetic to available potential energy.

The third term represents the effects of frictional dissipation. Since the frictional drag is generally in the opposite direction to the wind itself, this term represents a drain on the zonal kinetic energy.

The middle term will presently be shown to be the conversion from eddy kinetic energy to zonal kinetic energy. Zonal kinetic energy is increasing wherever there is a conversion of westerly momentum transport in a region in which the wind is already westerly and a divergence of westerly momentum transport out of a region in which the wind is already easterly and vice versa. At the jetstream level this term exhibits a negative extremum near 20° latitude, where westerly momentum is diverging out of a region of relatively weak (~15 m s^{-1}) westerlies on the equatorward flank of the jetstream and a somewhat stronger positive extremum near 45° latitude where the same amount of zonal momentum is being deposited by the eddies in a region of somewhat stronger (25 m s^{-1}) westerlies. Hence, it appears that this term represents a source of

kinetic energy for the zonal flow, that approximately balances the frictional dissipation.

Now let us consider the budget of eddy kinetic energy. We begin by applying (A5.10) first with $\psi = u$ and then with $\psi = v$ and adding the result to obtain

$$\frac{\partial \overline{K_E}}{\partial t} = -\frac{1}{g}\int_0^{p_0} \overline{\left[u^* v^*\right]} \frac{\partial [u]}{\partial y} dp - \frac{1}{g}\int_0^{p_0} \overline{\left[u^* \omega^*\right]} \frac{\partial [u]}{\partial p} dp - \frac{1}{g}\int_0^{p_0} \overline{\left[v^{*2}\right]} \frac{\partial [v]}{\partial y} dp - \frac{1}{g}\int_0^{p_0} \overline{\left[v^* \omega^*\right]} \frac{\partial [v]}{\partial p} dp$$
$$- \frac{1}{g}\int_0^{p_0} \overline{\left[u^* \frac{\partial \Phi^*}{\partial x} + v^* \frac{\partial \Phi^*}{\partial y}\right]} dp + \frac{1}{g}\int_0^{p_0} \overline{\left[u^* F_x^* + v^* F_y^*\right]} dp \qquad (5.2)$$

We neglect the two terms involving vertical fluxes of momentum on the first line on the basis of the scaling considerations discussed in §2.4, though there is no reason that we could not retain them if we wished. Comparing the two remaining terms on the first line, we note that extreme values of $\frac{\partial [u]}{\partial y}$, which occur on the flanks of the jetstream, are larger than extreme values of $\frac{\partial [v]}{\partial y}$, which occur near 30 and 60° latitude, by about a factor of 30. On the other hand, peak values of $\left[v^{*2}\right]$, which are observed ~50° latitude are about a factor of 4 larger than the largest values of $\left[u^* v^*\right]$, which are observed near the jetstream.[21] We also need to consider whether the eddy transports are large at the latitudes where the meridional gradients of [*u*] and [*v*] are large. We note that $\left[v^{*2}\right]$ is largest in the middle of the Ferrel cell, where the $\frac{\partial [v]}{\partial y}$ changes sign,while $\left[u^* v^*\right]$ is appreciable, not only in the core of the jet, but poleward and equatorward of it, where $\frac{\partial [u]}{\partial y}$ is quite large. Therefore, we are justified in neglecting the $\left[v^{*2}\right]\frac{\partial [v]}{\partial y}$ term, which involves the exchange of kinetic energy between the eddies and the mean meridional circulations. Hence, (5.2) reduces to

$$\frac{\partial \overline{K_E}}{\partial t} = -\frac{1}{g}\int_0^{p_0} \overline{\left[u^* v^*\right]} \frac{\partial [u]}{\partial y} dp - \frac{1}{g}\int_0^{p_0} \overline{\left[u^* \frac{\partial \Phi^*}{\partial x} + v^* \frac{\partial \Phi^*}{\partial y}\right]} dp + \frac{1}{g}\int_0^{p_0} \overline{\left[u^* F_x^* + v^* F_y^*\right]} dp \qquad (5.3)$$

Since the momentum transport across the poles is zero, it follows that $\frac{\partial}{\partial y}\overline{[u]\left[u^* v^*\right]} = 0$. Therefore, the second term in (5.1) is equal to the first term in (5.3) but for a sign reversal, so that these terms involve the conversion between $\overline{K_E}$ and $\overline{K_Z}$.[22] Hence, it is appropriate to label these terms as the conversion C_K in the Lorenz kinetic energy cycle, which is reproduced in Fig. 5.1.[23]

---

[21] These figures are based on comparisons of both transient and standing eddy quantities. For documentation, see Schubert et al. (1990)

[22] Note that the equality holds only in an average from pole to pole.

[23] If we retain the $[v^{*2}]/\partial[v]/\partial y$ term in (5.2) we have the option of formulating the kinetic energy

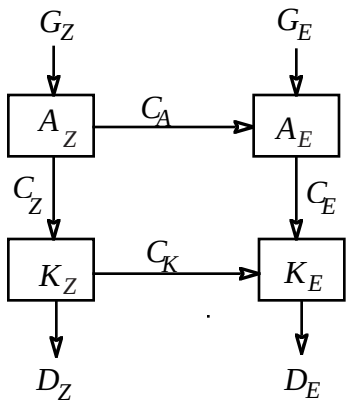

Fig. 5.1 The kinetic energy cycle, after Lorenz (1955).

The sign of this conversion in (5.3) depends upon whether the eddy transport of westerly momentum is directed up or down the meridional gradient of zonal wind. If it is down-gradient, the eddies will gain kinetic energy from the mean zonal flow. This is the mechanism by which waves can grow by barotropic instability. At the jetstream level the poleward momentum transports are strongest at the latitude of the zonally averaged jet, near 30°. Equatorward of that latitude they are up (counter) gradient, while poleward of that latitude, up to about 60°, where they undergo a sign reversal, they are down-gradient. It is evident from Fig. 2.2 that the meridional gradient of westerly momentum is stronger on the equatorward side than on the poleward side. In addition, note that the equatorward transports observed at higher latitudes are purely up-gradient. Hence, consistent with the analysis of the corresponding term in (5.1) we find that this conversion is primarily from the eddies to the zonal flow. Apparently, barotropic instability of the zonally symmetric flow is not the dominant energy source for the eddies.

The other terms in (5.3) may be recognized as the baroclinic conversion term labeled C_E in the cycle and the frictional dissipation labeled D_E. The baroclinic conversion must be large enough to balance dissipation plus the conversion to zonal kinetic energy. We know that circulations in baroclinic waves, monsoons and hurricanes are thermally direct, so it is reasonable to expect that C_E will be positive as labeled in Fig. 5.1 and quite large.

The corresponding equations for the time rates of change of A_Z and A_E are derived in an analogous manner. The resulting expressions are

$$\frac{\partial A_Z}{\partial t} = \frac{1}{g}\int_0^{p_0} \frac{\overline{P}\overline{[\alpha]}}{\sigma} dp + \frac{1}{g}\int_0^{p_0} \overline{[\omega]}\overline{[\alpha]} dp + \frac{1}{g}\int_0^{p_0} \frac{\overline{[Q]}\overline{[\alpha]}}{\sigma} dp \qquad (5.5)$$

and

---

cycle with separate reservoirs $[u]^2/2$ and $[v]^2/2$, which are connected by the Coriolis term.

$$\frac{\partial A_E}{\partial t} = -\frac{1}{g}\int_0^{p_0} \frac{\overline{[v^*\alpha^*]}}{\sigma}\frac{\partial \overline{\alpha}}{\partial y}dp + \frac{1}{g}\int_0^{p_0}\overline{[\omega^*\alpha^*]}dp + \frac{1}{g}\int_0^{p_0}\frac{\overline{[Q^*\alpha^*]}}{\sigma}dp \qquad (5.6)$$

The interpretation of these equations is analogous to that of (5.1) and (5.3). The first term on the right-hand-side, which involves the up or down gradient heat flux obviously represents the conversion C_A. This term must be in the sense of the arrow in Fig. 5.1, since the observed poleward eddy heat transport throughout the troposphere is down the gradient, from the warm tropics to the colder higher latitudes nearly everywhere.[24] This conversion can be viewed as distorting the shapes of the isotherms so as to make them less zonally symmetric and more wavelike, as shown in Fig. 5.2. Note how temperature advection is increasing the amplitude of the wave and, at the same time, weakening the zonally averaged meridional temperature gradient. Total available potential energy is conserved in this process, but the partitioning between the zonal and eddy reservoirs is altered.

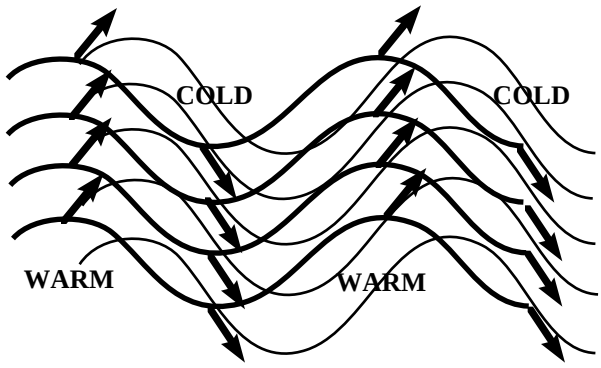

Fig. 5.2 Isotherms and streamlines in an idealized horizontal flow pattern in which eddy available potential energy is increasing at the expense of the available potential energy of the zonally symmetric background flow. Isotherms are denoted by heavy contours and streamlines by lighter contours.

The $\omega\alpha$ terms in (5.5)–(5.6) are identified with the baroclinic energy conversion terms C_Z and C_E, which have already been discussed in connection with the kinetic energy reservoirs. The $Q\alpha$ terms represent the generation of available potential energy by diabatic heating contrasts. It can be inferred from the distribution of net radiation at the top of the atmosphere discussed in Chapter 3, which is acting in the presence of a large equator to pole temperature gradient, that the zonally averaged term must be very large, particularly in the winter hemisphere.[25] Since we

[24] Countergradient heat fluxes are observed in parts of the lower stratosphere where the meridional temperature gradient reverses sign as seen in Fig. 4.1, but these conversions are localized and much weaker than those in the extratropical lower troposphere.

[25] The generation term is locally negative near the equatorial tropopause and at the mesopause (Fig. 5.1)

know that C_Z is quite small, it follows that in the long-term average the generation of zonal available potential energy must nearly balance the conversion to eddy available potential energy. Latent heat release in regions of precipitation is a source of eddy available potential energy for the monsoons and, to a somewhat lesser extent, for baroclinic waves. In the former, most of the heating occurs over the warm summertime continents while cooler air over the oceans is subject to a net heat loss through infrared cooling to space. In the latter, precipitation tends to occur preferentially in warm air masses. In the stratosphere, the diabatic heating can be described, to first order, by "Newtonian cooling" in which the temperature distribution tends to relax toward a radiative equilibrium field which is usually assumed to be zonally symmetric. In this prescription diabatic heating acts as a sink for eddy available potential energy. The negative value of G_E in Fig. 5.3 is questionable.

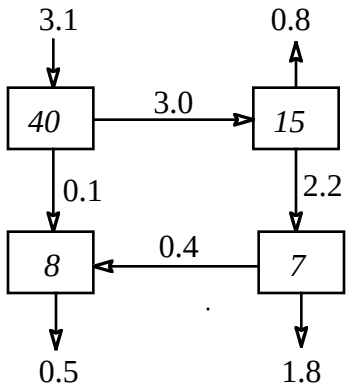

Fig. 5.3 Estimates of the annual average energy conversions and storage in the kinetic energy cycle after Oort (1964) based on rawinsonde station data in units of W m^{-2} for the conversions and 10^5 J m^{-2} for the storage in the various reservoirs. (Note that a conversion of 1 unit will change the storage in the adjacent reservoirs by just about 1 unit in one day.) Use Fig. 5.1 as a template.

Application to baroclinic waves

The poleward, down gradient heat transport near the lower boundary, as reflected in the conversion C_A, plays a central role in the linear theory of baroclinic waves. The most rapidly growing wave structures predicted by linear theory tend to be concentrated in the lower

---

where zonally averaged temperatures are far from radiative equilibrium and diabatic heating is acting to weaken the existing features in the $[\alpha']$ field.

troposphere and their wave axes exhibit a strong westward tilt with height. The relationship between the wind and temperature fields is as shown in Fig. 5.2. On latitude circles near the "stormtrack", warm, poleward air rises, while cooler, equatorward moving air sinks, converting available potential energy to kinetic energy. This conversion is essential to the amplification of the waves. Without it the eddy kinetic energy embodied in the amplitude of the *v*-component of the wind could not grow exponentially with the waves in the temperature field. On the other hand, it inhibits the growth of the temperature perturbations because poleward moving air cools as it rises and equatorward moving air warms as it sinks. The relative importance of the meridional temperature advection vs. the temperature changes induced by the vertical motions is determined by the slope of the air trajectories in the meridional plane as shown in Fig. 5.4. In constructing these trajectories it is assumed that the streamline and temperature fields in the waves are in quadrature as in Fig. 5.2. In the case of purely horizontal trajectories (left), the conversion $C_E = 0$ and the wind perturbations do not amplify. Locally in the waves, $\sigma\omega^*$ exactly cancels $-v^* \partial[T] / \partial y$ so that if the motion is adiabatic, the temperature field will not change with time. Since the waves do not amplify, it is clear that C_E must equal C_A. For exponential growth, it is essential that the slope be intermediate between these values as illustrated in the middle panel.

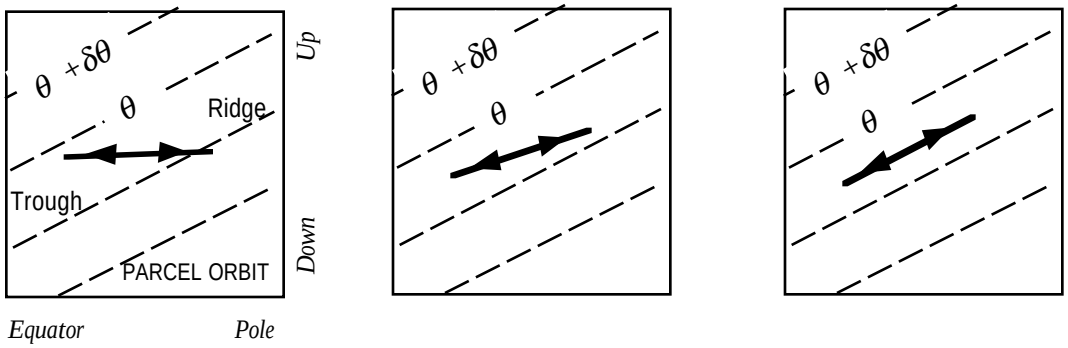

Fig. 5.4 Idealized orbits or trajectories of air parcels in waves in which the streamline and temperatures are in quadrature. Left: horizontal motion. Right: trajectories parallel to the isentropes. Middle: an intermediate slope.

The slope of the trajectories will be determined by the requirements for thermal wind balance, which depend upon the wavelength of the amplifying disturbances. We recall from Problem 1.3 that for wavelike disturbances with a prescribed vertical structure (other than pure barotropic), the ratio of K_E to A_E is proportional to the square of the zonal wavenumber. Hence, the trajectories in shorter waves need to be steeper than those in longer waves. For waves whose zonal wavelength is too short, the required slope will be steeper than the isentropes, in

which case the heat transport will become countergradient. This critical wavelength represents the "short wave cutoff" for baroclinic instability. Planetary waves, whose trajectory slopes are nearly horizontal, may be baroclinically unstable but they are less efficient at extracting energy from the A_z reservoir than synoptic-scale waves, because the perturbations in the meridional wind component do not amplify as rapidly. Most efficient, in this respect, are the waves in which the trajectory slopes are about half as large as the slopes of the isentropes.

As noted above, the normal modes associated with baroclinic instability tend to be confined to the lower troposphere and they exhibit only very weak momentum transports. In contrast, the observed baroclinic waves usually exhibit their largest amplitudes at the tropopause level, where they exhibit a systematic pattern of momentum transports, as was shown in Figs. 2.12 and 2.14. In order to understand these aspects of the structure of baroclinic waves it is necessary to consider them as finite amplitude disturbances evolving through a characteristic "life cycle", and modifying the shape of the mean flow. Simmons and Hoskins (1978) conducted a series of life cycle experiments in a high resolution primitive equation model with spherical geometry. Each integration was started from initial conditions consisting of a mean flow plus a small amplitude disturbance of normal mode form. We will show here the results from one of these integrations: the one with a westerly jet centered near 45°N[26], upon which a zonal wavenumber 6 disturbance (whose meridional and vertical structure is determined by solving the eigenvalue problem for the fastest growing baroclinic normal mode) is superimposed.

300 mb streamfunctions for 'Days 8-13' of the integration are reproduced in Fig. 5.5. During this period the waves develop a pronounced horizontal tilt, indicative of a poleward, countergradient transport of westerly momentum into the jet. The waves exhibit a distinct 'life cycle' characterized by an early period of exponential growth in a 'normal mode' form up to around Day 6 followed by a period of nonlinear growth and evolution from Day 6 to Day 10, ending with a period of rapid decay from Days 10-13.

Figure 5.6 shows the time history of the energy conversions during the life cycle of the waves. The conversions C_A and C_E grow exponentially up to about Day 6, throughout which time the other conversions are much weaker. C_A peaks on Day 8 followed by C_E about a day

---

[26] The maximum speed of the jet in this experiment is ~37 m s^{-1} Note that it is placed somewhat poleward of the observed jet.

Fig. 5.5 300 mb streamfunctions at 1 day intervals from Day 8 to Day 13 of a numerical integration of the life cycle of baroclinic waves (zonal wavenumber 6) in a primitive equation model with spherical geometry Latitude circles are drawn at 20° intervals starting at the equator. After Simmons and Hoskins (1978).

Fig. 5.6 Time history of the conversions in the numerical integration. Dotted lines represent the dissipation of eddy kinetic energy. After Simmons and Hoskins (1978).

later. Throughout the integration C_K is negative, indicating a conversion from eddy to zonal kinetic energy. This conversion peaks in Day 11, the time when the countergradient transport of westerly momentum in the previous figure is most pronounced. This process plays a major role in the abrupt decline in the amplitude of the waves around that time. Zonal kinetic energy is being converted to zonal available potential energy throughout the integration and eddy kinetic energy is being dissipated.

Note that in the time average over the complete life cycle there is a certain amount of "recycling" of zonal available potential energy. However, there is a substantial net loss through dissipation. Moreover, the structure of the mean flow changes during the course of the integration. The jet is displaced poleward of its original latitude and it is substantially sharpened and strengthened by the barotropic conversion that takes place during the decay stage. The baroclinic zone at the surface is just about eliminated, while the baroclinity in the upper troposphere increases somewhat.

Vertical cross sections of heat and momentum transports (not shown) are quite similar to the observed distributions for the transient eddies, but the momentum transports is displaced poleward of the observed. As in the real atmosphere, the strongest poleward momentum transports coincide with the jet.

Role of latent heat release

Apart from a small thermal diffusion term, which impacted only the smallest space scales in the model, the numerical experiments described in the previous subsection are essentially adiabatic: the G_E term cannot be a source of eddy available potential energy. Baroclinic waves in the real atmosphere (or more comprehensive models) can gain additional energy through the release of latent heat at longitudes at which temperatures in the waves are warmer than in the zonal average. At levels near 700 mb, where much of the latent heat release takes place, the warmest air and most of the precipitation tend to be coincident with the southerly flow one quarter of a wavelength downstream of the troughs of the waves. Hence, there is no question that $\left[Q^* T^*\right]$ is positive.

At the latitude of the monsoons, the meridional temperature gradients tend to be weak. Furthermore, we observed that the flow patterns associated with the monsoons exhibit little, if any westward tilt with height. Therefore it is evident that the conversion C_A must be very small. On the other hand, given the large release of latent heat over the warm continents, it is evident that both G_E and C_E are large and positive. Hence, in the monsoons, diabatic heating is the major source of eddy available potential energy, part of which is converted into eddy kinetic

energy as fast as it is generated so as to maintain the geostrophically appropriate ratio between the energy in the two reservoirs. Hurricanes exhibit a similar kinetic energy cycle.

In the stratosphere, where latent heat release is negligible, radiative heating tends to damp the eddies because the radiative equilibrium temperature field tends to be more zonally symmetric than the observed flow, in which the eddies are dynamically forced from below.

The energy cycle in the stratosphere

In §4.6 the reader was invited to verify that despite large values of the forcing terms P and G in the equations for the time rate of change of $[u]$ and $[T]$, the net eddy forcing (including the effects of the mean meridional circulations induced by the eddies) are not necessarily large. From the data shown in Fig. 4.8 it is evident that the poleward heat transport are directed down the zonally averaged temperature gradient while the momentum transports are, for the most part, directed up the gradient of zonal momentum[27]. Hence, like baroclinic waves, the stratospheric planetary waves are extracting energy from the mean flow by the conversion C_A and giving it back through the conversion C_K. In simulations of the stratospheric planetary waves with general circulation models it is observed that much of the time these two conversions proceed at almost exactly the same rate, which is also approximately equal to the rate of conversion C_E from eddy available potential energy to eddy kinetic energy. Furthermore, the eddy driven component of the mean meridional circulations converts zonal kinetic energy to zonal available potential energy at a comparable rate so that energy 'circulates' around the flow chart in Fig. 5.1 without changing the amounts of energy in any of the reservoirs.[28] Hence, by going through the laborious process of calculating all the conversions, one learns absolutely nothing about the sources and sinks of energy for the waves. The formalism that will be introduced in the next section will provide much more useful information concerning the interactions between the waves and the mean flow.

Question

5.1 The motions in stratospheric planetary waves are nearly adiabatic, $\left[v^*T^*\right] > 0$, $[T]$ decreases with latitude, and $[u]$ is larger than the phase speed of the waves. Under these conditions, prove that $\left[\omega^*\alpha^*\right] < 0$: i.e., that the circulations in the waves are thermally direct. (Hint: Make use of a sketch analogous to the right-hand panel of 3.14, but consider two different parcel orbits that intersect on a given latitude circle; one with upward motion and the other with downward motion.)

---

[27] The predominance of the countergradient transports is more striking when they are weighted by $\cos\phi$.

[28] Plumb (1979)

5.2 The transformed Eulerian mean equations

In §4.5 it was shown that $\partial[u]/\partial t$ is completely determined by the time rate of change of potential vorticity, as determined from the divergence of the forcing vector $\vec{\Gamma}$. It was also argued that the local eddy forcing of $\partial[u]/\partial t$ in the meridional plane is closely related to the poleward eddy transport of potential vorticity. In this section we will show that the two are, in fact, equal, and that the transport of potential vorticity, in turn, can be expressed as the divergence of a vectorial field, the Eliassen Palm flux, $\vec{E}$, which is an indicator of the group velocity of the waves in the meridional plane, as well as the net flux of zonal momentum by the waves and their induced mean meridional circulations. We will also show that the eddy component of the forcing vector $\vec{\Gamma}$ discussed in Chapter 4 is closely related to the meridional derivative of $\vec{E}$, and that the net rate of energy conversion between the eddies and the zonally symmetric part of the general circulation is related to the mass weighted integral of $\vec{E}\cdot\nabla[u]$.

Equations (4.6–7) can be rewritten in the form

$$\frac{\partial[u]}{\partial t} = f[v]^* + \nabla\cdot\vec{E} + [F_x] \tag{5.7}$$

$$\frac{\partial[\alpha]}{\partial t} = \sigma[\omega]^* + [Q] \tag{5.8}$$

where $[v]^* \equiv [v] + \dfrac{\partial}{\partial p}\dfrac{[v^*\alpha^*]}{\sigma}$ and $[\omega]^* \equiv [\omega] - \dfrac{\partial}{\partial y}\dfrac{[v^*\alpha^*]}{\sigma} = [\omega] + \dfrac{P}{\sigma}$ (5.9)

are the transformed mean meridional circulations and

$$\vec{E} \equiv \left(-[u^*v^*]\vec{j}, -f\frac{[v^*\alpha^*]}{\sigma}\vec{k} \right) \tag{5.10}$$

is the Eliassen-Palm flux. For the sake of clarity we have reintroduced the explicit notation for zonal averaging and we continue to use thickness (specific volume) in place of temperature. The poleward eddy heat transport $[v^*\alpha^*]/\sigma$ is, in effect, the streamfunction for the "correction" that is applied to the mean meridional circulations. It produces a heating or cooling equivalent to *P* and, in effect, takes the place of *P* in (4.2) and (4.7). It may be viewed as representing the 'Stokes drift' experienced by air parcels moving through the eddies as illustrated in Fig. 3.16. Note that in that idealized situation, the transformed Eulerian mean meridional circulation would be equivalent to the Lagrangian mean meridional circulation, which is identically equal to zero. Under steady state conditions in the real atmosphere, $\sigma[\omega]^* = [Q]$, the 'diabatically forced' part of the mean meridional circulation which can be identified with the Lagrangian mean meridional motions of air parcels. Hence, for example, in the upper troposphere the correction to the conventional mean meridional circulations cancels out the part of the Ferrel cell that is forced by

the eddy heat fluxes.

The eddy forcing term in (5.7) may be written in the form

$$\nabla \cdot \vec{E} = -\frac{\partial}{\partial y}\left[u^* v^*\right] - f\frac{\partial}{\partial p}\frac{\left[v^* \alpha^*\right]}{\sigma} \tag{5.11}$$

For the quasi-geostrophic scaling with $f = f_0$, and $q^* = \zeta^* - \partial\left[\alpha^* / \sigma\right] / \partial p$ it is readily verified that

$$\nabla \cdot \vec{E} = \left[q^* v^*\right] \tag{5.12}$$

and this identification with the poleward transport of potential vorticity is valid for more exact formulations. Hence, $\nabla \cdot \vec{E}$ may be regarded as the net eddy forcing of $\partial[u] / \partial t$. As in the thermodynamic energy equation (5.8), the transformed "diabatically forced" meridional mean circulation also plays a role.

In the winter stratosphere, where there tends to be a near balance between the convergence of the poleward heat transports by the planetary waves, as manifested in the term *P* and the warming or cooling associated with the wave-induced Eulerian mean meridional circulation $\sigma[\omega]$, the transformed equations provide a much more informative description of the dynamics of the zonally symmetric flow than the conventional equations that we considered in the previous chapter. Gone are the cancelling effects of the eddy fluxes and the induced mean meridional circulations. The transformed Eulerian mean meridional circulations that remain are usually much weaker than the conventional ones and (at least in some cases) more like the Lagrangian mean meridional circulation that a hypothetical "typical air parcel" (representing the center of mass of a large collection of parcels) would experience. The eddy forcing of the zonal flow is expressed as a single term $\nabla \cdot \vec{E}$ in the zonal momentum equation, which is recognized as the poleward transport of potential vorticity by the eddies.

Lest this transformation seem too good to be true, it should be pointed out that it doesn't work very well in the troposphere because the pathological situation that it was designed to correct does not exist there. Near the ground, where a near balance is observed between *P* and [*Q*], and $[\omega] \approx 0$ the meaning of the transformed mean meridional circulation is not at all obvious.

Since the acceleration of the mean flow by the eddies is given by $\nabla \cdot \vec{E}$, it follows that the flux of zonal momentum by the eddies (taking into account the mean meridional circulations that they induce) is simply $-\vec{E}$. The meridional component of $-\vec{E}$ is the momentum transport itself and the vertical component is the poleward heat flux, which transports momentum downward by inducing a mean meridional circulation cell with equatorward motion above and poleward motion below. This mechanism is embodied in the Ferrel cell, which removes westerly momentum from the upper troposphere and deposits it in the PBL.

The Eliassen-Palm flux has another, even more fundamental interpretation in terms of wave action and group velocity concepts. The "generalized Eliassen Palm" relation can be expressed in the form[29]

$$\frac{\partial A}{\partial t} + \nabla \cdot \vec{E} = D \qquad (5.13)$$

In this expression, D represents the role of diabatic heating and/or friction in generating or dissipating the eddies, as represented by the terms G_E and D_E in the kinetic energy cycle. A is a measure of "wave activity" which, in the quasi-geostrophic, beta-plane case can be approximated as $^1/_2[q]_y\left[\eta^{*2}\right]$, where η is the meridional displacement of air parcels in the eddies and $[q]_y$ is the meridional gradient of the quasi-geostrophic potential vorticity of the mean flow. Hence, wave action is closely related to the amplitude of Lagrangian parcel displacements. If $D = 0$, in (5.13) wave activity A is conserved and $\vec{E}$ traces its "flow" in the meridional plane. If $\partial / \partial t = 0$, as in a time averaged field, $\vec{E}$ traces the flow of wave activity from the region(s) in the meridional plane where the eddies are generated (e.g., by instabilities or by diabatic forcing as in the monsoons) to where they are dissipated by friction or radiative damping.

Fig. 5.7 shows the distribution of $\vec{E}$ in the life cycle simulation of baroclinic waves discussed in the previous section. Note how the packet of arrows proceeds upward toward the tropopause level[30] and then bends equatorward during the course of the integration, in agreement with the discussion of the energetics and life cycle of the waves in the previous section. Throughout the life cycle, $\vec{E}$ diverges out of the bottom boundary and the planetary boundary boundary layer in the vicinity of the "storm track". The corresponding region of convergence propagates upward and equatorward at the leading edge of the arrows that define the 'wave packet'. In the average over the complete life cycle, it is strongest near or just equatorward of the jetstream. Hence the waves are extracting zonal momentum from the mean flow in the vicinity of the jetstream and imparting it to the much weaker westerlies in the planetary boundary layer.

---

[29] The derivation is due to Andrews and Mc Intyre (1976, 1978). For more detailed tutorials on these concepts, see Andrews et al (1987) and Edmon et al. (1980)

[30] In pressure coordinates the arrows tend to shrink with increasing height, but the fluxes are nonetheless important in the wave-mean flow interaction because air density is decreasing with height at almost the same rate. For cross-sections covering substantial depths of the atmosphere it is preferable to use the *ln p* coordinate system and scale $\vec{E}$ accordingly.

Fig. 5.7 Meridional cross sections of Eliassen-Palm fluxes (arrows) in pressure coordinates as obtained from a simulation of the life cycle of baroclinic waves in a primitive equation model: (a) linear calculation for the initial perturbation representative of the early stages of the simulation; (b), (c) instantaneous cross sections for later (nonlinear) stages of the simulation; (d) time average over the entire life cycle. Contours indicate the divergence of the flux. After Simmons and Hoskins (1980).

By adding the conversions C_A and C_K in (5.3) and (5.6) it is readily verified that the net energy conversion from the mean flow to the eddies is simply $\vec{E} \cdot \nabla[u]$. Except for a small region equatorward of the jetstream near the tropopause level, $\vec{E}$ is directed up the gradient of $[u]$ in the meridional plane. The energy extracted from the mean flow in this numerical simulation is lost to frictional dissipation in the PBL and numerical damping of the smallest spatial scales that develop in association with fronts.

Figure 5.8 shows monthly averaged Eliassen Palm fluxes for two typical winter months. In order to make the arrows visible at the higher levels, they have been multiplied by exp(*z/H*), where *H* is scale height. Because of this scaling, the flux divergence, indicated by the contours can not be deduced quite as simply from visual inspection of the arrows as in the previous figure. A strong convergence / divergence couplet is evident ~60°N, with easterly forcing by the eddies in the middle and upper troposphere and westerly forcing in the PBL.[31] One stream of arrows bends equatorward, passes through the tropospheric jetstream, and converges into the subtropics. The other stream, which is greatly magnified by the scaling, proceeds more directly upward into the stratosphere toward the polar night jet and eventually bends equatorward. If the arrows don't bend very much, large convergence is inevitable in the vicinity of the polar night jet. On the other hand, if they bend soon enough and sharply enough, the convergence occurs at lower latitudes instead, and the jet is spared.

Fig. 5.8 Scaled Eliassen-Palm fluxes for January and February 1979, based upon NMC data. Both transient and standing eddies are included. After Baldwin (1987).

The amount of bending that the fluxes and the associated group velocities experience is determined by the potential vorticity gradient of the mean flow and the spectrum of zonal waveumbers and doppler shifted phase speeds of the disturbances responsible for the fluxes. A distribution of refractive index can be computed for each zonal wavenumber and ray tracing can be performed in the meridional plane.[32] Under some conditions the Eliassen-Palm fluxes are

[31] Analogous cross sections of the transient eddy contribution to the flux by Edmon et al. (1980) exhibit a secondary maximum in the convergence near the jetstream, in agreement with the numerical simulation shown in Fig. 5.7.

[32] Fundamental papers on this topic include Charney and Drazin (1968) which deals with the effects of

bent into westerly jetstreams as is evidently happening in the tropospheric jetstream. At higher levels the fluxes are usually refracted equatorward as they approach the polar night jet, but they are highly sensitive to the mean wind field such that even rather subtle changes in the shape or latitudinal position of the jet can enable them to propagate upward and sometimes even poleward, in which case they can precipitate a sudden warming in the polar cap region and a complete collapse of the polar night jet as described in detail in Chapter 6 of Andrews et al. (1987). These temporary lapses in the equatorward refraction of planetary wave activity are much rarer in the Southern winter circulation, where the polar night jet is stronger and the stationary waves are much weaker.

Away from critical levels where (5.13) applies, in the absence of transience and the generation or dissipation of the eddies by diabatic heating or frictional dissipation it reduces to the statement that $\nabla \cdot \vec{E} = 0$, which indicates that the net forcing of the mean flow by the eddies is zero. It follows that the important wave-mean flow interactions in the meridional plane must be taking place in precisely those places where one (or more) of these conditions does not apply. For example, baroclinic waves are generated near their 'critical (or steering) level' near 700 mb (3 km) and they are dissipated as they approach their 'critical latitude' near 20° at the jetstream level. Both regions lie close to the 10 m s^{-1} isotach, along which the zonal wind speed is comparable to the phase speed of the waves. As waves propagate into such a region in the meridional plane, their doppler-shifted frequency approaches zero and frictional dissipation and thermal damping have more and more time to act. It is in these same regions that the Lagrangian particle displacements in the waves become irreversible. Figure 5.9 shows low level (967 mb) isotherms and jetstream level IPV contours on Day 6 of a numerical simulation of the life cycle of a baroclinic wave. It is apparent that the occlusion process is already well underway at low levels and that a tongue of tropical air has become almost completely encircled by air originating at higher latitudes at the jetstream level. Even after the waves decay (as they do between Days 7 and 10 in this particular experiment) it is clear that the low level temperature field and the upper level potential vorticity field can never go back to the way they were. In contrast, at higher latitudes (45°N) at the jetstream level, which is situated far the 10 m s^{-1} wind line, the particle displacements grow up to Day 7 and then nearly completely collapse from Day 7 to Day 10. Hence, in the average over the complete life cycle of the wave, the distribution of potential vorticity in this region changes very little, consistent with the requirement that $\nabla \cdot \vec{E} \approx 0$.

---

vertical wind shear, and Dickinson (1968). For a comprehebsive discussion see Holton et al. (1987).

Fig. 5.9 Fields from a numerical simulation of the life cycle of baroclinic waves. (a) Temperature at the 967 mb level on Day 6; contour interval 5 K on Day 8. (b) Isentropic potential vorticity on the 350 K surface: contour interval 0.8 x 10^{-6} m^2 s^{-1} K kg^{-1}. The arrows in (b) are the flow field in this isentropic surface in a frame of reference moving with the phase speed of the waves. After Held and Hoskins (1985).

Problems

5.2 Prove that to the level of approximation of (4.1)–(4.4) $\vec{\Gamma} = \dfrac{\partial\left(\vec{E} \,/\, f\right)}{\partial y}$

5.3 Prove that the eddy geopotential flux vector

$$\vec{W} \equiv \left(\left[v^*\Phi^*\right]\vec{j},\ \left[\omega^*\Phi^*\right]\vec{k}\right) = \left([u]-c\right)\vec{E} \tag{5.14}$$

and give a dynamical interpretation of this result.

5.4 Show that for the more exact form of the governing equations for cartesian geometry

$$\frac{\partial[u]}{\partial t} = \left(f - \frac{\partial[u]}{\partial y}\right)[v] - [\omega]\frac{\partial[u]}{\partial p} + G + F \tag{5.15}$$

$$\frac{\partial[\alpha]}{\partial t} = -[v]\frac{\partial[\alpha]}{\partial y} + \sigma[\omega] + P + Q \tag{5.16}$$

where G and P now include the convergences of the vertical fluxes as well as the convergences of the meridional transports, the equation for the time rate of change of zonal momentum can be written in the transformed Eulerian mean form

$$\frac{\partial[u]}{\partial t} = \left(f - \frac{\partial[u]}{\partial y}\right)[v]^* - [\omega]^*\frac{\partial[u]}{\partial p} + \nabla\cdot\vec{E} + F$$

where $[v]^* \equiv [v] + \frac{\partial}{\partial p}\frac{\left[v^*\alpha^*\right]}{\sigma}$ and $[\omega]^* \equiv [\omega] - \frac{\partial}{\partial y}\frac{\left[v^*\alpha^*\right]}{\sigma} = [\omega] + \frac{P}{\sigma}$

as before, and the Eliassen-Palm flux now assumes the more general form

$$\vec{E} = \left(-\left[u^*v^*\right] - \frac{\partial[u]}{\partial p}\frac{\left[v^*\alpha^*\right]}{\sigma}\right)\vec{j}, \quad \left(-\left[u^*\omega^*\right] - \left(f - \frac{\partial[u]}{\partial y}\right)\frac{\left[v^*\alpha^*\right]}{\sigma}\right)\vec{k}$$

of which the previous definition may be recognized as a limiting case. Give an interpretation of each term. From an inspection of $\vec{E}$, show that the vertical component of the momentum flux is likely to be important in forcing the zonal flow in the tropics.

5.5 Following Holton and Dunkerton (1978), start with the linearized, quasi-geostrophic potential vorticity equation with an exponential growth or damping term

$$\frac{\partial q^*}{\partial t} = -[u]\frac{\partial q^*}{\partial x} - v^*\frac{\partial[q]}{\partial y} + \gamma q^*$$

and derive (5.13) where

$$A = \frac{1}{2}\frac{\left[q^{*2}\right]}{\partial[q]/\partial y} = \frac{1}{2}\left[\eta^{*2}\right]\frac{\partial[q]}{\partial y} \qquad \text{and} \qquad D = \frac{\gamma\left[q^{*2}\right]}{\partial[q]/\partial y} \tag{5.17}$$

5.3 Meridional energy dispersion and momentum transport

One of the outstanding features of the angular momentum balance in the earth's atmosphere is the maintenance of the surface easterlies in the subtropics and westerlies at higher latitudes by the poleward transport of westerly momentum across 30° latitude by the eddies. We are now in a position to consider the question of why the transports at that latitude are so consistently strong and poleward.

The linearized barotropic vorticity equation may be written in the form

$$\frac{\partial\zeta^*}{\partial t} = -[u]\frac{\partial\zeta^*}{\partial x} - v^*\frac{\partial\left(f + [\zeta]\right)}{\partial y} + \gamma\zeta^* \tag{5.18}$$

where the last term may be viewed as representing the combined effects of the divergence term $-f\nabla\cdot\vec{V}$ and the dissipation of small scale features associated with fronts and jetstreams. We will regard it as being a function of latitude. From the discussion of (1.18) it is evident that in thermally direct eddy circulations, γshould tend to be positive, favoring amplification of the vorticity perturbations and vice versa. If the ageostrophic circulations are neither thermally direct nor thermally indirect, dissipation should tend to dominate and γwill be weakly negative. Ageostrophic circulations driven by frictional drag within the PBL should also contribute to negative values of γwithin the free atmosphere. Hence, in the upper troposphere γshould

tend to be strongly positive near 50° latitude, where strong poleward heat transports and strong negative values of $\left[\omega^{*}\alpha^{*}\right]$ are observed in association with baroclinic waves and the stationary waves, and it should be weaker and may even be negative equatorward of 30° and in the polar regions. Multiplying (5.18) by ζ^{*} and zonally averaging, we obtain

$$\frac{1}{2}\frac{\partial\left[\zeta^{*2}\right]}{\partial t} = -\left[v^{*}\zeta^{*}\right]\frac{\partial\left(f+[\zeta]\right)}{\partial y} + \gamma\left[\zeta^{*2}\right] \tag{5.19}$$

Since we are interested in climatological mean conditions we can ignore the time derivative term. We recognize $\left[v^{*}\zeta^{*}\right]$ as *G*, the barotropic component of the eddy forcing of the mean zinal wind. Hence, (5.19) reduces to

$$G\frac{\partial\left(f+[\zeta]\right)}{\partial y} = \gamma\left[\zeta^{*2}\right] \tag{5.20}$$

For observed conditions in the earth's atmosphere, absolute vorticity increases monotonically with latitude except possibly within a degree or two near the equator and in small region around the poles. With these possible minor exceptions, *G* must be positive where γ is positive and vice versa. We have shown that *G* is largest ~50° latitude, precisely where we expect γ to be largest, and and it is most strongly negative in the subtropics of the winter hemisphere, where perturbations generated at higher latitudes are being damped as they approach their critical latitude. Hence, the eddies impart a westerly acceleration to the mean flow within the latitude belt in which they are forced, and an easterly acceleration within the latitudes in which they are damped.[33] This result is consistent with the notion that the transport of westerly momentum by the eddies is in the opposite sense as the flux of wave activity. It is also consistent with the 'kidney bean' or 'boomerang' shape of the baroclinic wave perturbations in Fig. 2.14.

A similar behavior is evident in numerical simulations of waves based on the barotropic vorticity equation. Figure 5.10 shows the vorticity perturbations generated when a circular vorticity source is inserted (at 30°N) into a mean flow consisting of pure superrotation (constant angular velocity, with westerlies). By Day 2.5, a circular region of cyclonic vorticity has developed over the source and a train of Rossby waves is beginning to develop downstream of it.. From a comparison with the panel for three days later it is evident that the phase velocity of the waves is nearly zero: individual features remain in virtually the same position, while new features develop as energy disperses downstream and in the meridional direction. The rate at which the leading edge of the new centers advances gives an indication of the group velocity of the waves. Note that the waves develop both equatorward and poleward of the latitude of the vorticity source. The former crosses the equator and returns via, a 'great circle route'. If the integration is continued indefinitely, the subsequent solution depends upon the amount of

[33] This derivation is due to Held (1976)

damping in the model. If the damping is very weak the returning part of the wavetrain interferes with the departing one to form a two-dimensional wave pattern with well defined nodes in the meridional as well as the zonal direction. As this pattern becomes established, one sees less and less of the northeast-southwest tilt required for a southward flux of wave activity. In the case of pure 'standing waves' in the meridional direction the fluxes of wave activity in the departing and returning parts of the wavetrains exactly cancel. If the damping is stronger, the solution model will reach a steady state solution qualitatively similar to the patterns shown in the figure. Wave activity is damped before it returns from the Southern Hemisphere, so the southward flux of wave activity and the northward transport of westerly momentum through the tropics continues to be strong. Since the streamfunction and vorticity patterns exhibit similar shapes for such wavelike patterns it is evident that there is a strong convergence of the eddy transport of westerly momentum into the latitude belt of the forcing. Analogous experiments have been carried out with the forcing on the equator and the results are also consistent with the above analysis: in this case the eddies produce a westerly acceleration on the equator.

References

Andrews, D.G., J.R.Holton, and. C.B. Leovy, 1987: *Middle Atmospheric Dynamics.* Academic Press, 488pp.

Andrews, D.G. and M.E. McIntyre, 1976a: Planetary waves in horizontal and vertical shear: The generalized Eliassen-Palm relation and mean-flow acceleration. *J. Atmos. Sci.,* **33**, 2031-2048.

Andrews, D.G. and M.E. McIntyre, 1976b: Planetary waves in horizontal and vertical shear: Asymptotic theory for equatorial waves in weak shear. *J. Atmos. Sci.,* **33**, 2049-2053.

Andrews, D.G. and M.E. McIntyre, 1978: Generalized Eliassen-Palm and Charney Drazin theorems for waves on axisymmetric flows in compressible atmospheres.. *J. Atmos. Sci.,* **35**, 175-185.

Baldwin, M.P., 1987: The propagation and mean-flow interaction of waves in the upper troposphere and lower stratosphere. PhD Thesis, Dep't. of Atmos. Sci., Univ. of Washington, 187 pp.

Charney, J.G. and P.G. Drazin, 1961: Propagation of planetary-scale disturbances from the

lower into the upper atmosphere. *J. Geophys. Res.,* **66**, 83-109.

Dickinson, R.E., 1968: Planetary Rossby-waves propagating through weak westerly waveguides. *J. Atmos. Sci.,* **25**, 984-1002.

Edmon, H.J., B.J. Hoskins and M.E. McIntyre, 1980: Eliassen-Palm cross-sections for the troposphere. *J. Atmos. Sci.,* **37**, 2600-2616.
Eliassen, A. and E. Palm, 1961: On the transfer of energy in stationary mountain waves. *Geophys. Publ.*, **22**, No.3, 1-23.

Held, I.M., 1975: Momentum transport by quasi-geostrophic eddies. *J. Atmos. Sci.,* **32**, 1494-1497

Held, I.M. and B.J. Hoskins, 1985: Large-scale eddies and the general circulation of the troposphere. In *Issues in Atmospheric and Oceanic Modeling: Part A Climate Dynamics* (S. Manabe ed.)., Academic Press, pp.1-31.

Holton, J.R. and T. Dunkerton, 1978: On the role of wave transience and dissipationin stratospheric mean flow vacillations. *J. Atmos. Sci.,* **35**, 740-744.

Hoskins, B.J. A.J. Simmons and D.G. Andrews, 1977: Energy dispersion in a barotropic atmosphere. *Quart. J. R. Meteorol. Soc.*, **103**, 553-567.

Lorenz, E.N., 1955: Available potential energy and the maintenance of the general circulation. *Tellus,* **7**, 157-167.

Oort, A.H., 1964: Estimates of the atmospheric energy cycle. *Mon. Wea. Rev.,* **9**2, 483-493.

Plumb, R.A., 1979: Eddy fluxes of conserved quantities by small amplitude waves. *J. Atmos. Sci.,* **36**, 1699-1704

Simmons, A.J. and B.J. Hoskins, 1978: The life cycles of some nonlinear baroclinic waves. *J. Atmos. Sci.,* **35**, 414-432

_____, 1980: Barotropic influences on the growth and decay of nonlinear baroclinic waves. *J. Atmos. Sci.*, **37**, 1679-1684.

6 THE CLIMATOLOGICAL-MEAN STATIONARY WAVES

6.1 Time mean vs. transient formalism

xx

6.2 The extratropical tropospheric stationary-waves: observational evidence

After Wallace, J.M., (1983): The climatological-mean stationary waves: Observational evidence. *Large Scale Dynamical Processes in the Atmosphere*, Academic Press, London, 27-53.

6.3 The extratropical tropospheric stationary-waves: interpretation

6.3.1 Early models

Beta-plane channel formalism...(meridional structure is largley ignored)

Charney and Eliassen (1949) A numerical method of predicting perturbations of the middle latitude westerlies. *Tellus,* **1**, 38-54.

Bolin, B. On the influence of the earth's orography on the general circulation of the westerlies. *Tellus,* **2**, 184-195.

Smagorinsky, J., 1953: The dynamical influence of large scale heat sources and sinks on the quasi stationary mean motions of the atmosphere. *Quart. J. Roy. Meteorol. Soc.*, **79**, 342-366.

6.3.2 Incorporation of spherical geometry

Hoskins, B.J., A.J. Simmons and D, Andrews, 1977: Energy dispersion in a barotropic atmosphere. *Quart. J. Roy. Meteorol Soc.*, **103**, 553-567.

Hoskins, B.J. and D.J. Karoly, 1981: The steady state linear response of a spherical atmosphere to thermal and orographic forcing. *J. Atmos. Sci.*, **38**, 1179-1196.

I.M. Held and B.J. Hoskins, 1985: Large-scale eddies and the general circulation of the troposphere. *Issues in Atmospheric and Oceanic Modeling. Part A: Climate Dynamics. Adv. in Geophysics*, **28** (Academic Press), 3-31.

6.3.3 Dymamics of longitudinally localized jetstreams

Namias, J. and P. F. Clapp, 1949: Confluence theory of high tropospheric jet streams. J. Meteorol., 6, 330-336.

Blackmon, M.L., J.M. Wallace, N.-C. Lau and S.L. Mullen, 1977: An observational study of the Northern Hemisphere wintertime circulation. J. Atmos Sci., 34, 1040-1053.

Nakamura, H., 1993: Horizontal divergence associated with zonally isolated jetstreams. *J. Atmos. Sci.*, **50**, 2310-2313.

6.4 The monsoons

Matsuno, T., 1966: Quasi-geostrophic motions in the equatorial area. *J. Meteorol. Soc. Japan*, **2**, 25-43. (response to a stationary mass source)

Webster, P.J., 1972: Response of the tropical atmosphere to local, steady forcing. *Mon. Wea. Rev.*, **100**, 518-541.

6.5 The stratospheric planetary-waves

Charney, J.G. and P.G. Drazin, 1961: Propagation of planetary-wves from the lower into the upper atmosphere. *J. Geophys. Res.*, **66**, 83-110.

7. THE TRANSIENT VARIABILITY

7.1 Frequency dependence

Variance fields • one-point correlation maps • concept of anisotropy • interpretation of contrasting high and low frequency anisotropy in terms of Rossby's dispersion relation Wallace and Lau (1985).

7.2 High frequency transients

Concept of 'stormtracks' as developed in Blackmon (1976), Blackmon et al. (1977, 1984*b*) and Wallace et al. (1988). Contrasting structure of the *u'* and *v'* fields. Horizontal structure, vertical structure, phase propagation, downstream energy dispersion • interpretation in terms of Rossby group velocity formula.

7.3 Diagnosis of the feedback of the transients upon the time-mean flow

The direct effect of fluxes associated with transients upon the zonally varying flow is readily evident when the governing equations are time averaged and written in flux form

$$\frac{\partial \bar{u}}{\partial t} = -\bar{u}\frac{\partial \bar{u}}{\partial x} - \bar{v}\frac{\partial \bar{u}}{\partial y} - \frac{\partial}{\partial x}\overline{u'u'} - \frac{\partial}{\partial y}\overline{u'v'} + f\bar{v}_a + F_x \qquad (7.1)$$

$$\frac{\partial \bar{v}}{\partial t} = -\bar{u}\frac{\partial \bar{v}}{\partial x} - \bar{v}\frac{\partial \bar{v}}{\partial y} - \frac{\partial}{\partial x}\overline{u'v'} - \frac{\partial}{\partial y}\overline{v'v'} - f\bar{u}_a + F_y \qquad (7.2)$$

where the small vertical advection terms have been omitted. Note that the transient terms involving $\partial / \partial x$, which were eliminated in the zonal averaging in previous chapters remain in the time averaged equations. We will show that these terms play quite different roles for the low and high frequency transients

For the high frequency transients associated with baroclinic waves, by far the largest of the flux terms is $-\partial\overline{v'v'}/\partial y$ in (7.2). It is large because (1) $\overline{v'v'}$ along the axis of the stormtracks is a factor of 2-3 larger than $\overline{u'u'}$ in the centers of the 'dumbell pattern' along the flanks of the stormtracks, which is in turn a factor of 2-3 larger than $\overline{u'v'}$ at the centers of the associated 'dipole pattern', and (2) $\partial / \partial y$ is particularly large because of the narrowness of the $\overline{v'v'}$ pattern in the meridional direction. The smallest of the four terms is $\partial\overline{u'v'}/\partial x$, since $\overline{u'v'}$ tends to be small and the zonal scale of its characteristic dipole pattern is broader than the meridional scale by a factor of 2-3. For low frequency transients with periods longer than 10 days, $\overline{u'u'}$ tends to be larger than $\overline{v'v'}$, particularly over the mid-latitude oceans as will be demonstrated in section 7.4. As at higher

frequencies, $\overline{u'v'}$ tends to be the smallest of the three flux terms and its patterns tend to be zonally elongated, such that $\partial\overline{u'v'}/\partial y >> \partial\overline{u'v'}/\partial x$. Hoskins James and White (1983) have shown that considerable simplification of the governing equations can be achieved by omitting the $\partial\overline{u'v'}/\partial x$ term, as detailed in the next section. [• vectorial representation of fluxes • divergent component of fluxes....not covered this year: see Lau and Wallace (1979).

7.3.1 The extended Eliassen-Palm flux

Analysis of the effects of the transients upon momentum budget in terms of (7.1) and (7.2) is not very helpful because it doesn't take into account the effect of the two-dimensional ageostrophic circulation induced by the transients. Just as the eddy-induced mean meridional circulations maintain thermal wind balance between time rates of change of [u] and [T], the two-dimensional ageostrophic circulation (u_a, v_a) serves to couple the time rates of change of $\bar{u}$ and $\bar{v}$ to keep them close to geostrophic balance with the pressure field and quasi-nondivergent.

The nature of this adjustment process can be illustrated by considering how the term $-\partial\overline{v'v'}/\partial y$ associated with the high frequency transients impacts the zonal flow at the jetstream level. If this term were abruptly turned on, it would drive a meridional diffluence $\partial\bar{v}/\partial y$ out of the stormtrack which would initially be unbalanced. The excess Coriolis force would induce a zonal ageostropic flow: eastward on the poleward (hereafter assumed to be northern) flank of the stormtrack and westward on the equatorward (southern) flank, which would in turn oppose the development of the diffluent meridional flow. (Hopefully this sounds familiar!) The continuity equation requires that $\bar{u}_a$ along the flanks of the stormtrack be accompanied by some combination of vertical velocity pertubations and $\bar{v}_a$ perturbations. The vertical velocity perturbations below the jetstream level will be characterized by ascent to the northwest (NW) and SE of the stormtrack and descent to the SW and NE. The associated adiabatic cooling and warming and hydrostatic pressure changes will lower the heights of pressure surfaces to the NW and SE of the stormtrack and raise them to the SW and NE, thereby creating east-west pressure gradients that are geostropically consistent with the induced diffluent meridional flow. This pattern of pressure changes implies westerly (easterly) accelerations of the geostrophic flow along the axis of the stormtrack to the west (east). The term in (7.1) that gives rise to these zonal accelerations is the ageostrophic meridional flow induced by the changes in the pressure field: e.g., to the west of the stormtrack falling pressure to the north and rising pressure to the south induces a northward ageostrophic flow, which forces a westerly acceleration in the zonal momentum equation. In effect, a clockwise ageostrophic circulation around the stormtrack transfers westerly momentum westward aling the axis of the stormtrack.

In the above example, the two-dimensional ageostrophic circulation and the associated vertical

motions (1) resist the changes in the meridional flow induced by the transients; (2) induce a pattern of pressure changes geostrophically consistent with the changes in the meridional flow; and (3) cause the zonal wind field to change in a manner geostrophically consistent with the pressure changes. In the process, westerly momentum is, in effect, transported westward along the axis of the stormtrack, even though there are no zonal momentum fluxes by the transients. The role of the three-dimensional 'secondary circulations' in this adjustment process is analogous to the role of the mean meridional circulations in the zonally averaged circulation.

The vorticity balance can help us to understand the nature of these changes in a more quantitative way. It is readily verified that

$$\overline{u\zeta} = \frac{\partial}{\partial x}\overline{uv} + \frac{\partial}{\partial y}\left(\frac{\overline{v^2} - \overline{u^2}}{2}\right) \quad \text{and} \quad \overline{v\zeta} = -\frac{\partial}{\partial y}\overline{uv} + \frac{\partial}{\partial x}\left(\frac{\overline{v^2} - \overline{u^2}}{2}\right) \tag{7.3}$$

The contribution of the transients to the time rate of change of $\bar{\zeta}$ is given by

$$-\nabla \cdot \overline{\vec{V}\zeta} = -\frac{\partial}{\partial x}\overline{u\zeta} - \frac{\partial}{\partial y}\overline{v\zeta} = \frac{\partial}{\partial x}\left(-\frac{\partial}{\partial x}\overline{uv}\right) - \frac{\partial}{\partial y}(\nabla \cdot \mathbf{E}) \tag{7.4}$$

where

$$\mathbf{E} \equiv -\left(\overline{u^2} - \overline{v^2},\ \overline{uv}\right) \tag{7.5}$$

The functional form of (7.4) suggests that the first term on the right hand side represents the forcing of $\partial\bar{v}/\partial x$ by the transients and the second term the forcing of $-\partial\bar{u}/\partial y$. .Since $\partial^2\overline{uv}/\partial y^2 >> \partial^2\overline{uv}/\partial x^2$, the second term must be much larger than the first, unless $\mathbf{E}$ is quasi-nondivergent. Hence, $\nabla \cdot \mathbf{E}$ functions as a zonal momentum source, and $-\mathbf{E}$ as a flux of zonal momentum by the transients: the horizontal component of an "extended Eliassen-Palm flux", as defined in Hoskins et al. (1983)

Both components of $\mathbf{E}$ relate to the anisotropy of the transients: the zonal component to their elongation along the *x* or *y* axes, and the meridional component to their elongation along a pair of axes oriented at a 45° angle relative to them. For example, transient eddies or waves that are elongated along the *y* axis transport zonal momentum westward; those elongated along a 45° (NE/SW) axis transport it northward; those elongated along the *x* axis transport it eastward, etc., as illustrated in the accompanying figure. Note that as the axis along which the transient eddies are elongated rotates through 180°, the direction of the zonal momentum flux rotates through a full circle. Eddy orientation can be described more quantitatively in terms of the correlation tensor discussed in §7.3.2.

E also has significance with respect to the barotropic energy conversion between the transients and the time-mean flow. By analogy with (5.3), the conversion from the mean flow to the transients is given by

$$C_K = -\overline{u'u'}\frac{\partial \bar{u}}{\partial x} - \overline{v'v'}\frac{\partial \bar{v}}{\partial y} - \overline{u'v'}\left(\frac{\partial \bar{v}}{\partial x} + \frac{\partial \bar{u}}{\partial y}\right) \tag{7.6}$$

The second term in parentheses tends to be much larger than the first because the zonal winds in the background climatology, which range as high as 70 m/s in the wintertime jetstream over Japan, tend to be much stronger than the meridional winds, and the meridional scale of these jetlike features in the $\bar{u}$ field tends to be narrower than in the more isotropic features that characterize the $\bar{v}$ field. If the smaller term is ignored, the conversion reduces to

$$C_K = \mathbf{E} \cdot \nabla \bar{u} \tag{7.7}$$

Hence, wherever **E** is directed up the gradient of $\bar{u}$, the transients are extracting kinetic energy from the mean flow and vice versa.

Hoskins James and White go on to show that **E** may be regarded as the horizontal component of a three-dimensional Eliassen-Palm flux vector, whose vertical component is proportional to the poleward heat flux by the transients, in analogy with (5.10). The net forcing of the time mean flow by the transients is given by the divergence of this three-dimensional vector and the net conversion between the mean flow and the transients is given by $\vec{\mathbf{E}} \cdot \nabla \bar{u}$ in three dimensions, where the vertical component represents the baroclinic conversion and the horizontal component the barotropic conversion. Subject to the restrictions discussed in §7.3.2, the extended Eliassen-Palm flux can also be regarded as the flux of transient wave activity from the regions where it is generated to the regions where it is dissipated.

[Discussion of observational data presented in Wallace and Lau (1985)]

7.3.2 The correlation tensor

Following the formalism developed in Hoskins et al., (1983) the horizontal velocity correlation tensor can be divided into isotropic and anisotropic (trace free) components

$$\begin{bmatrix} \overline{u'^2} & \overline{u'v'} \\ \overline{u'v'} & \overline{v'^2} \end{bmatrix} = \begin{bmatrix} K & 0 \\ 0 & K \end{bmatrix} + \begin{bmatrix} M & N \\ N & -M \end{bmatrix} \tag{7.8}$$

where $K = \left(\overline{u'^2} + \overline{v'^2}\right)/2$, $M = \left(\overline{u'^2} - \overline{v'^2}\right)/2$, and $N = \overline{u'v'}$.

The velocity correlation tensor conveys a considerable amount of information about the statistically averaged structure of the transient variability. It may be viewed as having an overall magnitude, indicated by *K*, and amounts of elongation along the (*x, y)* axes, and along a set of axes oriented at 45°/135° relative to the (*x, y)* axes, denoted by *M* and *N*, respectively. *M* is useful for diagnosing whether the transients are elongated in the zonal ($M > 0$) or meridional ($M<0$) directions. If the transients are elongated along an axis oriented at 45° relative to the (*x, y)* axes, then $M=0$, and the anisotropy would be characterized by the nonzero value of *N*, which would in this case be positive. In a similar manner, if the transient perturbations are elongated along an axis oriented at 135° relative to the (*x, y)* axes, then $M = 0$ and $N < 0$. For transients elongated along an arbitrary axis, both *M* and *N* may take on nonzero values.

Some simplification can be achieved by adopting a coordinate system oriented along the principal axes of the velocity correlation tensor, which lies at angle

$$\psi \equiv \frac{1}{2}\tan^{-1}\frac{N}{M}$$

relative to the *x* axis. Note that $0 < \psi < \pi$. Let u' and v' denote the velocity components in these rotated coordinates and M' and N' be the associated correlation terms. It is readily verified that *K* is not affected by this coordinate transformation and that

$$M' \equiv \left(\overline{u'^2} - \overline{v'^2}\right)/2 = \sqrt{M^2 + N^2} \quad \text{and} \quad N' = 0.$$

Hence, in these rotated coordinates, M' and ψ convey all the essential information about the anisotropy of the horizontal wind field. In addition, it is useful to define

$$\alpha \equiv M'/K$$

as a measure of the normalized anisotropy. It is evident that this *coefficient of anisotropy* may

take on a range of values from zero to one. For an isotropic horizontal wind field it would vanish; for motions constrained to one direction, as in Kelvin waves, it would assume a value of unity. An ellipse provides a useful visual analogue of the velocity correlation tensor. ψ defines the angle of its major axis and α is a measure of its ellipticity; for α=0 the ellipse degenerates into a circle and for α=1 it degenerates into a slit.

These statistics can be calculated for the transient variability as a whole or for the transient variability in any particular frequency band that one can isolate through the use of temporal filters. Fig. 1 in Wallace and Lau (1985) shows the distribution of α and ψ over the Northern Hemisphere during wintertime for the transient variability as a whole (top), for the high frequency transients that we associate with baroclinic waves (middle) and for low-frequency transients with periods longer than about 10 days (lower). The line segments are oriented perpendicular to the principal axis of the velocity correlation tensor, and their length scaled to be proportional to α. The sharp contrast between the structure of the high and low frequency fluctuations, which was pointed out in the previous section is evident in this figure. The east -west oriented line segments in the middle panel are indicative of an elongation of the high frequency fluctuations in the north-south direction, while the north-south orientation of many of the line segments in the lower panel is indicative of an elongation of the low frequency fluctuations in the east-west direction. Not surprisingly, the partial cancellation between the contributions from the high and low frequencies results in an overall lower level of anisotropy for the transient variability as a whole (top panel).

7.3.3 Local geopotential tendency diagnostics

After Lau and Holopainen (1984). Some of the figures are reproduced in Wallace and Lau (1985), Figs. 16 and 17.

7.3.4 Feedback of baroclinic waves upon low-frequency transients

After Lau (1988), Mullen (1987), Nakamura and Wallace (1990)

7.3.5 Control of the high frequency transients by the background flow

After James (1987), Nakamura (1992), Branstator (1994?),

7.4 Low-frequency 'normal mode behavior'

Observational evidence (NAO and PNA patterns) • barotropic instability of a zonally varying flow (after Simmons et al. 1983)• a stochastic perspective (after Nakamura et al. 1987).

7.5 Other low-frequency intraseasonal phenomena

Blocking after Nakamura (1994) • the Madden-Julian Oscillation • Kushnir-Branstator 'waves'

7.6 Orographic signatures in the transients

After Blackmon et al. (1979), Hsu and Wallace (1985), Hsu (1987)

7.7 Nonlinear aspects of the transients

Skewness after Nakamura and Wallace (1991); Cluster analysis, after Cheng and Wallace (1993)

7.8 Transient variability in the stratosphere

Lack of geographically dependent structure: Wallace (1996) Fig. 1

References

Blackmon M.L., 1976: A climatological spectral study of the Northern Hemisphere wintertime circulation. *J. Atmos. Sci.*, **33**, 1607-1623.

Blackmon, M.L., J.M. Wallace, N.-C. Lau and S.L. Mullen, 1977: An observational study of the Northern Hemisphere wintertime circulation. *J. Atmos Sci.*, **34**, 1040-1053.

Blackmon, M.L., R.A. Madden, J.M. Wallace and D.S. Gutzler, 1979: Geographical variations in the vertical structure of geopotential height fluctuations. *J. Atmos. Sci.*, **36**, 2450-2466.

Blackmon, M.L., Y.-H. Lee and J.M. Wallace, 1984a: Horizontal structure of 500-mb height fluctuations with long, intermediate and short time scales as deduced from lag-correlation statistics. *J. Atmos. Sci.*, **41**, 961-979.

Blackmon, M.L., Y.-H. Lee, J.M. Wallace and H. -H. Hsu, 1984*b*: Time variations of 500-mb height fluctuations with long, intermediate and short time scales as deduced from lag-correlation statistics. *J. Atmos. Sci.*, **41**, 981-991.

Branstator, G.W., 1995: Organization of strom track anomalies by recurring low frequency

circulation anomalies. *J. Atmos. Sci.,* **52**, ??

Chang, E.K.M., 1993: Downstream development of baroclinic waves as inferred from regression analysis. *J. Atmos. Sci.,* **50**, 2038-2053.

Cheng, X. and J.M. Wallace, 1993: Cluster analysis of the Northern Hemisphere wintertime 500-hPa height field. *J. Atmos. Sci.,* **50**, 2674-2696.

Hoskins, B.J., I.N James and G.H. White (1983): The shape, propagation and mean flow interaction of large-scale weather systems. *J. Atmos. Sci.,* **40**, 1595-1612.

Hsu, H. -H., and J.M. Wallace (1985) Vertical structure of wintertime teleconnection patterns. *J. Atmos. Sci.,* **42**, 1693-1710.

Hsu, H.-H., 1987: propagation of low level circulation features in the vicinity of mountain ranges. *Mon. Wea. Rev.,* **115**, 1864-1992.

James, I.N., 1987: Suppression of baroclinic instability in horizontally sheared flows. *J. Atmos. Sci.*, **44**, 3710-3720.

Lau, N.-C. Variability of the observed midlatitude stormtracks in relation to low-frequency changes in the circulation pattern. *J. Atmos. Sci.,* **45**, 2718-2743.

Lau, N.C. and E.O. Holopainen (1984): Transient eddy forcing of the time mean flow as identified by quasi-geostrophic tendencies. *J. Atmos. Sci.,* **41**, 313-328.

Lau, N.-C. and J.M. Wallace 1979: On the distribution of horizontal transports by transients in the Northern Hemisphere wintertime circulation, *J. Atmos Sci.,* **36**, 1844-1861.

Mullen, S.L., 1997: Transient eddy forcing of blocking flows. *J. Atmos. Sci.,* **44**, 3-22.

Nakamura, H.and J.M. Wallace, 1991: Observed changes in baroclinic wave activity during the life cycles of low frequency circulation anomalies. *J. Atmos. Sci.,* **47**, 1100-1117

Nakamura, H., 1992: Skewness of low-frequency fluctuations in the tropospheric circulation

during the Northern Hemisphere winter.. *J. Atmos. Sci.,* **48**, 1441-1448.

Nakamura, H.and J.M. Wallace, 1990: Observed changes in baroclinic wave activity during the life cycles of low frequency circulation anomalies. *J. Atmos. Sci.,* **47**, 1100-1117.

Nakamura, H., M. Tanaka, and J.M. Wallace, 1987: Horizontal structure and energetics of Northern Hemisphere wintertime teleconnection patterns. *J. Atmos. Sci.,* **44**, 3377-3391.

Nakamura, H., 1994: Rotational evolution of potential vorticity associated with a strong blocking flow configuration over Europe. Geophys. Res. Lett., 21, 2003-2006.

Plumb, R.A., 1986: Three-dimensional propagation of transient, quasi-geostrophic eddies and its relationship with eddy forcing of the time-mean flow. *J. Atmos. Sci.,* **43**, 1657-1678.

Simmons, A.J., J.M. Wallace and G.W. Branstator, 1983: Barotropic wave propagation and instability, and atmospheric teleconnection patterns. *J. Atmos. Sci.,* **40**, 1363-1392.

Wallace, J.M., 1996: Observed decade-to-century scale climate variability. In *Decadal Climate Variability, Dynamics and Predictability.*, J. Willebrand and D.L.T. Anderson eds., Springer Verlag NATO ASI Series, 493pp.

Wallace, J.M. and N.C. Lau, 1985: On the role of barotropic energy conversions in the general circulation. *Issues in Atmospheric and Oceanic Modeling. Part A: Climate Dynamics. Adv. in Geophysics,* **28** (Academic Press), 33-74.

Wallace, J.M., G.-H. Lim and M.L. Blackmon, 1996: Relationships between cyclone tracks, anticyclone tracks and baroclinic waveguides. *J. Atmos. Sci.,* **45**, 439-462.

8. CLIMATE VARIABILITY

8.1 The annual march

The canonical January / July polarity
The equatorial tropopause
The equatorial cold-tongue / ITCZ complex
Ozone (springtime maximum)

8.2 Interannual variability

the stratospheric QBO
ENSO
tropical Atlantic variability
the NAO
continental rainfall

8.3 Decadal variability

Pacific
Atlantic

8.4 Implications for global change

Fig. 5.10 The vorticity perturbations generated by a circular vorticity source centered at 30°N on the middle meridian is inserted into a westerly mean flow with constant angular velocity. The interval between latitude circles and meridians is 30°. Solid contours are positive and negative contours are dashed. After Hoskins et al., (1978).

APPENDIX 5 *Conservation equation for the variance of a scalar quantity*

Consider a scalar quantity ψ governed by the equation

$$\frac{\partial \psi}{\partial t} = -u\frac{\partial \psi}{\partial x} - v\frac{\partial \psi}{\partial y} - \omega\frac{\partial \psi}{\partial p} + \ldots\ldots\ldots \tag{A5.1}$$

where there may be additional source/sink terms. We will be concerned only about the advection terms. We begin by expanding ψ and the velocity components in terms of zonal mean and eddy components

$$\psi = [\psi] + \psi^*, \quad u = [u] + u^*, \quad \text{etc.}, \tag{A5.2}$$

which yields

$$\begin{aligned}\frac{\partial \psi}{\partial t} = &-[u]\frac{\partial [\psi]}{\partial x} - [u]\frac{\partial \psi^*}{\partial x} - u^*\frac{\partial [\psi]}{\partial x} - u^*\frac{\partial \psi^*}{\partial x} \\ &-[v]\frac{\partial [\psi]}{\partial y} - [v]\frac{\partial \psi^*}{\partial y} - v^*\frac{\partial [\psi]}{\partial y} - v^*\frac{\partial \psi^*}{\partial y} \\ &-[\omega]\frac{\partial [\psi]}{\partial p} - [\omega]\frac{\partial \psi^*}{\partial p} - \omega^*\frac{\partial [\psi]}{\partial p} - \omega^*\frac{\partial \psi^*}{\partial p} + \ldots\ldots ,\end{aligned} \tag{A5.3}$$

Next we zonally average, which yields

$$\frac{\partial [\psi]}{\partial t} = -[u]\frac{\partial [\psi]}{\partial x} - \left[u^*\frac{\partial \psi^*}{\partial x}\right] - [v]\frac{\partial [\psi]}{\partial y} - \left[v^*\frac{\partial v^*}{\partial y}\right] - [\omega]\frac{\partial [\psi]}{\partial p} - \left[\omega^*\frac{\partial \psi^*}{\partial p}\right] + \ldots \tag{A5.4}$$

Subtracting (A5.4) from (A5.3), we obtain an expression for the time rate of change of the eddy component

$$\begin{aligned}\frac{\partial \psi^*}{\partial t} = &-[u]\frac{\partial \psi^*}{\partial x} - u^*\frac{\partial [\psi]}{\partial x} - u^*\frac{\partial \psi^*}{\partial x} + \left[u^*\frac{\partial \psi^*}{\partial x}\right] \\ &-[v]\frac{\partial \psi^*}{\partial y} - v^*\frac{\partial [\psi]}{\partial y} - v^*\frac{\partial \psi^*}{\partial y} + \left[v^*\frac{\partial \psi^*}{\partial y}\right] \\ &-[\omega]\frac{\partial \psi^*}{\partial p} - \omega^*\frac{\partial [\psi]}{\partial p} - \omega^*\frac{\partial \psi^*}{\partial p} + \left[\omega^*\frac{\partial \psi^*}{\partial p}\right] + \ldots\end{aligned} \tag{A5.5}$$

Multiplying by ψ^*, we obtain

$$\begin{aligned}\frac{\partial\left(\psi^{*2}/2\right)}{\partial t} = \psi^*\frac{\partial \psi^*}{\partial t} = &-[u]\frac{\partial\left(\psi^{*2}/2\right)}{\partial x} - u^*\psi^*\frac{\partial [\psi]}{\partial x} - u^*\frac{\partial\left(\psi^{*2}/2\right)}{\partial x} + \psi^*\left[u^*\frac{\partial \psi^*}{\partial x}\right] \\ &-[v]\frac{\partial\left(\psi^{*2}/2\right)}{\partial y} - v^*\psi^*\frac{\partial [\psi]}{\partial y} - v^*\frac{\partial\left(\psi^{*2}/2\right)}{\partial y} + \psi^*\left[v^*\frac{\partial \psi^*}{\partial y}\right] \\ &-[\omega]\frac{\partial\left(\psi^{*2}/2\right)}{\partial p} - \omega^*\psi^*\frac{\partial [\psi]}{\partial p} - \omega^*\frac{\partial\left(\psi^{*2}/2\right)}{\partial p} + \psi^*\left[\omega^*\frac{\partial \psi^*}{\partial p}\right] + \ldots\end{aligned} \tag{A5.6}$$

Zonal averaging of this expression yields

$$\frac{\partial\left[\psi^{*2}/2\right]}{\partial t} = -[u]\frac{\partial\left[\psi^{*2}/2\right]}{\partial x} - \left[u^*\psi^*\right]\frac{\partial[\psi]}{\partial x} - \left[u^*\frac{\partial\left(\psi^{*2}/2\right)}{\partial x}\right] + 0$$

$$-[v]\frac{\partial\left[\psi^{*2}/2\right]}{\partial y} - \left[v^*\psi^*\right]\frac{\partial[\psi]}{\partial y} - \left[v^*\frac{\partial\left(\psi^{*2}/2\right)}{\partial y}\right] + 0$$

$$-[\omega]\frac{\partial\left[\psi^{*2}/2\right]}{\partial p} - \left[\omega^*\psi^*\right]\frac{\partial[\psi]}{\partial p} - \left[\omega^*\frac{\partial\left(\psi^{*2}/2\right)}{\partial p}\right] + 0 + ... \qquad \text{(A5.7)}$$

where the first and second terms on the right hand side on the top line also disappear in the zonal averaging. In order to put this expression into 'flux form', we add

$$0 = \left[\psi^{*2}/2\right]\left(\frac{\partial[u]}{\partial x} + \frac{\partial[v]}{\partial y} + \frac{\partial[\omega]}{\partial p}\right) \qquad \text{(A5.8)}$$

and

$$0 = \left[\psi^{*2}/2\right]\left(\frac{\partial u^*}{\partial x} + \frac{\partial v^*}{\partial y} + \frac{\partial \omega^*}{\partial p}\right) \qquad \text{(A5.9)}$$

and combine the terms on the right hand side with the corresponding advection terms in (A5.7) to obtain

$$\frac{\partial\left[\psi^{*2}/2\right]}{\partial t} = -0 - 0 - \left[\frac{\partial u^*\left(\psi^{*2}/2\right)}{\partial x}\right] + 0 \qquad \text{(A5.9)}$$

$$-\frac{\partial[v]\left[\psi^{*2}/2\right]}{\partial y} - \left[v^*\psi^*\right]\frac{\partial[\psi]}{\partial y} - \left[\frac{\partial v^*\left(\psi^{*2}/2\right)}{\partial y}\right] + 0$$

$$-\frac{\partial[\omega]\left[\psi^{*2}/2\right]}{\partial p} - \left[\omega^*\psi^*\right]\frac{\partial[\psi]}{\partial p} - \left[\frac{\partial \omega^*\left(\psi^{*2}/2\right)}{\partial p}\right] + 0 + ...$$

where the remaining term on the top line is zero. When this expresion is integrated over the entire mass of the atmosphere, noting that the vertical fluxes through the poles and the top and bottom of the atmosphere are equal to zero, the first and third terms on the second line vanish in the meridional integration and the corresponding terms on the third line vanish in the vertical integration leaving

$$\frac{1}{g}\int_0^{p_0}\frac{\partial\left[\psi^{*2}/2\right]}{\partial t}dp = -\frac{1}{g}\int_0^{p_0}\left[v^*\psi^*\right]\frac{\partial[\psi]}{\partial y}dp - \frac{1}{g}\int_0^{p_0}\left[\omega^*\psi^*\right]\frac{\partial[\psi]}{\partial p}dp + ... \qquad \text{(A5.10)}$$

If the above operations are performed based on time averaging, as opposed to zonal averaging; i.e., with $\psi = \overline{\psi} + \psi'$ $u = \overline{u} + u'$ etc., in place of (A5.2), it is readily verified that the term $-\overline{u'\psi'}\frac{\partial \overline{\psi}}{\partial x}$, which is the counterpart of the second term on the top line of (A5.7) does not vanish and the final result is

$$\frac{1}{g}\int_0^{p_0} \frac{\partial \overline{\psi'^2/2}}{\partial t} dp = -\frac{1}{g}\int_0^{p_0} \overline{u'\psi'}\frac{\partial \overline{\psi}}{\partial x} dp - \frac{1}{g}\int_0^{p_0} \overline{v'\psi'}\frac{\partial \overline{\psi}}{\partial y} dp - \frac{1}{g}\int_0^{p_0} \overline{\omega'\psi'}\frac{\partial \overline{\psi}}{\partial p} dp \qquad \text{(A5.11)}$$

4.5 A Lagrangian Perspective

In the absence of diabatic heating and friction, potential vorticity should be conserved. For any conservative tracer, χ, we can write

(

where v_L and ω_L are the Lagrangian mean meridional circulations. The distinction between Lagrangian and conventional Eulerian mean meridional circulations can be understood as follows. Suppose that we identify a large number of air parcels, equally spaced along a particular latitude circle, on a particular pressure level, and follow the subsequent motion of these marked parcels, as projected onto the meridional plane. Initially all the parcels occupy the same point in the plane, but within a few days they will disperse into a cloud which gradually spreads until it occupies the whole domain. Beyond some characteristic "memory time", clouds of marked parcels emanating from different points in the meridional plane are no longer distinguishable from one another. For time intervals much shorter than this "memory time" is it meaningful to identify the "center of mass" of the cloud of air parcels and follow it as it moves in the meridional plane. The Lagrangian mean meridional circulation is defined as the vectorial time rate of change of the position of this cloud. We will soon see that in the presence of eddies the Lagrangian mean meridional motions need not be the same as the Eulerian mean meridional motions.

Now if the zonal flow is not changing with time, under adiabatic and frictionless conditions, we can write

(

where P is the Ertel potential vorticity.

The advection can be zero only if [v] and [ ] are zero, of if the Lagrangian mean meridional motions happen to line up with contours of [P]. Contours of P in the earth's atmosphere tend to

be quasi-horizontal, with P increasing monotonically with height. Hence the Lagrangian mean meridional motion cannot follow along constant potential vorticity surfaces unless the atmosphere is systematically moving northward or southward. It follows that for steady, adiabatic, frictionless flow, the Lagrangian mean meridional circulations are zero.

It also follows from (4.19) that for adiabatic, frictionless, quasi-geostrophic flow

(

Hence, whenever the eddy fluxes are acting so as to produce significant changes in the zonal flow, they must be giving rise to substantial Lagrangian mean meridional circulations.

5.6 Wave Energy Fluxes

The distributions of the eddy fluxes of geopotential, [ ] and [ ], in the meridional plane give an indication of regions of generation and dissipation of the eddies. We recall from Section 1.4 that these fluxes can be interpreted in terms of the work that one part of the atmosphere does on the other part through mechanical stirring. In this section, we will show that the distribution of these so-called "wave energy fluxes" is closely related to the eddy forcing of the zonal flow, through the Eliassen- Palm fluxes. We will demonstrate this relationship by expressing [ ] and [ ] in terms of [ ] and [ ], for the special case of waves which exist in a steady state, in a dissipation-free environment.

Fig. 5.10

Let us consider the vertical flux of wave energy first. Fig. 5.10(a) shows an idealized eddy or wave in which there exists a perfect negative correlation between ω andΦ so that the wave energy flux is upward. We will assume that air is moving through the wave from west to east at the speed of the mean zonal wind [ ] minus the speed of propagation of the wave c and that the wave is neither growing nor decaying. We will further assume that the motion is entirely adiabatic. It can be seen from Fig. 5.10(a) that as a consequence of the sinking in the wave troughs and rising in the wave ridges, poleward moving air parcels must be warmer than equatorward moving parcels on the the same pressure level and hence there must be a net poleward eddy heat transport. We can demonstrate this result more formally and quantitatively by writing an expression for the time rate of change of temperature following a horizontal streamline moving with zonal velocity [u]-c, neglecting the non-linear horizontal advection terms u* T*/ x and v* T*/ y:

(

Then we multiply both sides by * and zonally average, making use of the identity

(

and the geostrophic approximation

(

which yields

(

This result is consistent with Fig. 5.10(a): given an eastward flow relative to the waves, an upward flux of geopotential or "wave energy" implies a poleward heat flux and vice versa. For westward flow relative to the waves the opposite conditions would prevail.

Now let us consider the meridional wave energy flux [v* *]. Fig. 5.10(b) shows an idealized eddy or wave in which there exists a negative correlation between v and , by virtue of a poleward, cross isobar flow in the wave troughs and an equatorward cross isobar flow in the ridges. (Since the geostrophic wind is incapable of transporting geopotential in the meridional direction (see Sec. , the sign and magnitude of [v* *] are completely determined by this cross-isobar component). In response to the cross-isobar flow, air parcels speed up as they move through the troughs and slow down as they move through the ridges. These accelerations and decelerations affect the zonal wind component because they are induced by meridional cross-isobar flow. It follows that the zonal wind must be stronger in the poleward flow, downstream from the troughs than in the equatorward flow, downstream from the ridges: hence [u*v]>0. Formally, we can write, using the same assumptions as in the previous derivation

5. Dynamics of a Geostrophically Balanced Vortex

The zonally averaged versions of (1) the zonal momentum equation, (2) the thermodynamic energy equation, (3) the thermal wind equation, and (4) the continuity equation together form a closed system of prognostic equations which can be solved as an initial value problem in order to forecast the future evolution of the zonally averaged zonal wind and temperature fields in response to time dependent distributions of diabatic heating, sources or sinks of zonal momentum, and eddy fluxes of heat and zonal momentum. At each time step, the distribution of mean meridional motions is derived as a by-product. The system of equations is, in many respects analogous to the quasi-geostrophic equations where zonal momentum is the analogue of vorticity and the mean meridional motions are the analogue of the ageostrophic motions which maintain the vorticity and temperature fields in a state of thermal wind balance.

The dynamics of a geostrophically balanced vortex were first discussed by Eliassen (1952) and applied more extensively to the diagnosis of mean meridional circulations in the earth's atmosphere by Kuo (1956). More recent reviews of this material can be found in Holton (1979: Section 10.4), Charney (1973), and Holton (1975), where these references are listed in order of increasing complexity of the treatment. This system of equations has been applied to the study of the annual cycle in the mesospheric jetstreams by Leovy (1964), the quasi-biennial oscillation by Wallace and Holton (1968) and it is currently being used by Haberle for diagnosis of the zonally symmetric component of the Martian circulation.

5.1 The Governing Equations

The full system of equations governing the time evolution of geostrophic, zonally symmetric motions on a spherical earth is derived in the Appendices. In this section we will deal with a simplified set based on Cartesian geometry, which retains only the leading terms.

Q diabatic heating rate in deg K per unit time.

F the frictional source or sink of zonal momentum/unit mass.

G $-\partial/\partial y[u^*v^*]$: the source or sink of zonal momentum/unit mass due to meridional eddy transports.

E $-\partial/\partial y[v^*T^*]$: the time rate of change of temperature due to meridional eddy transports.

With these assumptions the set of equations that we will be discussing is exactly analogous to the quasi-geostrophic equations. The more exact treatment in the Appendix which retains the spherical geometry and the vertical eddy fluxes is in some sense more exact than the quasi-geostrophic treatment. The simplified equations retain all the effects that we wish to discuss here. The simplified equations are

(

(

(

(

This set of equations involves four unknowns: [u], [T], [ ] and [ ]. We can reduce it to three equations in three unknowns by expressing the mean meridional motions in terms of the gradient of the streamfunction ( ); that is

(

Use of the steam function insures that (5.4) is satisfied. Since all the terms in (5.1)-(5.4) are zonally averaged anyway, we can drop the brackets notation and write

(

(

(

(

Before proceeding any further, let us reflect upon the nature of time dependent solutions of (5.6)-(5.8). At any instant in time, u is changing in response to the distributions of F and G, while T is changing in response to the distribution of B and Q which, for all we know, are entirely unrelated to those of F and G. Yet despite the lack of any dependable relation between G, F, B and Q, we know that T and u are changing in a manner that is consistent with the thermal wind equation: i.e., the meridional temperature gradient can't change unless the vertical wind shear changes, and vice versa. How does the temperature field know how the wind field is changing, and vice versa? Any change in one field without a compensating change in the other immediately creates a small departure from geostropic balance (that is, the zonal wind suddenly finds itself subgeostrophic or supergeostrophic). The resulting imbalance between the meridional components of the pressure gradient force and the Coriolis force gives rise to an acceleration in the meridional direction and hence to mean meridional motions together with vertical velocities as required by the continuity equation. Hence it is the terms involving mean meridional motions (the terms) in (5.6) and (5.7) which keep the zonal wind and temperature fields in thermal wind balance. The ageostrophic flow plays an analogous role in the quasigeostrophic system.

5.2 Some Examples

In order to better understand how the mean meridional motions perform this balancing act, let us consider a few specific examples:

Fig. 5.1

The annual cycle in the mesosphere: At the times of the solstices the zonal flow at

mesospheric levels is characterized by a matched pair of mid-latitude jetstreams with westerlies in the winter hemisphere, as described in Fig. 5.1. With the approach of the equinoxes, temperatures at the stratopause level begin to warm over the pole which is experiencing late winter. The warming is reflected in the thickness field, so that geopotential height in polar latitudes at mesospheric levels must rise. As the heights over the polar region rise, the meridional pressure gradient weakens and the westerly jet in middle latitudes finds itself supergeostrophic. (Its supporting temperature gradient is literally being cut out from underneath it by the radiative warming at the polar stratopause). In response to this supergeostrophic flow the unbalanced equatorward Coriolis force induces a meridional circulation up the pressure gradient toward lower latitudes. This equatorward flow is accompanied by ascent over the pole at the stratopause level whose adiabatic cooling counteracts but doesn't completely cancel the radiative warming. Meanwhile, in the late summer hemisphere the easterly jet is also finding itself in a supergeostrophic state as the polar regions begin to cool off at the stratopause level. The unbalanced Coriolis force induces a flow toward the pole which is accompanied by subsidence over the pole, whose adiabatic warming counteracts but doesn't completely cancel the radiative cooling. These relationships are illustrated in Figs. 5.2 and 5.3.

Fig. 5.3

Note that the mean meridional circulation in Fig. 5.2 takes the form of a single cell extending from pole to pole. The circulation is thermally indirect, with rising over the colder pole and sinking over the warmer pole and cross-isobar flow toward higher pressure. In effect, the mean meridional circulation is trying (without complete success) to maintain the existing meridional temperature gradient at the stratopause level, but in so doing, it is destroying the jetstreams. Kinetic energy is being converted into available potential energy which, in turn, is being destroyed by radiative heating over the cold pole and radiative cooling over the warm pole. The mesospheric jetstreams and the meridional temperature gradients at the stratopause level are both weakening at rates which are just sufficient to keep them in thermal wind balance. If the decrease in the temperature gradient gets a little bit ahead of the decrease in the strength of the jets, the winds will become more supergeostrophic and the mean meridional circulation in Fig. 5.2 will speed up a little so that the balance is restored.

Shortly after the time of the equinox, the mesospheric jets in Fig. 5.1 completely disappear. At precisely the same time the pole-to-pole temperature gradient at the stratopause level reverses so that the springtime pole becomes warmer than the autumn pole. The mean meridional circulation continues in the same sense as in Fig. 5.2 only from this point on it is thermally

direct, with rising over the warmer pole, sinking over the colder pole, etc. This continuing mean meridional circulation gives rise to a new pair of jets whose polarity is the opposite of those that existed previously. This later situation is illustrated in Fig. 5.4 and 5.5.

Fig. 5.5

With the approach of the equinox, temperatures at the stratopause level eventually attain radiative equilibrium and the radiative heating and cooling stop. In the absence of other forcing the mean meridional circulation would also grind to a halt and the zonal wind and temperature fields would remain in thermal wind equilibrium. A few months later, radiative heating and cooling resume with the opposite polarity, which leads to the development of a mean circulation whose sense is opposite to that in Figs. 5.2 and 5.4.

In the situation considered above the only forcing was in the diabatic heating field Q. Although the Q term appears only in the Thermodynamic Energy Equations (5.7), the forcing was felt by the zonal wind through the - / p term in (5.6). Now let us consider a situation in which the forcing comes from the eddy flux terms B and G.

Eddy Fluxes in the Mid-latitude Troposphere: In the mid-latitude troposphere during winter, the eddies produce strong poleward fluxes of heat and zonal momentum. At 50°N, 500 mb the momentum forcing G is positive and increasing with height. Hence, the eddies are acting to increase the existing vertical wind shear; making the westerlies increase more rapidly with height. The poleward eddy heat flux is near its maximum at 50°N, so that B is increasing with latitude; from negative values to the south, to positive values to the north. Hence B/ y>0 and B is acting to reduce the existing mean temperature gradient; producing cooling to the south and warming to the north. These relationships are illustrated in Fig. 5.6.

Fig. 5.6

From the standpoint of the acceleration of the zonal flow, it is evident that the eddy fluxes of zonal momentum and heat are working at cross purposes: the former are acting directly to accelerate the westerly flow at 50°N at the jetstream level while the latter are acting indirectly, through their induced mean meridional motions, to decelerate it. The net result, to first order, is zero acceleration. However, from the standpoint of the induction of mean meridional circulations, it is evident that the two kinds of fluxes are both contributing to make the westerlies supergeostrophic at the jetstream level, thus inducing an equatorward flow which constitutes the upper branch of the Ferrel cell. The Coriolis force associated with this equatorward flow

cancels the momentum forcing G, while the adiabatic heating and cooling associated with the corresponding vertical motions cancels the thermal forcing B. If there were no eddy fluxes, there would be no need for a Ferrrel cell as a mechanism for keeping the mean zonal wind and temperature fields in thermal wind balance. In this sense we can think of the Ferrel cell as being driven by the eddies.

In the two examples considered with this section, some rather general conclusions can be drawn. If one type of forcing (G, F, B or Q) is considered in isolation, it must contribute to inducing mean meridional circulations, which will always act so as to oppose the forcing. Despite this opposition, the zonal flow and its associated temperature field will change in the sense in which the forcing is acting. The changes will occur in such a way that the zonal wind and temperature fields remain in thermal wind balance. The particular example that we considered involved forcing through the Q term. However, it is easily verified that these conclusions are valid for any of the forcing terms.

The combined effect of forcing from eddy fluxes B and G is inherently more complex. In the particular example that we considered, G and B were distributed in such a way as to produce little or no net forcing of the zonal flow (that is to say, u/ t 0, but they worked together to force a strong mean meridional circulation. One can imaging other distributions (hypothetical ones, at least) which might produce a strong forcing of the zonal flow and little or no man meridional circulations, or some of both. It remains to be seen whether, in the example described above, G and B just heppened to be distributed so as to produce no net forcing of the mean zonal flow or whether there is some fundamental reason why they opposed one another.

5.3 The Omega Equation

We can gain a clearer understanding of the forcing of mean meridional motions by diabatic heating, friction, or eddy fluxes if we eliminate the time dependent terms in (5.6) and (5.7) and solve directly for in terms of G, F, B, and Q. To this end we differentiate (5.6) with respect to pressure, and (5.7) with respect to latitude and substitute the right hand sides of both equations into (5.8) to obtain, after some minor rearranging,

(

where A( ) is an elliptic operator. The distributions of A( ) and in the meridional plane should be qualitatively similar but of opposite sign, with the distribution being smoother. Hence, distinct maxima and minima in should correspond roughly to centers of circulation cells in the meridional plane. By our definition, the Ferrel cell should circulate around a maximum in the field and the Hadley cell around a minimum.

In the middle of the Ferrel cell G is increasing with height (decreasing with pressure) and B is increasing with latitude from negative values to the south of the maximum in [v*T*] to

positive values to the north of it, as shown in Fig. 5.6. Hence, both terms in (5.9) are contributing to producing negative values of A( ) which results in a local minimum and maximum in itself. F also contributes to producing negative values of A( ) near the top of the planetary boundary layer in middle latitudes because of the presence of surface westerlies. The reader is invited to verify that the F, G, and Q terms all contribute to positive values of A( ) in the vicinity of the Hadley cell.

In Appendix 5a it is shown that if the eddy wind field can be assumed to be quasi nondivergent, it follows that

(

where is relative vorticity. If we substitute this expression into (5.9) and assume that Q and F are negligible, the resulting expression bears a strong resemblance to the quasi-geostrophic "omega equation". In the omega equation the "forcing" for an elliptic operator involves the vertical derivative of the vorticity advection and the Laplacian of the heat flux, whereas in (5.9) it involves the vertical derivative of [v* *] and / y [v*T*].

For a geometrical interpretation of (5.9) we can write it in the form

(

and expressing it as

(

where

(

and ( ) is the divergence operator in the meridional plane, with ln p as vertical coordinate. Note that ln p is approximately equivalent to an inverted height scale; j and are unit vectors in the y and ln p (downward) directions. The distribution of X can be determined by observations or it can be specified for various hypothetical distributions of B, Q, G and F. A schematic distribution of X for the Northern Hemisphere wintertime troposphere is depicted in Fig. 5.7. It can be seen that X, as we have defined it, radiates out of thermally indirect circulation cells and into thermally direct ones. Fig. 5.7 (a) can be interpreted as the direct eddy forcing of the mean meridional circulations. The

Fig. 5.7

other components of the forcing shown in panels (b) and (c) are more difficult to interpret because F is determined by the distribution of zonal wind at the earth's surface, and Q is determined by the distributions of temperature and precipitation; surface wind, temperature and precipitation, in turn, are determined by the mean meridional circulations and the eddy fluxes.

A more exact analogue of (5.9) can be derived from the complete zonally averaged versions

of the zonal momentum equation and the First Law. The resulting equation contains a mixed second order term and first order terms and , but it is still elliptic, provided that angular momentum decreases with latitude on surfaces of constant potential temperature, which corresponds to the criterion for stability with respect to axially (zonally) symmetric disturbances. Given suitable boundary conditions (e.g., = 0 at the earth's surface and at the poles), (5.9) or its more complete counterpart can be solved by conventional numerical methods. For a discussion of the complete equation, see Wallace and Holton (1968).

We have now considered four different methods of inferring the mean meridional motions:

(1) Direct estimates of [v] on the basis of wind data, and inference of [ ] from the continuity equation, given suitable top or bottom boundary conditions. This method is the most straightforward in principle, but it is difficult because [v] is one or two orders smaller than v at individual longitudes, so that sampling errors may be larger than [v] itself.

(2) Inference of [v] from the zonally averaged zonal momentum equation (2.), where [u]/ t, and G are estimated on the basis of observed data and the meridional advection term [ ] [u]/ p is assumed to be negligibly small. For seasonal mean statistics the time rate of change term can often be neglected. As in (1), [ ] can be inferred from [v] on the basis of the continuity equation. This method yields results to within about 20% accuracy for the strength of the Ferrel cell.

(3) Use of the First Law to estimate [ ], from which [ ] is inferred through the use of the continuity equation. As in (2), the time rate of change term can often be neglected. This method is of some use for the Hadley cell.

(4) Use of the diagnostic equation (5.9) of its more complete counterpart, which, in effect, represents a combination of (2) and (3) which results in an elimination of the time dependent terms.

If the zonal flow is changing with time and if its future evolution is not known, the / t terms will be difficult to estimate accurately, so that methods (2) and (3) will not be reliable. In this situation, (4) will give the best estimate of the mean meridional motions.

It is of interest to compare these four methods of inferring the mean meridional motions to the four methods of estimating large-scale vertical velocity at a fixed point in space and time. Method (2) is analogous to the kinematic method and it is subject to similar limitations with regard to sampling errors because of the smallness of . Method (2) is analogous to the vorticity budget approach, in which one infers divergence as a residual from the vorticity equation and integrates vertically (usually downward from a "top" boundary condition) to obtain vertical velocity. Method (3) is clearly analogous to the adiabatic method (see 8.7 of Wallace and Hobbs 1977)) which estimates the local vertical velocity as a residual from the

First Law. Method (4) is analogous to diagnostic equations for , from which the time dependent terms have been eliminated. The simplest of these diagnostic equations is the quasi-geostrophic omega equation, analogous to (5.9) and the most complete is based on numerical solution of the primitive equations, without any simplifications.

5.4 The Potential Vorticity Equation

In order to deduce the changes in the zonally averaged wind and temperature fields which should occur in response to forcing from the G, F, B and Q fields it is necessary to eliminate the terms involving mean meridional circulations from (5.6) and (5.7). To this end we (2) differentiate (5.6) with respect to latitude, treating f as a slowly varying function of latitude so that v f/ y can be neglected in comparison to f v/ y, (2) multiply (5.7) by f/ and then differentiate it with respect to pressure, (3) add the two equations, and (4) reverse all the signs to obtain

(

where e have reintroduced the brackets notation for zonal averages for the sake of clarity. Henceforth we will treat the static stability σ as a function of pressure only.

At this point it is convenient to introduce the quasi-geostrophic potential vorticity

(

which is discussed further in Appendix 2. From an inspection of the First Law, it is readily verified that under adiabatic flow conditions the local value of T/ is a measure of the (Lagrangian) vertical displacement of that air parcel from any arbitrary reference (pressure) level; it has units of pressure, so that its vertical derivative is dimensionless. We can resolve (5.13) into zonally symmetric and eddy components, in the usual manner, with

(

and

Substituting (5.14) into (5.12) we have

(

Hence, zonally symmetric quasi-geostrophic potential vorticity can be increased locally by zonal momentum sources which increase - (u)/ y (the first term), or by heat sources which act to make (T)/ p more negative (the second term). Alternatively, the two terms can be thought of as sources (or sinks) of vorticity and static stability, respectively.

Now let us consider the form of the poleward eddy flux of quasi-geostrophic potential vorticity. Multiplying (5.15) by v*, and zonally averaging, we obtain

(

which can be rewritten in the form

(

since is not a function of longitude, we can take it outside the brackets in the last term. Then, substituting for v*/ p from the thermal wind equation, and making use of the identity

(

we can eliminate the last term, which leaves us with

(

where the two terms on the right-hand side can be identified with the poleward transports of relative vorticity and static stability, respectively. Substituting from (5.10) for [*v*] it can be written as

(

Substituting (5.18) into (5.16) and rearranging, we obtain

(

The first term on the right-hand side may be recognized as the meridional convergence of the eddy flux of potential vorticity. With the assumptions we have made in deriving (5.19) this term has no counterpart involving the vertical fluxes of q. Note the analogy to the conventional quasi-geostrophic potential vorticity equation which contains no vertical advection term. Notably absent are terms involving mean meridional circulations. The absence of such terms is no accident, since we purposely set out to eliminate them in the first place.

The fact that mean meridional motions have no effect on quasi-geostrophic potential vorticity can be understood as follows. Such motions exert the largest influence in changing the vorticity in regions where [v] is changing rapidly with latitude. For example, equatorward of the jetstream, in the upper branch of the Hadley cell the f[v] term in (5.10 is positive whereas poleward of the jetstream, in the upper branch of the Ferrel cell it is negative. Hence in the vicinity of the jetstream, the mean meridional circulations are contributing to increasing the relative vorticity. However, in this same region, [[/ p>0 and the mean vertical motions are producing a vertical stretching of layers between isentropes, thus reducing the static stability. The net result is zero change in potential vorticity. A similar compensation exists wherever there is a strong divergence of [v].

Since the zonal flow can change only if [q] changes (assuming fixed boundary conditions), it follows from (5.19) that in the absence of diabatic heating and friction, the mean zonal flow can change if and only if the eddies produce a meridional transport of quasi-geostrophic potential vorticity. In the absence of such transports, the eddy forcing G and B will drive mean meridional circulations which completely cancel their effects on the zonal wind and temperature fields, leaving these fields unchanged. We have already seen in Section 5.2 that such condition commonly prevail in the middle latitude troposphere near the center of the Ferrel cell. In this region the two terms on the right-hand side of (5.17) tend to cancel, so that [q*v*] 0. The zonal

momentum and heat fluxes cooperate to drive the Ferrel cell which cancels the effects of the G and B terms in (5.1) and (5.2), respectively.

Now let us consider three different types of situations in which the zonal flow will change in response to eddy forcing

(a) Suppose that in some localized region in the meridional plane [*v*]>0 as a result of a convergence in the poleward flux of westerly momentum, but there are no poleward heat fluxes. In this case [q*v*]>0 and the flow should change by becoming more westerly in the region of eddy forcing. Some mean meridional motions will develop in response to the forcing because the zonal wind in the region of eddy forcing. Some mean meridional motions will develop in response to the forcing because the zonal wind in the region of eddy forcing will tend to depart from thermal wind balance as it becomes more westerly. This imbalance will drive an equatorward flow which will give rise to a negative f[v] term which opposes the westerly acceleration. The associated vertical motions will generate horizontal temperature gradients above and below the region of eddy forcing, as illustrated in Fig. 5.8a. The development of these temperature gradients will allow the geostrophically balanced component of the zonal flow to become more westerly. Hence the zonal wind will gradually become more westerly in response to the forcing, but not as fast as one would think from considering G alone.

Fig. 5.8

(b) Suppose that in some localized region the poleward eddy heat flux is increasing with height as indicated in Fig. 5.8b, but there are no momentum fluxes. Again, [q*v*]>0 and the zonal flow should change in the same sense as in (a). As the temperature gradients change in response to the eddy forcing, the zonal flow will depart from thermal wind balance, but in the opposite sense as in (a). Hence the induced mean meridional circulation will be poleward, and it will give rise to westerly acceleration. Again, the mean meridional circulations will resist the forcing; this time by producing adiabatic warming and cooling in opposition to the B term. The net result is qualitatively the same as in (a) with a westerly acceleration occurring in response to a poleward flux of potential vorticity.

(c) Suppose that the forcings in (a) and (b) are superimposed. In this case both types of fluxes will contribute to a positive [q*v*], so the resulting change in the zonal flow will be correspondingly larger than in (a) and (b). If the zonal wind and temperature changes resulting from the eddy fluxes just happen to be perfectly geostrophically balanced, then there will be no induced mean meridional circulations to oppose the forcing. Because of this fortuitous coincidence, the two forcing terms on the right-hand side of (5.9) exactly cancel so that A( )=0.

From the above examples it is evident that a poleward flux of potential vorticity is associated with westerly accelerations and vice versa. Hence, the relationships derived in this section can

be used in a qualitative way to infer the sense of the zonal wind changes induced by the eddies. It is interesting to consider this relationship in light of (5.10) which relates the eddy momentum flux forcing G to the poleward vorticity flux. Since [u] on any pressure surface and latitude circle is directly proportional to the circulation, which, in turn, is equal to the integral of the vorticity of the flow on that pressure surface within the polar cap region enclosed by that latitude circle, it is evident that the eddies can increase [u] only if they transport vorticity poleward across the latitude circle, into the polar cap region. In a similar manner, the poleward flux of potential vorticity is a measure of the geostrophically balanced zonal wind acceleration, which cannot be cancelled out by mean meridional circulations.

5.5 The Eliassen-Palm Flux

We can gain an extremely useful geometrical insight into the poleward eddy flux of potential vorticity by writing (5.17) in the form

(

where

(

is a vector in the meridional (y,p) plane. Here j and k are the unit vectors in the y and p (downward) directions. F is the pressure coordinates version of the so-called "Eliassen-Palm flux" which is e tensively used in the recent literature on wave-zonal flow interactions. It was first derived by Eliassen and Palm (1960) in a treatise on mountain-induced planetary waves and it is central to the concept of "wave action" as defined in Andrews and McIntyre (1978). The relation of the Eliassen-Palm flux to general circulation statistics will be discussed in a forthcoming paper by McIntyre, Edmon and Hoskins.

A schematic illustration of the distribution of F in the troposphere is shown in Fig. 5.9. From this distribution it appears that F is nearly non-divergent except in the upper branch of the Hadley cell, near 20°N, where there is definitely some convergence due to the increase in [u*v*] with latitude, and near the earth's surface in middle latitudes, where there is divergence due to the increase of [v*T*] with height in the planetary boundary layer. Note that most of the upward F in middle latitudes emanates from the ground.

Fig. 5.9

In the upper branch of the Hadley cell the eddies are apparently acting so as to decelerate the zonal flow, while in the mid-latitude planetary boundary layer they are acting so as to accelerate it. Yet despite this eddy forcing, the zonal flow remains in an approximately steady state. In order to reconcile these results it is necessary to postulate that the Hadley and Ferrel cells both contain components which are not directly forced by the eddies. The Hadley cell is partially driven by the meridional heating gradient. It is this thermally driven component of the

Hadley circulation which supplies the zonal momentum that is carried poleward by the eddies at the tropopause level. In a similar manner, it is only because the Ferrel cell contains a frictionally driven component that it is able to absorb the westerly momentum that the eddies deposit in the mid-latitude planetary boundary layer.

5.5 A Lagrangian Perspective

In the absence of diabatic heating and friction, potential vorticity should be conserved. For any conservative tracer, , we can write

(

where v_L and ω_L are the Lagrangian mean meridional motions. The nature of these motions can be understood as follows. Suppose that we identify a large number of air parcels, equally spaced along a particular latitude circle, on a particular pressure level, and follow the subsequent motion of these marked parcels, as projected onto the meridional plane. Initially all the parcels occupy the same point in the plane, but within an arbitrarily short time interval, they will disperse into a cloud which will gradually grow with time until it occupies the whole domain, at which time the parcels have, in effect, lost the memory of where they came from. For periods much shorter than this "memory time" is it meaningful to identify the "center of mass" of the cloud of air parcels and follow it as it moves in the meridional plane. The Lagrangian mean meridional motion is defined as the vectorial time rate of change of the position of this cloud. We will soon see that in the presence of eddies the Lagrangian mean meridional motions need not be the same as the Eulerian mean meridional motions.

Now if the zonal flow is not changing with time, under adiabatic and frictionless conditions, we can write

(

where P is the Ertel potential vorticity.

The advection can be zero only if [v] and [ ] are zero, of if the Lagrangian mean meridional motions happen to line up with contours of [P]. Contours of P in the earth's atmosphere tend to be quasi-horizontal, with P increasing monotonically with height. Hence the Lagrangian mean meridional motion cannot follow along constant potential vorticity surfaces unless the atmosphere is systematically moving northward or southward. It follows that for steady, adiabatic, frictionless flow, the Lagrangian mean meridional circulations are zero.

It also follows from (5.19) that for adiabatic, frictionless, quasi-geostrophic flow

(

Hence, whenever the eddy fluxes are acting so as to produce significant changes in the zonal flow, they must be giving rise to substantial Lagrangian mean meridional circulations.

5.6 Wave Energy Fluxes

The distributions of the eddy fluxes of geopotential, [ ] and [ ], in the meridional plane give an indication of regions of generation and dissipation of the eddies. We recall from Section 1.4 that these fluxes can be interpreted in terms of the work that one part of the atmosphere does on the other part through mechanical stirring. In this section, we will show that the distribution of these so-called "wave energy fluxes" is closely related to the eddy forcing of the zonal flow, through the Eliassen- Palm fluxes. We will demonstrate this relationship by expressing [ ] and [ ] in terms of [ ] and [ ], for the special case of waves which exist in a steady state, in a dissipation-free environment.

Fig. 5.10

Let us consider the vertical flux of wave energy first. Fig. 5.10(a) shows an idealized eddy or wave in which there exists a perfect negative correlation between ω andΦ so that the wave energy flux is upward. We will assume that air is moving through the wave from west to east at the speed of the mean zonal wind [ ] minus the speed of propagation of the wave c and that the wave is neither growing nor decaying. We will further assume that the motion is entirely adiabatic. It can be seen from Fig. 5.10(a) that as a consequence of the sinking in the wave troughs and rising in the wave ridges, poleward moving air parcels must be warmer than equatorward moving parcels on the the same pressure level and hence there must be a net poleward eddy heat transport. We can demonstrate this result more formally and quantitatively by writing an expression for the time rate of change of temperature following a horizontal streamline moving with zonal velocity [u]-c, neglecting the non-linear horizontal advection terms u* T*/ x and v* T*/ y:

(

Then we multiply both sides by * and zonally average, making use of the identity

(

and the geostrophic approximation

(

which yields

(

This result is consistent with Fig. 5.10(a): given an eastward flow relative to the waves, an upward flux of geopotential or "wave energy" implies a poleward heat flux and vice versa. For westward flow relative to the waves the opposite conditions would prevail.

Now let us consider the meridional wave energy flux [v* *]. Fig. 5.10(b) shows an idealized eddy or wave in which there exists a negative correlation between v and , by virtue of a poleward, cross isobar flow in the wave troughs and an equatorward cross isobar flow in the ridges. (Since the geostrophic wind is incapable of transporting geopotential in the meridional

direction (see Sec. , the sign and magnitude of [v* *] are completely determined by this cross-isobar component). In response to the cross-isobar flow, air parcels speed up as they move through the troughs and slow down as they move through the ridges. These accelerations and decelerations affect the zonal wind component because they are induced by meridional cross-isobar flow. It follows that the zonal wind must be stronger in the poleward flow, downstream from the troughs than in the equatorward flow, downstream from the ridges: hence [u*v]>0. Formally, we can write, using the same assumptions as in the previous derivation

(

where the subscript a denotes the ageostrophic component of v. Again, we multiply by , zonally average, rearrange the left-hand side and substitute for / from the geostrophic equation to obtain

(

and since $v^*=v_g^*+v_a^*$ and $[v_g^*\Phi^*]=0$, we can, if we wish, drop the a subscript. The result is consistent with Fig. 5.10(b): given an eastward flow relative to the waves an equatorward flux of geopotential implies a poleward flux of zonal momentum and vice versa. For westward flow relative to the waves, the opposite conditions prevail.

The wave energy flux in the meridional plane is closely associated with the Eliassen-Palm flux, since at any local point, from (5.20), (5.24) and (5.25), we have

(

so that W and F are everywhere in the same (or opposite) direction. In most of the earth's lower atmosphere, where [u]>c the eddy flux of geostrophically balanced westerly momentum is in the opposite sense to the flux of wave energy, so that the eddies are imparting westerly momentum to the zonal flow in regions of the meridional plane where they are being generated by baroclinic instability, mountains, etc. and they are extracting westerly momentum from the zonal flow in regions where they are being dissipated by radiative damping and friction.

The so-called "critical lines" in the meridional plane, where [u]=c are of special interest because they act as barriers to the flux of wave energy, as defined in (5.24) and (5.25). As wave energy propagates toward one of these critical lines, the fluxes of geopotential fluxes become progressively weaker and the waves become more and more susceptible to dissipative processes. Eddies generated by baroclinic instability in middle latitudes encounter such a situation when they propagate into the region equatorward of the jetstream where there is a strong convergence of the Eliassen-Palm flux. Critical lines are also intimately linked to certain kinds of instabilities which serve as mechanisms for generating eddies. Baroclinically unstables waves have a "steering level" and barotropically unstable waves have a "steering latitude", both of which may be viewed as critical lines in the meridional plane.

Now let us examine the behavior of the wave energy flux W the special situation of steady state waves which do not force the zonal flow. We will assume that the phase speed of the waves is independent of latitude and height and that there are no critical lines in the region of interest. For these special conditions we can write

(

Combining these expressions, we obtain

(

Substitution for [u]/ p from the thermal wind equation yields

(

Hence, the eddies are capable of producing a nonzero, local wave energy flux divergence, even when they are not accelerating the mean zonal flow. It follows that the Eliassen-Palm flux F is more useful than the wave energy flux W as a basis for diagnosing the interactions between the eddies and the mean zonal flow. The two terms on the right-hand side of (5.27) can be interpreted as the local rates at which the eddies extract energy from the mean zonal wind and temperature fields by barotropic and baroclinic processes, respectively. Note that these terms can both be positive, locally, without resulting in any growth of the eddies, or any weakening of the mean flow. In such a situation, the eddy kinetic energy gained locally from the zonal flow would, in effect, be exported by the wave energy fluxes (as indicated by 5.27) and the local effects of the eddies on the mean zonal wind and temperature fields would be cancelled by an eddy-induced mean meridional circulation. Locally, the kinetic energy budget could be viewed as depicted in Fig. 5.11.

Fig. 5.11

APPENDIX II

THE ZONAL MOMENTUM BALANCE

The equation that governs the local time rate of change of zonal wind can be written in the form

(

A complete derivation of this equation is given in Holton (1972) p. 21-28*. The advective terms can be rewritten in the form

(

where the term in parentheses vanishes because of the continuity of mass. Substituting back into (A.2.1) and making use of the identity

(

we obtain

(

When we zonally average, the terms $-\partial/\partial x(u^2)$ and $-\partial\Phi/\partial x$ drop out because of the identity

(

[34]

Next we expand the [uv] and [uw] terms, making use of (A. 1.11), to obtain

(

Then we expand the mean meridional motion terms in the form

(

and

(

Substituting back into (A 2.4) and making use of the zonally averaged continuity equation in spherical coordinates

(

we obtain, after some minor rearranging,

(

As an alternative method of deriving (A 2.5) we can start with the equation governing the angular momentum of a fixed, zonally symmetric annulus, bounded by latitudinal "walls" at y and y + y and pressure levels p and p + p, as shown in the accompanying figure. The only processes capable of changing the integrated angular momentum within the annulus are advection across the boundaries of the annulus and frictional torques acting within the annulus. Such torques will be assumed to be small unless the annulus is contiguous with the earth's surface. The net advection of angular momentum across the latitudinal walls is given by

(

where the zonal integration is carried out around a complete latitude circle and the vertical integration is carried out from level p down to p + p. Expanding Mv in a Taylor series expansion in y, and keeping only the linear term, the above expression reduces to - (Mv/ y) dx dp y, which is an accurate representation, provided that y is sufficiently small. Furthermore, if p is sufficiently small, this expression can be vertically integrated to obtain - Mv/ y) dx y p, or, using (A 1.2), -2 R cos y p [M]/ p. [In writing the vertical advection term in pressure

[34] Here the equation has been written in pressure coordinates and the small terms uw/R_E and $2\Omega w \cos\phi$ have been neglected. It is easily shown that these terms are at least 2 orders of magnitude smaller than the corresponding terms in v.

coordinates we are implicitly neglecting the vertical convergence or divergence associated with the variation in y with height. It is this effect which leads to the small (uw tan)/R term which is neglected in (A 2.1) (see footnote, p. A7). Now let us